THE UNIVERSITY OF CALGARY

The role of SERCA3 in lymphocyte calcium signaling and activation

by

Carla Sciarretta

A THESIS

SUBMITTED TO THE FACULTY OF GRADUATE STUDIES

IN PARTIAL FULFILLMENT OF THE REQUIREMENTS FOR THE

DEGREE OF MASTER OF SCIENCE

DEPARTMENT OF BIOCHEMISTRY AND MOLECULAR BIOLOGY

CALGARY, ALBERTA

JANUARY, 2000

ABSTRACT

In lymphocytes, antigen receptor activation causes the IP_3-mediated release of Ca^{2+} from intracellular stores, consequently stimulating Ca^{2+} influx at the plasma membrane. Two Ca^{2+} pumps, SERCA2b and SERCA3, replenish the calcium stores of these cells. I tested the hypothesis that SERCA3 has a unique role in regulating lymphocyte Ca^{2+} signaling and activation, using cells isolated from *serca3*$^{-/-}$ mice. Compared to wild-type cells, the rate of decline of $[Ca^{2+}]_i$ following antigen receptor stimulation was significantly reduced in *serca3*$^{-/-}$ splenic B cells and thymocytes, but not in splenic T cells. The latter, however, secreted significantly reduced levels of IL-2 when treated with potent pharmacological stimuli. Moreover, the Ca^{2+} stores of these cells were found to be more depleted, and their Ca^{2+} influx pathway reduced when compared to wild-type cells. These results suggest that SERCA3 expression is critically important for lymphocyte function when the Ca^{2+} handling requirements of the cell are high.

ACKNOWLEGEMENTS

I would like to thank my supervisor, Dr. Jonathan Lytton, for allowing me to work in his lab, and for providing me with a tremendous amount of support and guidance. I would also like to thank my committee members, Dr. Julie Deans and Dr. Paul Schnetkamp, for all their encouragement and suggestions, and Dr. Gary Kargacin for agreeing to be my external examiner.

I am grateful to Dr. Gary Shull for providing us the *serca3*$^{(-/-)}$ mice, and Dr. Lynne Liu for supplying us with her preliminary data. I thank Dr. Aziz Amrani, and Sherri Thiessen for teaching me a lot about handling the animals, and Laurie Robertson for her assistance with flow cytometry.

I thank my wonderful lab-mates RuoMei, Steve, Jeremy, Xiao-Fang, Charu, Hui and XinJiang for their friendship and positive attitudes! Finally, I would like to thank my mom and dad, Claudia, Todd and Gail for their *endless* encouragement!!

To my mom and dad

TABLE OF CONTENTS

LIST OF TABLES

LIST OF FIGURES

LIST OF ABBREVIATIONS

$[Ca^{2+}]_i$: Intracellular free Ca^{2+} concentration

Ab: Antibody

Ach: Acetylcholine

ATP: Adenosine triphosphate

ATPase: Adenosine triphosphatase

BAPTA: 1,2-bis(2-Aminophenoxy)ethane-N,N,N',N'-tetraacetic acid

BCR: B cell receptor

bp: Base pair

BSA: Bovine serum albumin

cDNA: Complementary deoxyribonucleic acid

ConA: Conconavalin A

CRAC: Calcium release activated calcium

DAG: Diacylglycerol

DMSO: Dimethyl sulfoxide

DNA: Deoxyribonucleic acid

EDTA: Ethylene diamine tetra-acetic acid

ELISA: Enzyme-linked immunosorbent assay

ER: Endoplasmic reticulum

FBS: Fetal bovine serum

FITC: Fluorescein isothiocynate

FL-1: Fluorescence 1 detector

FL-2: Fluorescence 2 detector

FL-3: Fluorescence 3 detector

F_{max}: Maximum fluorescence of fluo-3

F_{min}: Minimum fluorescence of fluo-3

F_{Mn}: Fluorescence of Fluo-3 in the presence of Mn^{2+}

HBS: Hepes-buffered saline

HBSS: Hanks balanced salt solution

IgD: Immunoglobulin D

IgG: Immunoglobulin G

IgM: Immunoglobulin M

IL-2: Interleukin-2

IP_3: Inositol 1,4,5-triphosphate

IP_3R: Inositol 1,4,5-triphosphate receptor

ITAM: Immunoreceptor tyrosine-based activation sequence motif

kDa: Kilodalton

mAb: Monoclonal antibody

MAPK: Mitogen activated protein kinase

$MnCl_2$: Manganese chloride

mRNA: Messenger ribonucleic acid

NFAT: Nuclear factor of activated T cells

PAGE: Polyacrylamide gel electrophoresis

PBS: Phosphate buffered saline

PCR: Polymerase chain reaction

PE: R-phycoerythrin

PerCP: Peridinin chlorophyll protein

PI: Propidium iodide

PIP_2: Phosphatidylinositol 4,5-bisphosphate

PKC: Protein kinase C

PLCγ: Phospholipase C γ

PMA: Phorbol 12-myristate 13-acetate

PMCA: Plasma membrane Ca^{2+} ATPase

PTK: Protein tyrosine kinase

SDS: Sodium dodecyl sulphate

SERCA: Sarco(endo)plasmic reticulum Ca^{2+}-ATPase

SOC: Store-operated channel

SR: Sarcoplasmic recticulum

TCR: T cell receptor

CHAPTER ONE: INTRODUCTION

In lymphocytes, an increase in the intracellular free Ca^{2+} concentration ($[Ca^{2+}]_i$) is one of the earliest events observed following the stimulation of antigen receptors (Imboden et al., 1985; Tsien et al., 1982). This rise in intracellular Ca^{2+} levels is the result of both the release of Ca^{2+} from intracellular storage compartments associated with the endoplasmic reticulum, and the influx of Ca^{2+} from the extracellular space. Numerous studies have subsequently demonstrated the critical importance of the Ca^{2+} signal in regulating aspects of lymphocyte maturation and activation (Donnadieu et al., 1992; Nakayama et al., 1992; Negulescu et al., 1996; Timmerman et al., 1996). Given its central role in mediating antigen receptor-induced responses, much research has been focused on the identification of proteins and mechanisms involved in the regulation of the Ca^{2+} signal.

The Sarco(endo)plasmic Reticulum Ca^{2+}-ATPase (SERCA) Ca^{2+} pumps modulate $[Ca^{2+}]_i$ by replenishing intracellular stores of Ca^{2+}, making the ion available for subsequent release and signal transduction. SERCA proteins therefore play an important role in the initiation, maintenance and termination of Ca^{2+} signals. Lymphocytes are one of a select number of cell types that express the third isoform of the SERCA pump (Wu et al., 1995), suggesting this isoform that it may be uniquely involved in regulating Ca^{2+} signaling in these cells.

This introduction provides a review of the relevant literature pertaining to the initiation of Ca^{2+} signaling in lymphocytes, and the role that SERCA3 may play in regulating these processes. It begins with an overview of calcium regulation and signal transduction.

I. Calcium Ion and Signal Transduction

Ionized calcium is a ubiquitous second messenger and increases in its intracellular concentration serve as signals that mediate a diverse number of cellular processes, including cell proliferation and differentiation, apoptosis, and the secretion of molecules from the cell (Clapham, 1995). The maintenance of Ca^{2+} homeostasis is therefore critically important for cell function.

The resting concentration of intracellular free calcium ($[Ca^{2+}]_i$) is approximately 100 nM, which is several thousand fold lower than the concentration found extracellularly. In addition to this concentration gradient, the membrane potential of approximately –70 mV, also favours Ca^{2+} entry. Therefore, a substantial electrochemical gradient facilitates the passive entry of Ca^{2+} into cells through channels that are regulated by hormones, second messengers or changes in membrane potential.

Cytosolic Ca^{2+} levels are regulated by the active or facilitated transport of Ca^{2+} across membranes into either the extracellular space or intracellular storage compartments. This removal is achieved by two predominant mechanisms. One mechanism involves exchanger proteins, which couple the extrusion of Ca^{2+} from the cell with the diffusion of Na^+ into the cell down its electrochemical gradient (Blaustein and Lederer, 1999), while the other involves ATP-dependent calcium pumps, which utilize the energy of ATP to actively remove Ca^{2+} from the cytosol (Pozzan et al., 1994). Two types of pumps are expressed in cells. One type is the plasma membrane Ca^{2+} ATPase (PMCA) calcium pump, and the other type is the SERCA calcium pump, which decreases cytosolic Ca^{2+} levels by pumping the ion into intracellular storage compartments present within the sarcoplasmic or endoplasmic reticulum (SR and ER, respectively) (Clapham, 1995; Pozzan et al., 1994).

Due to the pervasive distribution of the SR/ER throughout the cell, the existence of storage compartments within these organelles facilitates the removal of Ca^{2+} from the

cytosol at distances from the plasma membrane. However, these stores do not solely function in providing a buffer for large increases in $[Ca^{2+}]_i$, they also play a dynamic role in cells. Due to the biochemical properties of the proteins associated with the Ca^{2+} pools of the SR/ER, these stores are able to rapidly exchange Ca^{2+} with the cytosol, and thus represent a major source of signaling Ca^{2+} in the cell. Ca^{2+} is accumulated within these stores by the activity of SERCA pumps, and is maintained in the organelle through low affinity/high capacity interactions with calcium binding proteins such calreticulin and other chaperones present in the ER (Pozzan et al., 1994). Ca^{2+} is released through ryanodine receptor Ca^{2+} channels in the SR, or IP_3-regulated channels in the ER (Clapham, 1995). The release of stored Ca^{2+} generates a transient increase in $[Ca^{2+}]_i$, due to the intrinsic inactivation of the release channels (Meszaros et al., 1998), as well their regulation by both phosphorylation and the local concentration of Ca^{2+} (Clapham, 1995).

Released Ca^{2+} can trigger numerous cellular events including the contraction of skeletal muscle, and the initiation of signaling pathways in non-excitable cells (Clapham, 1995). Moreover, in non-excitable cells the sensitivity of IP_3-gated channels for its ligand is regulated in a biphasic nature by $[Ca^{2+}]_i$, resulting in the generation of propagating waves of released Ca^{2+} along the ER (Berridge, 1997). The frequency and amplitude of these waves are regulated by numerous processes, including the rate and amount of IP_3 production, the subcellular location of the Ca^{2+} release channels, the re-uptake of Ca^{2+} by SERCA pumps (Camacho and Lechleiter, 1995; Camacho and Lechleiter, 1993), and the influx of extracellular Ca^{2+} (Girard and Clapham, 1993; Lewis and Cahalan, 1995). Variations in the frequency and amplitude of the Ca^{2+} signal appear to encode information that has significant consequences for cellular function since both can activate multiple signaling pathways depending on the affinity of these events for Ca^{2+} (Berridge, 1997; Dolmetsch et al., 1997; Dolmetsch et al., 1998; Li et al., 1998). For example, increases in

intracellular Ca^{2+} levels of different amplitudes following antigen receptor stimulation, have been shown to specifically activate different types of transcription factors, thereby mediating the expression of particular genes (Dolmetsch et al., 1997).

The concentration of free Ca^{2+} within the intracellular stores of the ER not only determines the magnitude of Ca^{2+} release, but also modulates the "capacitative" entry of Ca^{2+} through store-operated channels (SOC) at the plasma membrane (Hofer et al., 1998; Putney, 1990; Putney, 1993). The signal that couples the depletion status of intracellular stores to the activation of Ca^{2+} influx is not well understood, but may involve a diffusible calcium influx factor that is released upon store depletion (Csutora et al., 1999; Randriamampita and Tsien, 1993), or a mechanism that leads to a direct interaction between IP_3 receptors in the ER and SOCs at the plasma membrane (Patterson et al., 1999; Yao et al., 1999). The capacitative entry of Ca^{2+} through SOCs is believed to serve many functions in cells. It provides the necessary Ca^{2+} for replenishing depleted stores, as well as facilitates the propagation of Ca^{2+} waves and the prolongation of Ca^{2+} signals that are necessary for stimulating gene expression (Berridge, 1997; Fanger et al., 1995; Girard and Clapham, 1993).

Numerous types of Ca^{2+} SOCs have been identified, including the Trp family of proteins, and calcium release activated calcium (CRAC) channels (Lewis and Cahalan, 1995). Although CRAC channels have not as yet been cloned or purified, the characteristics of the current associated with them reveal that they are highly selective for Ca^{2+}, and do not conduct Ca^{2+} spontaneously, but instead are associated with a current that is temporally linked to changes in $[Ca^{2+}]_i$ (Lewis and Cahalan, 1995). Furthermore, CRAC channels are inhibited by membrane depolarization and blocked by Ni^{2+} and Cd^{3+} (Lewis and Cahalan, 1995). The channels formed when mammalian Trps are expressed have been

shown to be non-selective for Ca^{2+}, suggesting that the highly selective CRAC channels are encoded by a different gene (Birnbaumer et al., 1996).

The intracellular Ca^{2+} stores of the SR/ER, and the Ca^{2+} channels, pumps and binding proteins associated with them, therefore play an important role in regulating cellular Ca^{2+} homeostasis at rest and during signal transduction, by mediating the rapid initiation and termination of Ca^{2+} signals, which can be localized to particular areas within the cell. By accumulating Ca^{2+} within intracellular pools, SERCA pumps regulate the $[Ca^{2+}]_i$, as well as the availability of stored Ca^{2+} for release, the influx of extracellular Ca^{2+}, and the frequency of Ca^{2+} waves.

II. The SERCA Family of Calcium Pumps

Biochemical studies first identified the SERCA Ca^{2+} pump in rabbit skeletal muscle as the protein responsible for the ATP-dependent transport of Ca^{2+} in sarcoplasmic reticulum (SR) membrane fractions (MacLennan, 1970). A family of SERCA proteins have subsequently been identified, and have been shown to be present in the SR or ER (Pozzan et al., 1994).

Mechanism of Ca^{2+} transport

SERCA pumps are P-type ATPases that form a phosphoprotein intermediate during the course of their reaction cycle (MacLennan et al., 1997). During this cycle, SERCA proteins undergo four major reversible changes in conformation (Figure 1). Formation of the E_1P intermediate occurs following the occupation of two high affinity Ca^{2+}-binding sites, and subsequent phosphorylation of SERCA by ATP. Phosphorylation results in the Ca^{2+} becoming occluded and no longer able to exchange with cytoplasmic Ca^{2+}. The transition to the E_2P intermediate is rate limiting, and is followed by the loss of Ca^{2+} to the

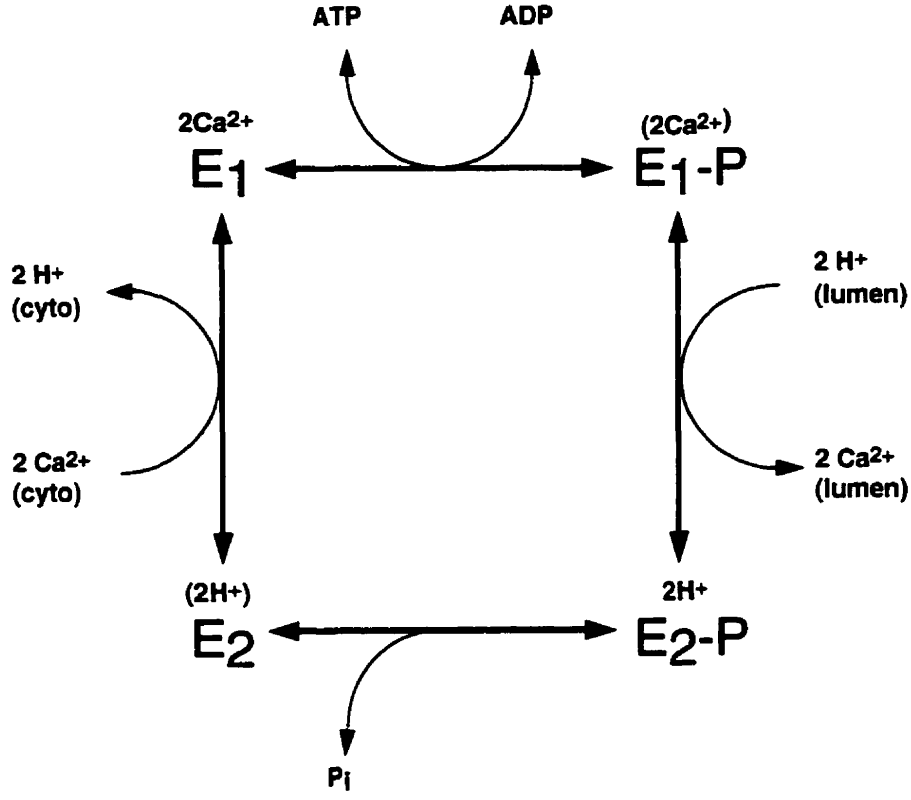

Fig. 1. **Reaction cycle of Ca^{2+} transport by SERCA pumps.** The four reversible conformations of the enzyme (E) are shown. Brackets around Ca^{2+} and H^+ indicate that the ions are occluded. Phosphorylation (P) of the enzyme by ATP occurs after the binding of 2 Ca^{2+}. Transition from the E_1-P conformation to E_2-P results in the loss of Ca^{2+} to the lumen of the SR/ER. Subsequent hydrolysis of enzyme in E_2-P conformation results in the transition to the E_2 conformation, which converts back to E_1, thereby regenerating the 2 high affinity Ca^{2+} binding sites (Adapted from MacLennan et al. (1997).

lumen of the SR/ER due to the low Ca^{2+} affinity of the E_2 conformation. E_2P is then hydrolyzed, and the E_2 form of the enzyme converts back to the E_1 conformation, regenerating the two high affinity Ca^{2+}-binding sites (MacLennan et al., 1997).

SERCA Isoforms

At least seven SERCA isoforms are encoded by three different alternatively spliced genes; the SERCA1 gene, *ATP2A1*, SERCA2 gene, *ATP2A2*, and SERCA3 gene, *ATP2A3*. The primary sequences of the isoforms are highly conserved suggesting that they have essentially identical transmembrane topologies and tertiary structure; characterized by 10 transmembrane spanning segments that are connected to a large cytoplasmic head by a stalk-like structure, and a small lumenal region (Zhang et al., 1998) (Figure 2). Although they share a similar overall structure, and perform a qualitatively similar role in cells (the removal of Ca^{2+} from the cytoplasm through the loading of intracellular stores), numerous differences between the SERCA proteins with respect to their structure, function, and tissue distribution have been identified.

The SERCA isoforms expressed in the SR are SERCA1 and SERCA2a. The SERCA1 isoform is found exclusively in fast-twitch skeletal muscle (Wu et al., 1995). Two developmentally regulated alternatively spliced species are transcribed from the SERCA1 gene (SERCA1a and SERCA1b) that differ by seven amino acids at their carboxyl termini (Brandl et al., 1987). The SERCA2 gene also encodes two alternatively spliced transcripts, producing the SERCA2a and SERCA2b proteins that, similar to the SERCA1 isoforms, differ at their carboxyl termini. SERCA2b possesses an extended hydrophobic sequence of approximately 50 amino acids that forms an additional transmembrane spanning segment, with the C-terminal region residing in the lumen of the SR/ER (Bayle et al., 1995; Campbell et al., 1992). SERCA2a is expressed in cardiac and

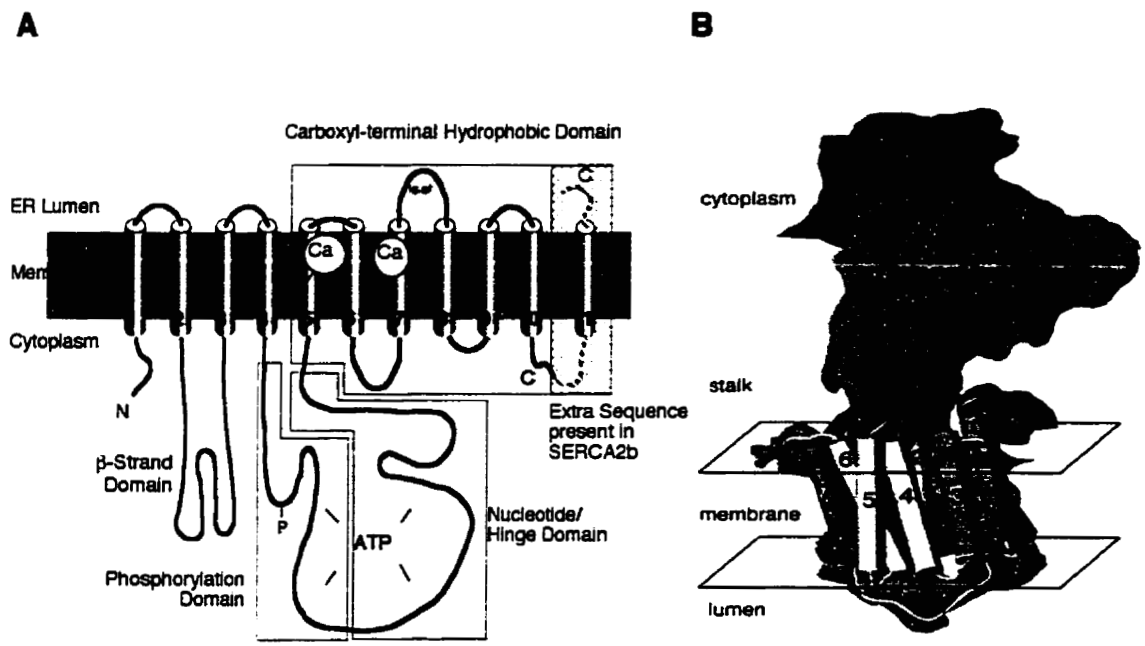

Fig. 2. **The structure of SERCA Ca^{2+} pumps.** **A.** Illustration of the proposed membrane topology. **B.** Model for the arrangement of the transmembrane regions shown in A, based on the electron density map of SERCA. The helices shown in yellow form a cavity leading to the Ca^{2+} binding sites. The red dot indicates a bound Ca^{2+} ion (the other ion binds in a region behind helix 5). Adapted from Zhang et al. (1998).

slow-twitch skeletal muscle, whereas SERCA2b is an ubiquitously expressed form of the Ca^{2+} pump (Lytton et al., 1989; Wu et al., 1995).

It has recently been demonstrated that both the human and mouse SERCA3 genes encode for at least three alternatively spliced transcripts that are expressed in a select number of non-muscle tissue (Dode et al., 1998; Ozog et al., 1998; Poch et al., 1998). In the mouse, these transcripts encode for functional proteins of either 994, 1039 or 1027 amino acids, that differ at the extreme C-terminal region, such that the last six amino acids of the 994 amino acid isoform are replaced with stretches of either 45 or 33 amino acids to produce the other two proteins (Dode et al., 1998; Ozog et al., 1998). The physiological functions of these different isoforms are not yet known. In addition, unlike the C-terminal region of SERCA2b, the results of hydropathy analysis do not indicate that the C-terminal tails of the SERCA3 isoforms form transmembrane spanning segments (Dode et al., 1998).

SERCA2b and SERCA3: Differences in structure, function and patterns of expression

SERCA2b and SERCA3 represent the non-muscle isoforms of the Ca^{2+} pump. At the amino acid level, the two proteins share ~75% identity, differing mainly in the region of the nucleotide binding domain and the carboxyl terminus (Burk et al., 1989). These differences in primary sequence likely contribute to the distinct biochemical properties of SERCA3 that are believed to result from an alteration of the conformational equilibrium of the isozyme (Lytton et al., 1992; Toyofuku et al., 1992). SERCA3 appears to have a faster reaction cycle compared to SERCA2b, as suggested by its faster rate of Ca^{2+} transport and ATP hydrolysis (Lytton et al., 1992). In addition, SERCA3 has been shown to have an altered pH dependence, functioning maximally at a pH of 7.2-7.4, which is higher than the pH required for optimal activity of the other isoforms (pH 7) (Lytton et al., 1992).

The two proteins also differ with respect to their affinities for Ca^{2+}. The apparent Ca^{2+} affinity of rat SERCA3 ($K_{1/2}$~ 1.1 μM) is much lower compared to that of rat SERCA2b ($K_{1/2}$ ~ 0.27 μM) (Lytton et al., 1992). Similarly, the Ca^{2+} affinity of the 994 amino acid form of mouse SERCA3 has been shown to be lower than that of pig SERCA2b ($K_{1/2}$ = 2.2 μM vs $K_{1/2}$ = 0.19 μM, respectively). The differences in the reported $K_{1/2}$ values may be due to differences in the assay systems used, but consistently reveal that SERCA3 has a lower apparent affinity for Ca^{2+} than SERCA2b. Based on this observation it has been suggested that SERCA3 may be localized to an area with elevated levels of Ca^{2+}, since at a normal resting $[Ca^{2+}]_i$ this isozyme would be inactive (Lytton et al., 1992; Toyofuku et al., 1992).

SERCA3 is expressed in the ER of a limited number of non-muscle tissues, including epithelial and endothelial cells, lymphoid cells, platelets, and cerebellar Purkinje neurons (Anger et al., 1993; Bobe et al., 1998; Dode et al., 1998; Wu et al., 1995; Wuytack et al., 1994). In these cells, SERCA3 is always co-expressed along with SERCA2b, although the two isoforms differ in their relative levels of expression among different cell types (Wu et al., 1995). Using quantitative Northern blot analysis, Wu et al showed that rat SERCA3 mRNA is most abundant in the lung, cerebellum, gastrointestinal tract and lymphoid tissues, however its contribution to the total SERCA mRNA varied widely in these tissues. In the cerebellum, for example, SERCA3 mRNA represented only 10% of the total SERCA mRNA, whereas in the small intestine and lung the SERCA3 message comprised 33% of the total SERCA mRNA. Two tissues in which SERCA3 mRNA was more abundant than SERCA2b mRNA were the large intestine and thymus (69% and 68% of total SERCA transcripts, respectively). *In situ* hybridization studies on thymic tissue revealed SERCA3 expression to be restricted to the cortical regions, which are areas of thymocyte maturation (Abbas et al., 1997), whereas SERCA2b expression was

evenly distributed throughout the tissue. SERCA3 and SERCA2b were found to be similarly expressed in the spleen and lymph node. Closer examination of the relative expression levels of SERCA3 and SERCA2b in T cells and non-T cells of the spleen (the latter representing predominately B cells) revealed that SERCA3 mRNA is more abundant than SERCA2b mRNA in B cells, but both are equally represented in splenic T cells.

The functional significance of two isoforms being expressed in the same cell type is unclear. Based on their structural and biochemical differences, and their different levels of expression in certain cells types, it has been hypothesized that the two isoforms may regulate physically distinct Ca^{2+} stores. Immunocytochemical analysis of endogenously expressed SERCA2b and SERCA3 in Jurkat T cells, or overexpressed human SERCA3 or SERCA2b in human embryonic kidney cells, showed the two proteins possess indistinguishable reticular patterns of expression (Poch et al., 1998). It is possible, however, that immunocytochemical techniques may not be sufficiently sensitive to identify subtle differences in the subcellular localization of the SERCA isoforms in these cells. Similar analysis of polarized salivary gland ancinar and duct cells showed SERCA2b and SERCA3 were localized to different subcellular regions (Lee et al., 1997). In certain cell types, then, SERCA3 and SERCA2b may regulate different pools of intracellular Ca^{2+}.

The Physiological Roles of SERCA Calcium Pumps

SERCA pumps modulate intracellular Ca^{2+} levels by replenishing intracellular pools present within the SR/ER. As described above, the isoforms differ both structurally and functionally. Moreover, they are expressed in a tissue specific manner. Together, these findings suggest that their expression is important for regulating the particular Ca^{2+} handling requirements of the cells in which they are expressed.

The first direct evidence that SERCA pumps have a dynamic role in regulating Ca^{2+}

signaling came from overexpression studies in *Xenopus* oocytes (Camacho and Lechleiter, 1995; Camacho and Lechleiter, 1993). In these studies overexpression of SERCA proteins altered the frequency and amplitude of Ca^{2+} waves in response to cellular stimulation, revealing that SERCA activity may be important for signaling cellular responses that are dependent on oscillating levels of Ca^{2+} .

With the exception of brain cerebelleum and large intestine, which express quite high levels of SERCA mRNA, non-muscle tissues express only 2 to 20% of the SERCA content of skeletal muscle (Wu et al., 1995). It is in skeletal muscle cells, therefore, that the specific biological roles of SERCA proteins are best understood. As described above, muscle cells express either SERCA1 (fast-twitch skeletal muscle cells) or SERCA2a (slow-twitch skeletal muscle and cardiac cells). SERCA1 and SERCA2a are critically important for lowering intracellular Ca^{2+} levels following muscle cell contraction, thereby mediating relaxation, as wells as replenishing the SR stores needed to re-initiate contraction (Pozzan et al., 1994). It is well established that SERCA2a activity conributes to the inotropic and chronotropic cardiac response to β-adrenergic receptor stimulation, due to the phosphorylation of the SERCA2a inhibitor, phospholamban (Pozzan et al., 1994). Phospholamban phosphorylation results in the release of SERCA2a inhibition, increasing the rate at which Ca^{2+} is lowered, hence speeding relaxation, and increasing the SR Ca^{2+} load. This in turn leads to enhanced Ca^{2+} release and stronger contraction. Recently, our understanding of SERCA2a function has been furthered by gene inactivation and transgenic studies in mice. Ablation of the *serca2* gene causes embryonic lethality (Periasamy et al., 1999), revealing the critical importance of SERCA2 for viability. The role of this gene in the regulation of cardiac cell contraction and relaxation has been demonstrated more clearly, however, by studies that examined cardiac function in tissue isolated from mice heterozygous for a *serca2* mutation (Periasamy et al., 1999), as well as in cells isolated

from mice overexpressing a SERCA2 transgene (He et al., 1997).

Additional information regarding the physiological functions of SERCA pumps has also been obtained through the study of genetic diseases associated with mutations in the SERCA genes. Mutations in *serca1* are associated with Brody's disease, an inherited disorder characterized by stiffness and cramps in the muscles, revealing the critical role of SERCA1 in mediating the relaxation of fast-twitch skeletal muscle (Odermatt et al., 1996). In addition, mutations of the SERCA2 gene have recently been identified as being the cause of Darier-White disease, a rare skin disorder (Sakuntabhai et al., 1999). This discovery has revealed a role for SERCA2b in mediating the differentiation of epidermal cells, as well as epidermal cell adhesion (Sakuntabhai et al., 1999).

In all these studies, an interesting observation has been that the alteration in SERCA pump expression can be compensated for to varying degrees. For example, cells heterozygous for a *serca2* mutation upregulate the expression of the remaining copy of the gene (Periasamy et al., 1999). In cardiac cells overexpressing a SERCA2 transgene, the expression of the Na^+/Ca^{2+} exchanger and phospholamban were shown to be altered (He et al., 1997). Similarly, cardiac cells overexpressing SERCA1a showed a decrease in the expression of endogenous SERCA2a (Loukianov et al., 1998). In addition, the difficulty in establishing transgenic mouse models that overexpress SERCA proteins has been discussed (Loukianov et al., 1998). SERCA expression is regulated at both the level of transcription and translation, as revealed by the low level increases in mRNA expression from transgenes, and even lower levels of expression of the protein (He et al., 1997; Ji et al., 1999). Together, these findings demonstrate that cells utilize mechanisms to compensate for alterations in SERCA expression, and reveal that cells tightly regulate proteins involved in maintaining Ca^{2+} homeostasis.

Although a significant amount of information is currently available regarding the

physiological roles of the SERCA1 and SERCA2a isforms, much less is understood about the biological roles of the non-muscle isoforms, SERCA2b and SERCA3. Two recent studies have shown that the expression of SERCA2b and SERCA3 are differentially regulated during myeloid cell differentiation (Launay et al., 1999) and T cell activation (Launay et al., 1997), suggesting that the relative expression levels of these SERCA pumps may be important for regulating Ca^{2+} homeostasis during signal transduction.

Recently a gene-targeting approach has been used to develop a mouse model to examine the physiological role of SERCA3 (Liu et al., 1997). These animals show no overt abnormalities, and matings of animals homozygous for the mutation produce viable young. Aortic rings isolated from SERCA3-deficient mice, however, showed a reduced relaxation in response to acetylcholine (Ach) compared to those of wild-type mice (Liu et al., 1997). Ach, acting through its G-protein-coupled receptor on endothelial cells, stimulates relaxation of precontracted aortic rings by producing NO through an IP_3-mediated Ca^{2+} release mechanism (Liu et al., 1997). Ca^{2+} imaging experiments performed on isolated aortic endothelial cells showed that the acetylcholine-responsive Ca^{2+} stores in the mutant cells were more depleted than those of wild-type control cells (Liu et al., 1997). Moreover, the stores in the *serca3*$^{(-/-)}$ cells were not replenished following the removal of acetylcholine. Therefore, the alteration in Ca^{2+} signaling caused by SERCA3 ablation in endothelial cells, may have contributed to the relaxation deficit observed in the aortas (Liu et al., 1997).

Examination of trachea isolated from these same mice revealed that they have a reduced rate of relaxation following pre-contraction (Kao et al., 1999). The relaxation was mediated by the surrounding epithelial cells, which normally express SERCA3. Although not directly tested, their results suggest that SERCA3 expression in epithelial cells is important for the regulation of Ca^{2+} signals that mediate epithelium-dependent relaxation of tracheal smooth muscle. Finally, it has recently been reported that various mutations in the

SERCA3 gene may contribute to the genetic susceptibility to Type II diabetes (Varadi et al., 1999). SERCA3 expression therefore has important consequences for the functioning of the cells in which it is expressed. Moreover, the results of Liu et al. revealed that SERCA3 regulates intracellular Ca^{2+} levels in endothelial cells in a manner that is not compensated for by the presence of SERCA2b. The physiological role of SERCA3 in lymphocytes, however, is not known.

III. Antigen Receptor-mediated Signaling in Lymphocytes

Early Signal Transduction from Antigen Receptors

Lymphocytes are classified into two main cell types, cells that act against intracellular pathogens (T cells) and cells that protect against extracellular pathogens (B cells). Both cell types express antigen-specific receptors on their cell surfaces. Although the T cell receptor (TCR) and the B cell receptor (BCR) differ in their overall structure and ligand specificities, the two receptors share many features in common. In addition, stimulated TCRs and BCRs appear to recruit similar families of effector molecules, and utilize common signal transduction pathways to mediate cellular responses.

The TCR and BCR are oligomeric transmembrane spanning proteins that lack intrinsic enzymatic activity, and are organized such that their ligand binding and signal transduction regions are localized in distinct subunits (Kurosaki, 1999; Qian and Weiss, 1997; Weiss and Littman, 1994). In the TCR, two variable chains recognize and bind antigen (Weiss and Littman, 1994). In the BCR, the ligand binding subunit is a surface immunoglobulin (sIg) possessing variable regions that confer ligand specificity (Kurosaki, 1999). In both receptors, the ligand binding subunits are coupled non-covalently to invariant signal transducing subunits (Kurosaki, 1999; Weiss and Littman, 1994). These

subunits possess immunoreceptor tyrosine-based activation sequence motifs (ITAMs) in their extended cytoplasmic domains, that have been shown to be critical for the ability of the TCR and BCR to relay information into the cell interior (Kurosaki, 1999; Qian and Weiss, 1997; Reth, 1989; Weiss and Littman, 1994). The TCR and BCR can be stimulated by the binding of antigen, as well as through cross-linking with monoclonal antibodies (mAb). For TCRs, this can be accomplished using a secondary antibody to cross-link primary mAbs directed against their CD3ε subunits, whereas BCRs can be stimulated by cross-linking their surface Ig molecules using specific mAbs.

Stimulation of the TCR and BCR results in the aggregation of their cytoplasmic chains, and the recruitment of protein tyrosine kinases (PTKs) of the Src, Syk/ZAP-70 and Tec families to the receptor complex (Kurosaki, 1997; Qian and Weiss, 1997; Weiss and Littman, 1994). The initiation of phosphorylation events by the PTKs results in the activation of the phosphatidylinositol 3' kinase, mitogen-activated protein kinase (MAPK), and phospholipase Cγ (PLCγ) signaling pathways, all of which are important for the production of second messengers responsible for triggering the intracellular events that culminate in the induction of appropriate cellular responses (Dasgupta et al., 1992; Gold and Aebersold, 1994; Gold et al., 1992; Imboden and Stobo, 1985; Iwashima et al., 1994; van Oers et al., 1996; Wange and Samelson, 1996).

The cellular responses induced following antigen receptor activation can vary depending on the developmental stage of the cell. In maturing lymphocytes, the stimulation of the TCR and BCR are important for the apoptotic elimination of self-reactive cells and the survival of cells capable of recognizing forgein antigen (Abbas et al., 1997). The stages of maturation of both B and T cells can be defined by the temporal expression of particular surface proteins. For T cells these proteins include CD4 and CD8 (Abbas et al., 1997). T cells mature in the thymus. Within this organ, the most immature cells express neither CD4

nor CD8 on their cell surface ($CD4^-CD8^-$). As maturation proceeds, thymocytes express both CD4 and CD8 ($CD4^+CD8^+$). These double positive cells undergo a process of selection resulting in the survival of cells capable of recognizing foreign antigen (positive selection), and the death or inactivation of cells that recognize self antigen (negative selection). The surviving cells develop further into mature single $CD4^+$ or $CD8^+$ positive thymocytes, which are classified as "helper" T cells and "cytotoxic" T cells, respectively, that migrate from the thymus to peripheral organs such as the spleen, where they encounter forgein antigen.

The CD4 and CD8 surface molecules function as co-receptors that facilitate antigen recognition by binding to the major histocompatibility complex that is expressed on the surface of an antigen presenting cell, and to which the antigen peptide is bound. The cytoplasmic tails of both CD4 and CD8 are associated with protein tyrosine kinases that are thus recruited to the TCR when antigen is present. The recruitment of these kinases to the vicinity of the TCR is believed to facilitate signal transduction from the ligated receptor (Janeway and Bottomly, 1994).

In mature lymphocytes, the signaling pathways initiated following antigen binding can trigger cellular activation; a process characterized by morphological changes, and the initiation of gene transcription leading to cellular proliferation, and the acquisition of immunological functions, including the secretion of antibodies by B cells and lymphokines by T cells (Crabtree and Clipstone, 1994; DeFranco, 1997; Weiss et al., 1987). Paradoxically, antigen receptor ligation can also induce the apoptotic death of mature lymphocytes, due to the transcription and secretion of Fas ligand, which can lead to the activation of caspases following its receptor binding (Berridge, 1997).

The specific signals that cause a cell to either proliferate or die are not clearly understood. Numerous factors appear to play a role in determining the ultimate response of

lymphocytes to antigen binding, including the nature of the antigen (self vs foreign), the number of receptors engaged (Ashton-Rickardt et al., 1994), the developmental stage of the cell, and the initiation of additional signaling pathways following the ligation of co-receptors or accessory molecules on the surface of lymphocytes (Kishimoto and Sprent, 1999; Kurosaki, 1999; Ward, 1996). An example of the latter type includes the CD28 molecule, which is expressed on the surface of T cells. CD28 stimulation by either its endogenous ligand, B7, or mAbs *in vitro*, initiates the co-stimulatory signals that are required for the expression of interleukin-2 and T cell proliferation following TCR activation (Janeway and Bottomly, 1994; Stein et al., 1994).

Calcium Signaling in Lymphocytes

When examined in a population of cells, the increase in $[Ca^{2+}]_i$ that occurs soon after antigen receptor stimulation is biphasic in nature; characterized by an initial rapid spike followed by a lower sustained plateau in $[Ca^{2+}]_i$. In lymphocytes, the initiation of this Ca^{2+} signal is attributed to the activation of the PLCγ pathway (Dasgupta et al., 1992; Imboden and Stobo, 1985; Kurosaki, 1999; Sugawara et al., 1997; Takata et al., 1995). Figure 3 highlights the known pathways that are activated following antigen receptor stimulation leading to the initiation of Ca^{2+} signaling in lymphocytes. Activated PLCγ catalyses the conversion of phosphatidlyinositol 4,5-bisphosphate (PIP_2) to diacylglycerol (DAG) and inositol 1,4,5-triphosphate (IP_3) (Berridge and Irvine, 1989). DAG is a regulator of protein kinase C (PKC), whose activation is important for the initiation of additional signaling pathways downstream of the antigen receptor (Truneh et al., 1985). IP_3 induces a biphasic

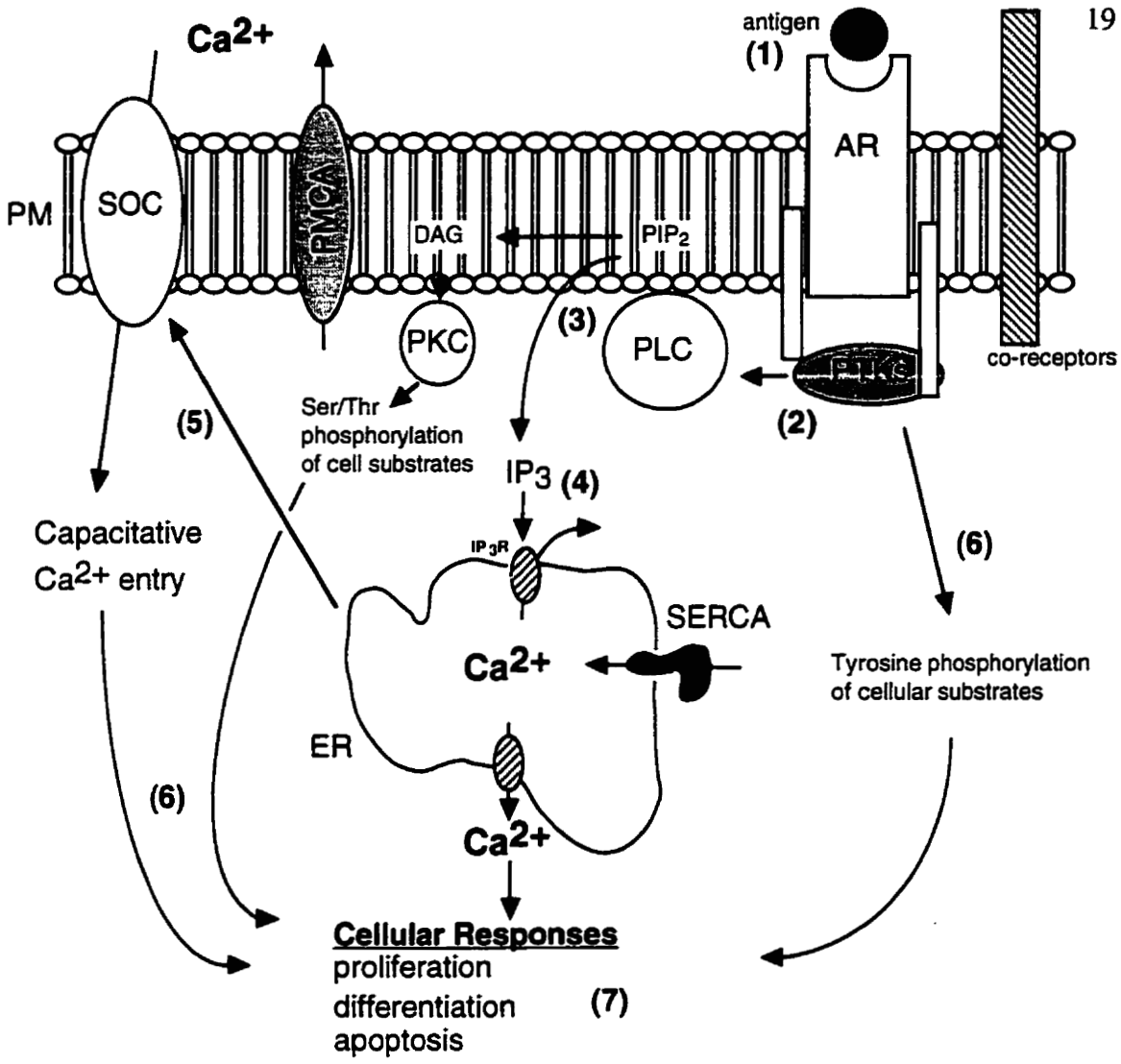

Fig. 3. **Signaling pathways activated by antigen receptors.** Receptor ligation (1) initiates phoshorylation cascades by recruited protein tyrosine kinases (PTKs) (2), resulting in phosholipase C (PLC) activation (3) and the IP_3-mediated release of Ca^{2+} from the ER (4). Depletion of ER stores activates Ca^{2+} entry at the plasma membrane (PM), through store-operated channels (5) (SOC). Ca^{2+}-dependent and independent (6) signals converge to mediate cellular responses to antigen binding (7). AR, antigen receptor; PIP_2, phophatidylinositol 4,5-bisphosphate; IP_3, inositol 1,4,5-trisphosphate; IP_3R, IP_3 receptor; DAG, diacylglycerol; PKC, protein kinase C; PMCA, plasma membrane Ca^{2+} ATPase pump; ER, endoplasmic reticulum. Adapted from Izuierdo and Cantrell (1992)

increase in $[Ca^{2+}]_i$ by binding to its receptor (IP_3R), a Ca^{2+} channel expressed on the ER, resulting in the release of stored Ca^{2+} from this organelle (Clapham, 1995).

The importance of IP_3 in initiating Ca^{2+} signaling in lymphocytes is demonstrated by the finding that receptor-induced mobilization of intracellular Ca^{2+} is abolished in DT40 B cells possessing null mutations in all three isoforms of the IP_3R (Sugawara et al., 1997). The release of Ca^{2+} from intracellular stores contributes to the initial transient peak in $[Ca^{2+}]_i$ observed following antigen receptor stimulation (Harnick et al., 1995; Takata et al., 1995). The release of stored calcium in lymphocytes may also be mediated by ryanodine recepters, which have recently been shown to be expressed in these cells (Hakamata et al., 1994; Sei et al., 1999).

Functional responses associated with this rapid increase in $[Ca^{2+}]_i$ include changes in T cell shape and motility (Negulescu et al., 1996). However, this initial transient increase is not sufficient for the expression of interleukin-2 (IL-2) (Gelfand et al., 1988; Goldsmith and Weiss, 1988), the principle cytokine responsible for the induction of T cell proliferation (Cantrell and Smith, 1984; Meuer et al., 1984), and whose expression serves as a marker of early T cell activation induced by antigen receptor ligation (Crabtree and Clipstone, 1994).

The transcription of IL-2, as well as T cell commitment, to activation require a sustained increase in $[Ca^{2+}]_i$ of ~200 nM for at least two hours (Wacholtz and Lipsky, 1993; Weiss et al., 1987). In lymphocytes, sustained increases in Ca^{2+} levels are dependent on the influx of extracellular Ca^{2+} (Timmerman et al., 1996; Tsien et al., 1982), which is believed to occur through the mechanism of capacitative Ca^{2+} entry (Gouy et al., 1990; Hofer et al., 1998; Mason et al., 1991; Putney, 1990; Putney, 1993; Zweifach and Lewis, 1993). Examination of the influx current generated in lymphocytes suggests that Ca^{2+} entry occurs predominately through CRAC channels (Fanger et al., 1995; Lewis and Cahalan,

1995). Additional molecules in lymphocytes that may mediate extracellular Ca^{2+} influx include L-type Ca^{2+} channels (Akha et al., 1996), and CD20 in B cells (Bubien et al., 1993; Kanzaki et al., 1997; Kanzaki et al., 1995).

When observed at the level of single cells, the sustained plateau phase of the Ca^{2+} transient appears as a series of asynchronous oscillating bursts of $[Ca^{2+}]_i$ (Donnadieu et al., 1992; Li et al., 1998; Negulescu et al., 1994). These oscillations are due to the repetitive release and re-uptake of Ca^{2+} by intracellular stores, as well as the influx of Ca^{2+} through CRAC channels (Camacho and Lechleiter, 1993; Donnadieu et al., 1992; Donnadieu et al., 1992; Girard and Clapham, 1993).

The sustained increase in $[Ca^{2+}]_i$, and the frequency and amplitude of the Ca^{2+} oscillations that comprise it, has been shown to mediate numerous cellular responses in lymphocytes following receptor activation, including the maintenance of interactions between T cells and antigen presenting cells, as well as lymphocyte proliferation, differentiation and death (Donnadieu et al., 1992; Nakayama et al., 1992; Negulescu et al., 1996; Timmerman et al., 1996). In maturing thymocytes, for example, high amplitude calcium elevations induced following TCR ligation are associated with the removal of self-reactive cells, whereas low amplitude calcium signals are associated with the survival of self-tolerant cells (Mariathasan et al., 1998). Oscillating levels of intracellular Ca^{2+} of different frequencies and amplitudes can also induce gene transcription in mature lymphocytes (Dolmetsch et al., 1998; Negulescu et al., 1994; Tsien et al., 1982). A particularly well characterized mechanism by which changes in $[Ca^{2+}]_i$ signals the onset of gene expression in lymphocytes involves the activation of the Ca^{2+}/calmodulin-dependent serine/threonine phosphatase, calcineurin (Crabtree and Clipstone, 1994; O'Keefe et al., 1992; Shibasaki et al., 1996; Venkataraman et al., 1994).

The importance of calcineurin for antigen receptor-mediated cellular responses is demonstrated by the following findings. Inhibition of calcineurin by immunosuppressive drugs inhibits the transcription of IL-2 in T cells (Clipstone and Crabtree, 1992; O'Keefe et al., 1992). Moreover, expression of a Ca^{2+}-independent constitutively active mutant calcineurin can synergize with phorbol 12-myristate 13-acetate (PMA), an activator of PKC, to stimulate IL-2 expression, thereby replacing the normal requirement for an increase in $[Ca^{2+}]_i$ (O'Keefe et al., 1992).

Calcineurin stimulates gene expression in lymphocytes by regulating members of the nuclear factor of activated T cells (NFAT) family of transcription factors (Loh et al., 1996; Shibasaki et al., 1996; Wesselborg et al., 1996), which are required for IL-2 expression (Chow et al., 1999). Activated calcineurin is believed to dephosphorylate associated NFAT proteins, resulting in the unmasking of a nuclear localization signal and thus their rapid translocation to the nucleus (Rao et al., 1997; Shibasaki et al., 1996). It has subsequently been demonstrated that oscillating Ca^{2+} levels of a particular frequency and amplitude are associated with NFAT-dependent gene expression (Dolmetsch et al., 1997; Dolmetsch et al., 1998; Li et al., 1998). These oscillations may result in the periodic activation of calcineurin that is sufficient to maintain NFAT in a dephosphorylated state, and thereby located in the nucleus (Crabtree and Clipstone, 1994).

NFAT proteins transcriptionally activate genes in cooperation with other transcription factors, that are also activated in response to the ligation of antigen receptors or co-receptors. For IL-2 expression, these transcription factors include AP-1, nuclear factor κB, stimulatory protein-1 (SP-1) and cREL (Chen et al., 1998; Crabtree and Clipstone, 1994; McCaffrey et al., 1993; Schwartz, 1997). Therefore, gene expression in lymphocytes involves the convergence of numerous signaling pathways in which changes

in cytosolic Ca^{2+} levels are a critical component (Jacinto et al., 1998; Su et al., 1994; Timmerman et al., 1996; Woodrow et al., 1993).

SERCA3 and Lymphocyte Calcium Signaling

From the above discussion it is clear that Ca^{2+} signaling plays a prominent role in mediating responses of lymphocytes to antigen receptor stimulation. The Ca^{2+} signal is generated by both the release of Ca^{2+} from intracellular stores and the sustained influx of extracellular Ca^{2+}, and depends upon the coordinated action of numerous proteins. By maintaining the filling status of intracellular Ca^{2+} stores, SERCA pumps regulate the availability of Ca^{2+} for release, and the activation of Ca^{2+} influx through store-operated channels at the plasma membrane.

Such a role for SERCA activity in antigen receptor-induced Ca^{2+} signaling is supported by the results of numerous studies in which SERCA pumps were inhibited by thapsigargin. Thapsigargin specifically inhibits all forms of the SERCA Ca^{2+} pumps, resulting in an increase in $[Ca^{2+}]_i$ due to the leak of stored Ca^{2+} from the ER by a mechanism that is not well understood (Lytton et al., 1991; Thastrup et al., 1990). Thapsigargin treatment of Jurkat T cells produced a Ca^{2+} current that was indistinguishable from the current characteristic of CRAC channels, suggesting that SERCA proteins regulate the Ca^{2+} pools that mediate Ca^{2+} influx in response to antigen (Zweifach and Lewis, 1993). In rat thymocytes and a human $CD4^+$ T cell line, the elevated $[Ca^{2+}]_i$ induced following the depletion of thapsigargin-sensitive Ca^{2+} stores was not increased further in response to TCR activation, nor was an increase in $[Ca^{2+}]_i$ observed when the order in which these stimuli were applied was reversed (Gouy et al., 1990; Lewis and Cahalan, 1995), suggesting that SERCA proteins regulate Ca^{2+} pools that are mobilized upon TCR activation.

Additional studies have also demonstrated a role for SERCA proteins in regulating cellular responses in lymphoid cells. The inhibition of SERCA activity by thapsigargin was found to be sufficient to induce expression of the α-chain of the IL-2 receptor in human peripheral and Jurkat T cells (Sei and Reich, 1995), and in combination with PMA treatment to induce IL-2 expression in $CD8^+$ mouse T cell hybridoma cells (Negulescu et al., 1994). In addition, thapsigargin alone could stimulate the apoptotic death of immature rat thymocytes (Jiang et al., 1994). Therefore, ample experimental evidence suggests that SERCA proteins regulate intracellular Ca^{2+} stores associated with capacitative Ca^{2+} entry in lymphocytes, and as a consequence, play an important role in mediating cellular responses in these cells.

What is unclear, however, is the functional significance of the co-expression of SERCA3 and SERCA2b in lymphocytes. In endothelial and epithelial cells, where Ca^{2+} signaling is also critically important for cell function, mutation of *serca3* results in alterations in Ca^{2+}-mediated responses to cellular stimulation (Kao et al., 1999; Liu et al., 1997). SERCA3 possesses a lower affinity for Ca^{2+}, and has a faster rate of turnover than SERCA2b (Lytton et al., 1992). The high expression levels of SERCA3 in lymphoid cells, particularly in B cells and thymocytes where it predominates over SERCA2b, suggests a functional role for this isoform in regulating cytosolic Ca^{2+} levels, in a manner that is distinct from that of SERCA2b.

Additional support for this hypothesis has been obtained from recent studies by Launay et al., who showed that SERCA3 and SERCA2b expression is differentially regulated in Jurkat T cells activated by Ca^{2+} ionophore and PMA treatment (Launay et al., 1997). Western blot analysis revealed that SERCA3 protein levels were reduced by 40% after 12 hours of stimulation, and by 90% following 48 hours of stimulation. Conversely, SERCA2b expression levels increased slightly during this same time period. These results

demonstrate that Jurkat cells regulate the functional status of their intracellular Ca^{2+} stores, and suggest that SERCA3 and SERCA2b contribute to Ca^{2+} homeostasis in distinct ways during T cell activation (Launay et al., 1997). Decreases in SERCA3 may contribute to the maintenance of a sustained elevation of $[Ca^{2+}]_i$ that is required for cellular activation, since a reduction in the SERCA3-associated Ca^{2+} pool could stimulate a sustained degree of Ca^{2+} influx.

IV. Hypothesis and Objectives

The purpose of this research project was to gain a better understanding of the physiological role of SERCA3. Specifically, it was aimed at determining if SERCA3 expression is important for mediating antigen-receptor induced Ca^{2+} signaling and cellular activation. **Based on the findings summarized above, it was hypothesized that SERCA3 functions in maintaining the filling status of antigen receptor-associated Ca^{2+} stores, and is therefore involved in regulating the magnitude of Ca^{2+} release and entry in response to antigen receptor stimulation. Moreover, by regulating Ca^{2+} influx, it was hypothesized that SERCA3 activity contributes to T cell activation.**

This hypothesis was tested using splenocytes and thymocytes isolated from mice with an inactive gene for SERCA3 (Liu et al., 1997), or wild-type animals. The objectives of my research were as follows:

Objective 1: Determine the role of SERCA3 on the maturation of T cells in the thymus and the representation of B cells and T cell subsets in the spleen.

Objective 2: Assess SERCA2b expression levels in lymphocytes lacking SERCA3

Objective 3: Determine if SERCA3 has a functional role in mediating T cell activation in response to cellular stimulation.

Objective 4: Determine the role of SERCA3 in regulating kinetic changes in $[Ca^{2+}]_i$ following antigen receptor stimulation.

CHAPTER TWO: MATERIALS AND METHODS

I. Genotyping of mice

Litters resulting from crosses of mice heterozygous for the *serca3* mutation were genotyped by performing a polymerase chain reaction (PCR) on genomic DNA isolated from biopsied tails. The DNA was isolated by incubating tails overnight at 37°C in 400 µL of Tail Buffer (100 mM Tris (pH 8.5), 10 mM EDTA, 200 mM NaCl, 0.2% SDS), to which Proteinase K (Boehringer Mannheim) was added at a final concentration of 0.75 mg/mL. Resulting debris was removed by centrifugation at 13,000 x *g* for 3-4 minutes. The DNA was precipitated using 95-100% ethanol, and washed using 70% ethanol. The final DNA pellets were resuspended in 100 µL 10 mM Tris (pH 8.5), 1 mM EDTA. PCR was performed using three primers simultaneously, two specific for *serca3* and one specific for the neomycin resistance gene. The conditions of the reaction were set such that fragments of either 260 bp or 142 bp, corresponding to a disrupted gene or wild-type gene, respectively, were amplified (Liu et al., 1997). PCR products were separated using 5% acryl-bisacrylamide gel electrophoresis, and visualized by ethidium bromide staining.

II. Isolation of mouse splenocytes and thymocytes

Six to eight week old mice homozygous for the *serca3* deletion, or sex- and age-matched wild-type mice, were killed by cervical dislocation under non-sterile conditions, and their dissected spleens and thymi were transferred to petri dishes containing bicarbonate- and Hepes-buffered Hank's Balanced Salt Solution (HBSS) (Life Technologies). The tissues were subsequently transferred to a second dish of HBSS under sterile conditions, where they were homogenized using frosted microscope slides. For

experiments involving the kinetic analysis of $[Ca^{2+}]_i$ by flow cytometry, the homogenate was subsequently filtered through a 44 μM nylon mesh (Small Parts Inc.) in order to remove any traces of non-cellular material. In all cases, the homogenized cells were pelleted at 1,500 rpm (International Equipment Company, Rotor 215) at room temperature for 5 minutes. Erythrocytes in the splenocyte preparations were lysed by resuspending the cell pellet in a hypotonic solution of Tris-buffered ammonium chloride (17mM Tris, 144mM NH_4Cl, pH 7.2), and incubating at room temperature for 10 minutes with periodic mixing (Coligan et al., 1997). Thymocyte preparations were treated similarly if erythrocytes were present. In these instances, the cells of the other member of the experimental pair were treated identically. Following hemolysis, the cell preparations were washed twice in a large volume of HBSS. The final cell pellets was resuspended in 10 mL HBSS, and the number of live cells counted using Trypan Blue dye (0.22% (v/v) final) and a Hausman Hemocytometer.

III. Protein isolation and immunoblotting

Freshly isolated splenocytes and thymocytes were washed once in 5 mL PBS (PBS: 130 mM NaCl, 3 mM KCl, 8 mM Na_2HPO_4, 2 mM KH_2PO_4, pH 7.2) containing 0.5 M EDTA, resuspended in 1 mL PBS/EDTA, transferred to microcentrifuge tubes, and pelleted at 5,000 x *g* for 1 min. Cells were cooled on ice and subsequently lysed with 70- to 100 μL/10^7 cells ice-cold lysis buffer (25 mM Tris, 1% Triton X-100, 0.5% deoxycholate, 140 mM NaCl, 10 mM EDTA, pH 7.5), plus a freshly added tablet of a protease inhibitor cocktail (Boehringer Mannheim). Cells were incubated on ice for 30 minutes with periodic vortexing. The nuclear fraction was removed by centrifugation at 13,000 x *g* for 15 minutes in the cold room. Protein concentrations of cell lysates were determined by a Bradford dye binding assay using a BioRad Protein Assay Kit and bovine

gamma-globulin as standard. An equivalent volume of lysis buffer was included in the preparation of protein standards. Cell lysate corresponding to a desired quantity of protein was added to an equal volume of 4X SDS sample buffer, and then separated by SDS-PAGE using a 7.5% gel (Ausubel et al., 1997). The gel was subsequently electrophoretically transferred onto nitrocellulose membranes.

For immunoblotting, membranes were blocked for 1 hour in PBS containing 0.1% Tween20, 5% non-fat milk powder, and 1% BSA. Primary antibodies used for the detection of SERCA proteins and their working concentrations were as follows:

• N1	polyclonal serum; recognizes all SERCA isoforms (developed previously in our lab)	1:4000
• C4	polyclonal purified IgG; recognizes all SERCA isoforms (developed previously in our lab)	2 µg/mL
• PA1-910	polyclonal affinity purified; anti-SERCA3 (Affinity Bioreagents Inc.)	2 µg/mL
• 2A7-A1	monoclonal; anti-SERCA2 (Affinity Bioreagents Inc.)	8 µg/mL

In all cases, primary antibodies were diluted in PBS/0.1% Tween20/1% non-fat milk/0.2% BSA, and incubated with membranes for 1 hour. Membranes were then washed 4 times (5 minutes each) in 0.1% Tween20/ PBS. Primary antibodies were detected using horseradish peroxidase conjugated secondary antibodies (goat anti-mouse IgG or goat anti-rabbit IgG; Jackson Immnuochemicals) diluted 1:10,000 in 0.1% Tween-20/PBS, and incubated with blots for 30 minutes. Following 4 washes (5 minutes each), membranes

were incubated with Pierce Super Signal enhanced chemiluminescence solutions and the signal visualized using Kodak BioMax film.

For the subsequent analysis of actin expression, blots were washed twice (10 minutes each) in 0.1% Tween20/PBS to remove the chemiluminescent reagent, blocked again for 1 hour, and then probed with a monoclonal anti-actin antibody (Boehringer Mannheim) used at 0.1 μg/mL, following the same protocol as described above.

IV. *In vitro* stimulation of splenocytes and IL-2 assay

Freshly isolated splenocytes were resuspended at 2.5 x 10^3 viable cells/μL in complete RPMI medium (RPMI medium supplemented with 9% FBS, 90 U/mL penicillin and 90 μg/mL streptomycin) (all Life Technologies). 2.5 x 10^5 cells (100 μL) were then plated in 96-well dishes. 100 μL of treatment compound diluted in complete medium was subsequently added to each well of cells to obtain the desired final concentration in 200 μL total. Control wells received 100 μL of cell culture medium alone. The final concentrations of the compounds used to stimulate the cells were as follows:

- 10 μg/mL plate-bound anti-mouse CD3ε mAb

  Wells were pre-coated with anti-mouse CD3ε mAb by adding 50 μL of 10 μg/mL of antibody in Coating Buffer (50 mM Tris, 150 mM NaCl, pH 9.5) to each well, and incubating overnight at 4°C. Before cells were plated, the wells were washed twice with 5% FBS/RPMI to remove excess antibody.
- 10 μg/mL plate-bound anti-mouse CD3ε + 10 μg/mL soluble anti-mouse CD28 (Pharmingen)
- 5 μg/mL Conconavalin A (ConA) (Sigma)
- 10 nM PMA (Sigma) + 100 nM A23187 (Boehringer Mannheim)

- 10 nM PMA alone
- 100 nM A23187 alone

Nine wells per treatment condition were used. The cells were cultured in a humidified 37°C incubator with 5% CO_2 for 24 hours, after which time the supernatants were collected. Supernatants from three wells were pooled, therefore triplicate samples were obtained for each treatment condition. The harvested supernatants were stored at -80°C.

The IL-2 concentration in the harvested supernatants was determined using a sandwich Enzyme-linked Immunosorbent Assay (ELISA) kit (Genzyme). Microtitration plate wells were coated with 5 µg/mL of anti-mouse IL-2 antibody diluted in Coating Buffer (100 mM carbonate, pH 9.5), and incubated overnight at 4°C. Following 3 washes in 0.05% Tween-20/PBS, wells were blocked with 4% BSA/PBS for 2 hours at 37°C. The blocking solution was then decanted and 100 µL of cell culture supernatant, or 0- to 1000 pg/mL of recombinant mouse IL-2 standard serially diluted in complete cell culture medium, were added to each well, in duplicate, and incubated for 1 hour at 37°C. Following the removal of unbound IL-2 by washing, the wells were incubated with 0.2 µg/mL of a biotinylated anti-mouse IL-2 antibody diluted in 0.05% Tween-20/1% BSA in PBS, for 1 hour at 37°C. Following 5 washes, antibody-antigen complexes were detected by adding a 1:1200 dilution of horseradish peroxidase-conjugated strepavidin to each well, and incubating for 15 minutes at 37°C. Unbound strepavidin was removed by washing, wells were subsequently reacted with a prepared substrate solution of tetramethylbenzidine and hydrogen peroxide (Sigma). The reactions were stopped after 20 minutes with the addition of 2N H_2SO_4.

The optical density of each well was determined using a microplate reader set at 450 nm. To correct for optical imperfections in the plates, absorbance readings at 570 nm were automatically subtracted from those made at 450 nm. The calculated mean absorbance of samples and standards from duplicate wells were corrected by subtracting the average absorbance obtained with the 0 pg/mL standard. The IL-2 concentrations of the samples were determined from the standard curves generated.

V. Cell viability assay

Propidium iodide (PI) intercalation and flow cytometry (Sasaki et al., 1987) were used to assess the viability of $CD4^+$ and $CD3\varepsilon^+$ splenic T cells at the time of isolation, and following 24 hours of stimulation. 2.5 x 10^5 viable splenocytes were plated in 96-well dishes in quadruplicate, and cultured in complete medium alone, or stimulated with either 10 nM PMA plus 100 nM A23187 or 10 µg/mL plate-bound anti-CD3ε plus 10 µg/mL soluble anti-CD28 mAbs. The cells were harvested following 24 hours of culturing in a 37°C/5% CO_2 incubator. Pooled samples were stained with either FITC-anti-CD4, FITC-anti-CD3ε, or an FITC-conjugated isotype control mAbs (see section VII. below, for the staining protocol). At the time of analysis, 5 µg/mL PI was added to the cell samples. The percentage of viable cells, which were cells excluded from PI staining, was calculated based on the percentage of stained cells, after correcting for background fluorescence registered before the addition of PI.

VI. Flow Cytometry

The method of flow cytometry was used in many of the experiments described below, because it provides a powerful and convenient way of simultaneously examining different parameters and cell types within a mixed population of cells, thus making the

purification of a desired subpopulation unnecessary. For the purposes of this thesis, a brief description of flow cytometry, and how it was used, is presented below.

Flow cytometry describes the measurement of fluorescence and light scattering emitted by whole cells present within a flowing stream of solution (Takahashi et al., 1999). These measurements are made using a flow cytometer. When a tube of cells in suspension is placed in the machine, a single-file stream of cells is hydrodynamically forced into the centre of a surrounding sheath of fluid, and directed into the path of a laser beam (Takahashi et al., 1999). The beam of light is used for the excitation of a fluorophore, or for the analysis of cell size and structure by light scattering (Takahashi et al., 1999). The flow cytometer used in the experiments described in this thesis is a FACScan™ (Becton Dickinson), equipped with a single argon-ion laser light source that emits an excitation wavelength of 488 nm. This flow cytometer also possesses two light scattering detectors that monitor light scattered in the forward direction and at right angles when the laser beam hits a cell. The degree of light scattered in the forward direction is proportional to cell size, whereas the degree of side scatter is proportional to cell granularity. The FACScan is also equipped with three fluorescence detectors; the fluorescence 1 (FL1), FL-2 and FL-3 detectors, which detect light of 530 nm, 575 nm, and 675 nm, respectively.

Specific cell types of interest within a mixed population of cells can be selected, or "gated", for examination based on their light scattering properties, and by using fluorophore-conjugated monoclonal antibodies (mAbs) directed against cell-type specific surface antigens. In the experiments outlined below, fluorophore-conjugated Abs were used to identify and examine B cells of the spleen, and subpopulations of thymic and splenic T cells. These fluorophores included Fluorescein Isothiocyanate (FITC), which has a fluorescence emission maximum of ~520 nm when excited by 488 nm light, R-phycoerythrin (PE), which has an emission maximum of ~576 nm, and Peridinin

Chlorophyll Protein (PerCP), which has an emission spectrum that peaks at ~677 nm. Other fluorophores used included the calcium indicating dye, fluo-3, and propidium iodide (PI). When excited with 488 nm light, the emission maxima of fluo-3 and PI are ~526 nm and ~600 nm, respectively. Therefore, the fluorescence emissions of FITC and Fluo-3 were captured by the FL1 detector, PE and PI fluorescence were registered by the FL-2 detector, and PerCP fluorescence was captured by the FL-3 detector. Fluorescence and light scattering data were digitalized and analyzed by computer using CellQuest software (Becton Dickinson).

In order to examine multiple parameters simultaneously, different fluorophores, specific for each parameter of interest and possessing different emission maxima, are used in the same cell sample. A potential drawback of multi-colour analysis is that overlap exists in the emission spectra of some fluorophores, which may result in the fluorescence signal emanating from one fluorophore being registered by an inappropriate detector. This could potentially lead to the misidentification of cells as positive for a cell surface antigen, and the attainment of artifactual histogram shapes. The effects of spectral overlap are removed by a process called compensation, which involves the electronic subtraction of unwanted signal from an inappropriate detector (Givan, 1992). For the experiments described in this thesis, compensation was initially set by examining cell samples stained with each fluorophore individually, and was then optimized using a cell sample in which both fluorophores were present (Rijkers et al., 1990).

VII. Surface antigen staining and two-colour analysis by flow cytometry

1 x 10^6 freshly isolated viable splenocytes or thymocytes were aliquoted into 4 mL centrifuge tubes. The cells were washed twice, resuspended in 50 µL FACS buffer (1% FBS, 0.1% sodium azide in PBS, and subsequently stained with combinations of the

following mAbs: FITC-anti-CD3ε, FITC- or PE-anti-CD4, PE-anti-CD8α, and PerCP-anti-B220 (all Pharminagen). In addition, FITC-anti hamster IgG or PE-conjugated anti-rat IgG mAbs (both Immunotech) were used as isotype-matched negative controls for non-specific binding. As suggested by the suppliers, thymocytes were cultured at 37°C for 2-4 hours before staining with anti-CD3ε to enhance the ability of the antibody to detect CD3ε. All mAbs were used at 1 $\mu g/10^6$ cells as recommended. Following 20 minutes of incubation at room temperature in the dark, the cells were washed twice and resuspended at a concentration of 2 x 10^6 cells/mL in FACS buffer, or 2% formaldehyde/PBS if not analyzed immediately. Single colour or two-colour analyses were performed using flow cytometry. Lymphocytes were gated based on their light scattering properties. Within this gate, cells were identified as being positive for a surface antigen if their fluorescence emission was above the background level, which was determined using unstained cells or isotype control samples, and was set at a value that routinely gave <2% positive cells in these control samples.

VIII. Kinetic analysis of changes in $[Ca^{2+}]_i$

Fluo-3 loading and surface antigen staining

The Ca^{2+} indicating dye, fluo-3, is considered one of the most suitable Ca^{2+} indicators for use in flow cytometry (Takahashi et al., 1999), based on a number of its properties. Its absorption spectrum closely matches the emission output (488 nm) of the excitation light source in FACScan flow cytometers. In addition, it undergoes a 40- to 100-fold increase in fluorescence intensity upon binding Ca^{2+} (Kao, 1994; Minta et al., 1989), therefore sufficiently amplifying the Ca^{2+} signal for detection (Takahashi et al., 1999).

For the loading of cells with dye, a protocol based on those previously described by

others (Thomis et al., 1997; Vandenberghe and Ceuppens, 1990) was used with some modifications. 2 x 10^7 freshly isolated, viable splenocytes or thymocytes were resuspended at 1 x 10^7 cells/mL in HBSS containing 4 μM of the acetoxymethyl ester form of fluo-3 plus 0.01% Pluronic F-127 (both Molecular Probes), and incubated in the dark in a 37°C water bath for 20 minutes with periodic mixing. The cells were subsequently washed in 50 mL of HBSS without fluo-3, followed by a second wash in 50 mL of Hepes-Buffered Saline solution (HBS: 137 mM NaCl, 5 mM KCl, 1 mM Na_2HPO_4, 5 mM dextrose, 0.1% w/v bovine serum albumin, 1mM $CaCl_2$, 0.5 mM $MgCl_2$, 25 mM Hepes, pH 7.4). The final pellet was resuspended at 2 x 10^6 cells/mL in HBS, and 1 mL (2 x 10^6 cells) was transferred to 4 mL centrifuge tubes. The cells were then pelleted and resuspended in 100 μL HBS in preparation for surface antigen staining.

For experiments aimed at examining T cell responses, $CD4^+$ or $CD8^+$ T cells were identified by staining with PE-conjugated anti-CD4 or CD8α mAbs, respectively (Pharmingen). In addition, cells were simultaneously incubated with an unconjugated anti-CD3ε mAb (Pharmingen). Splenic B cells were identified by staining $CD4^+$ and $CD8^+$ T cells simultaneously, and then gating on the unstained population. Background levels of PE fluorescence were set using cell samples labeled with a PE-conjugated anti-rat IgG mAb (Immunotech). In all cases, 1 μg of mAb was used per 10^6 cells. The cells were incubated at room temperature in the dark for 20 minutes. They were subsequently washed three times, and the final cell pellets were resuspended in HBS at 1.5 x 10^6 cells/mL, a concentration that initial experiments had revealed to be satisfactory for the kinetic analysis of fluo-3 fluorescence. The cell samples were kept at room temperature until analyzed.

For experiments aimed at examining the Ca^{2+} influx pathway, an identical dye loading and surface staining protocol was used with three exceptions; (i) cell samples contained 4 x 10^6 cells, (ii) cells were not pre-labeled with an anti-CD3ε mAb, and (iii)

HBS prepared without $CaCl_2$ was used for the final three washes and for the resuspension of cell pellets.

Cellular stimulation and kinetic analysis of fluo-3 fluorescence

For the kinetic analysis of changes in $[Ca^{2+}]_i$, cells were continuously acquired and measurements of fluo-3 fluorescence were accumulated in time intervals of one second. For each experiment, antigen receptor stimulation was induced after a 30 second baseline measure of fluo-3 fluorescence intensity. Splenic T cells and thymocytes were stimulated by cross-linking anti-CD3ε mAbs with 5 µg/mL or 10 µg/mL, respectively, of a goat anti-hamster IgG secondary antibody (Pharmingen). B cells were stimulated by cross-linking surface IgG with 10 µg/mL F(ab')2 rabbit anti-mouse IgG (Zymed Laboratories, Inc.). Data was acquired for an additional ten minutes following the addition of Abs. At the end of each experiment, a calibration procedure was performed in order that arbitrary fluorescence values could be converted to measures of $[Ca^{2+}]_i$ (see below). The calibration involved sequentially forcing the fluo-3 dye present within cells into two states; either saturated with Ca^{2+} or Ca^{2+}-free (Grynkiewicz et al., 1985), using a protocol based on those previously described by others (Hesketh et al., 1983; Kao, 1994). Intracellular Ca^{2+} was increased to saturating levels by adding the Ca^{2+} ionophore, A23187 (Boehringer Mannheim Biochemicals), to a final concentration of 10 µM, and data was collected for 5 minutes. $MnCl_2$ was subsequently added at a final concentration of 3 mM in order to displace Ca^{2+} from the dye, and incubated with the cells for 10 minutes. The resultant fluo-3 fluorescence intensity was then measured for an additional 3 minutes.

Experiments essentially identical to those just described were performed on splenocytes resuspended in nominally Ca^{2+}-free HBS, with the following exceptions. Fluo-3 fluorescence measurements were accumulated over time intervals of two seconds. At the

time of the experiment, BAPTA was added to the cells at a final concentration of 2 mM in order to chelate Ca^{2+} to trace levels. Following a 30 second baseline measure of fluo-3 fluorescence, 5 μg/mL anti-CD3ε mAb and 1 μM thapsigargin was added to the cells. The antibody was subsequently cross-linked with 50 μg/mL goat anti-hamster IgG 60 seconds later. Following 8 minutes of data acquisition, A23187 was added to the cells at a final concentration of 100 nM. Fluo-3 fluorescence intensity was monitored for another 8 minutes. This was followed by the addition of 3 mM (final concentration) $CaCl_2$, and data acquisition was resumed for an additional 5 minutes. At the end of each experiment, a calibration procedure was performed using 10 μM A23187 and 3 mM $MnCl_2$, as described above.

Because no gates were imposed on the cell samples before the initiation of data collection, the acquired data represented changes in fluo-3 fluorescence intensity from all cell types capable of responding to the applied stimulus. At the completion of an experiment, the response of specific subpopulations of cells to antigen receptor stimulation was determined by first gating on lymphocytes based on their light scattering properties, and then examining the fluo-3 kinetic profile of desired cells based on whether they were positive or negative for a given surface antigen. The fluo-3 fluorescence data acquired over two time intervals were then converted to a measure of median fluorescence. All of these analyses were performed using FlowJo software (Treestar).

Calculation of $[Ca^{2+}]_i$

The median fluorescence intensity values obtained for each time interval were converted to a median measure of $[Ca^{2+}]_i$ using the following formula (Grynkiewicz et al., 1985):

$$[Ca^{2+}] = K_d \frac{(F - F_{min})}{(F_{max} - F)}$$

In this equation, K_d represents the effective dissociation constant of fluo-3 for Ca^{2+}, and is equal to 400 nM based on *in situ* and *in vitro* calibrations performed by others (Minta et al., 1989; Schnetkamp et al., 1991). F represents the median fluo-3 fluorescence of the experimental samples. F_{max} represents the fluorescence intensity of fluo-3 when saturated with Ca^{2+}, and for the experiments described here, was made equal to the mean fluorescence observed following the addition of 10 μM A23187 to the cells. F_{min} represents the fluorescence of fluo-3 in its metal-free state. This value was calculated based on the F_{max} value, and the mean fluo-3 fluorescence intensity observed in the presence of 3 mM $MnCl_2$, termed F_{Mn}. The difference between the fluorescence intensities corresponding to F_{Mn} and F_{min} is one-fifth the difference between F_{max} and F_{min} (ie. $F_{Mn} - F_{min} = 1/5\ (F_{max} - F_{min})$) (Vandenberghe and Ceuppens, 1990). Rearranging the equation, F_{min} was calculated as follows:

$$F_{min} = (1.25 \times F_{Mn} - 0.25 \times F_{max})$$

Calculation of half-time ($t_{1/2}$) of decay

Rate constants for the decay portion of kinetic curves were derived from a computerized least squares minimization fit of the data to exponential equations using MacCurveFit software (Kevin Raner Software; www.home.aone.net/krs). The half-time ($t_{1/2}$) of the decay was then calculated by dividing the natural log of one-half by the derived rate constant and changing the sign (ie. $t_{1/2} = -(\ln 0.5/b)$; where b represents the rate constant).

Some of the curves were best fit to double exponential equations, thus producing two rate constants corresponding to a fast and a slow component, with the fast component making the greatest contribution to the transient. The *serca3*$^{(-/-)}$ and *serca3*$^{(+/+)}$ experimental pairs consistently differed with respect to the fast component of the curve, but not the slow component. Therefore, in order to compare members of an experimental pair the rate constants for the slow component of the curves were made the same (usually this value correspond to that of the wild-type cell sample), the curves were re-fit, and a new $t_{1/2}$ of the decay was calculated based on the rate constant obtained for the fast component of each curve.

IX. Statistical analysis of data

Tests of statistical significance were performed using pair-wise t-tests of the means. Data in the form of percentages or fractions were transformed by taking the inverse sine of the square root to obtain samples with normal distributions (Ausubel et al., 1997). The transformed data were then compared using pair-wise t-tests.

CHAPTER THREE: RESULTS

I. Characterization of *serca3*$^{(-/-)}$ splenocytes and thymocytes

Expression patterns of B cells and T cells in *serca3*$^{(-/-)}$ mice

During lymphocyte maturation, the ligation of the BCR and TCR can induce either the death or differentiation of immature B cells and T cells, respectively. As described in Chapter 1, the stages of maturation of T cells in the thymus can be defined by the expression patterns of CD4 and CD8 on the surface of these cells. Cells double positive for CD4 and CD8 undergo intense selection, resulting in the death of self-reactive cells and the survival of cells capable of recognizing foreign antigen. Changes in intracellular Ca^{2+} levels have been shown to be an important component of the signaling pathways that mediate these responses (Mariathasan et al., 1998; Nakayama et al., 1992). For example, elevations in $[Ca^{2+}]_i$ are associated with thymocytes that have contacted self-antigen, and are undergoing negative selection (Nakayama et al., 1992). SERCA3 is abundantly expressed in lymphoid cells, particularly in maturing thymocytes (Wu et al., 1995). Given the role of antigen receptor-induced Ca^{2+} signaling pathways for the maturation of B cells and T cells, initial experiments were aimed at determining if SERCA3 has a role in the maturation of these cell types.

The expression of B cells and T cells in the spleen, and the distribution of subpopulations of T cells in both the spleen and thymus of *serca3*$^{(-/-)}$ mice were compared with those of *serca3*$^{(+/+)}$ mice, using flow cytometry and fluorophore-conjugated antibodies directed against cell-specific surface markers. B cells were identified using an antibody against the surface molecule B220 (CD45R), which is a membrane-bound tyrosine

phosphastase expressed on all mature B cells (Abbas et al., 1997). T cells were identified by staining the CD3ε subunit of the TCR. The distribution of $CD4^+$ and $CD8^+$ T cells in the spleen and thymus were determined using antibodies specific for these two surface proteins.

Beginning with a general examination of the thymocytes of both genotypes, it is evident that these cells could be divided into three predominant groups based on their expression levels of CD3ε (Figure 4), with about 30% falling in the background range (fluorescence values less than 10), a small fraction expressing very high levels of CD3ε (fluorescence values above 100), and the majority expressing low levels of the surface protein (fluorescence levels between 10 and 100). As shown in Figure 5 and summarized in Table 1, more than 95% of the isolated thymocytes were positive for either CD4 or CD8, and 80-85% were positive for both. Double positive cells undergo intense selection, with only a small percentage surviving and maturing into single positive cells (10-15% CD4 single positive and 3% CD8 single positive; Figure 5 and Table 1). Two colour analysis of CD3ε and CD4 (or CD8) expression showed that CD4 (or CD8) positive cells expressed a varied degree of CD3ε on their cell surface (Figure 5; Table 1). Therefore, the vast majority of mouse thymocytes were double positive for CD4 and CD8, and about 60% of them expressed low levels of CD3ε (Table 1). Interestingly, as shown in Figure 5, the group of cells expressing the highest levels of CD3ε were predominately $CD4^+$ single positive thymocytes.

Comparison of the thymocytes isolated from SERCA3-deficient and wild-type control mice revealed that the disruption of *serca3* did not affect the percentage of immature and maturing T cells in the thymus, as determined by the surface expression of CD4 and CD8 (Figure 5 and Table 2). In addition, the expression levels of CD4 and CD8, as well as

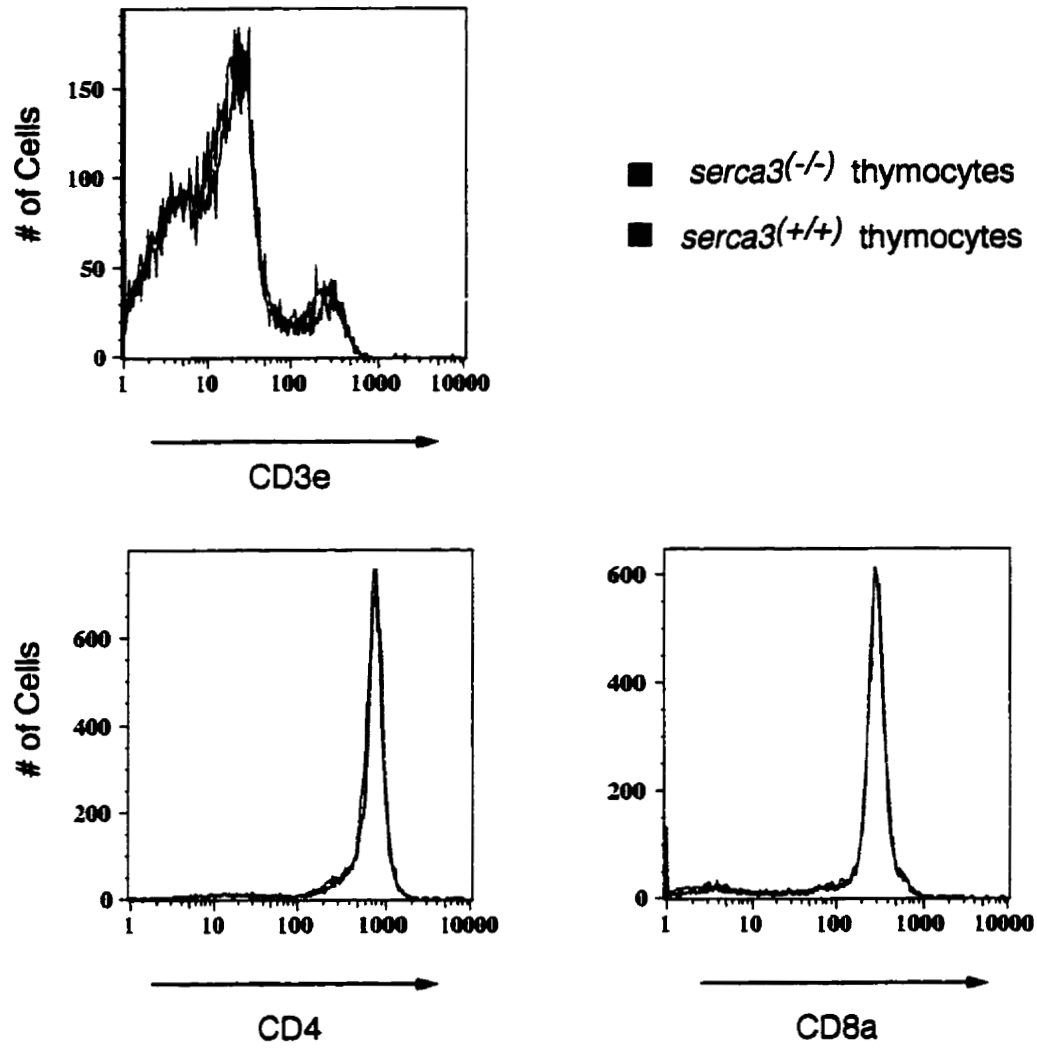

Fig. 4. **Expression levels of surface proteins on thymocytes isolated from wild-type and SERCA3-deficient mice.** Superimposed histograms are shown illustrating the fluorescence intensity of wild-type (■) and SERCA3-deficient (■) cells stained with fluorophore-conjugated antibodies to the indicated lymphocyte surface proteins. Cell samples were analyzed by flow cytometry, as described in Materials and Methods. A representative result from two experiments is shown.

Fig. 5. **Fluorescence-activated cell sorting analysis of thymocytes isolated from wild-type and SERCA3-deficient mice.** Dot plots of the co-expression of the indicated T cell surface proteins as determined by two-colour flow cytometric analysis using fluorophore-conjugated antibodies, are shown. Representative results from two experiments are presented. The axes indicate increasing fluorescence intensity. The gates (horizontal and vertical lines) defining positive versus negative staining were based on the analysis of similar cells labelled either with isotype control antibody, or without antibody. The percentages of cells stained by one, both, or neither, primary antibody are indicated in the appropriate quadrants of the graphs.

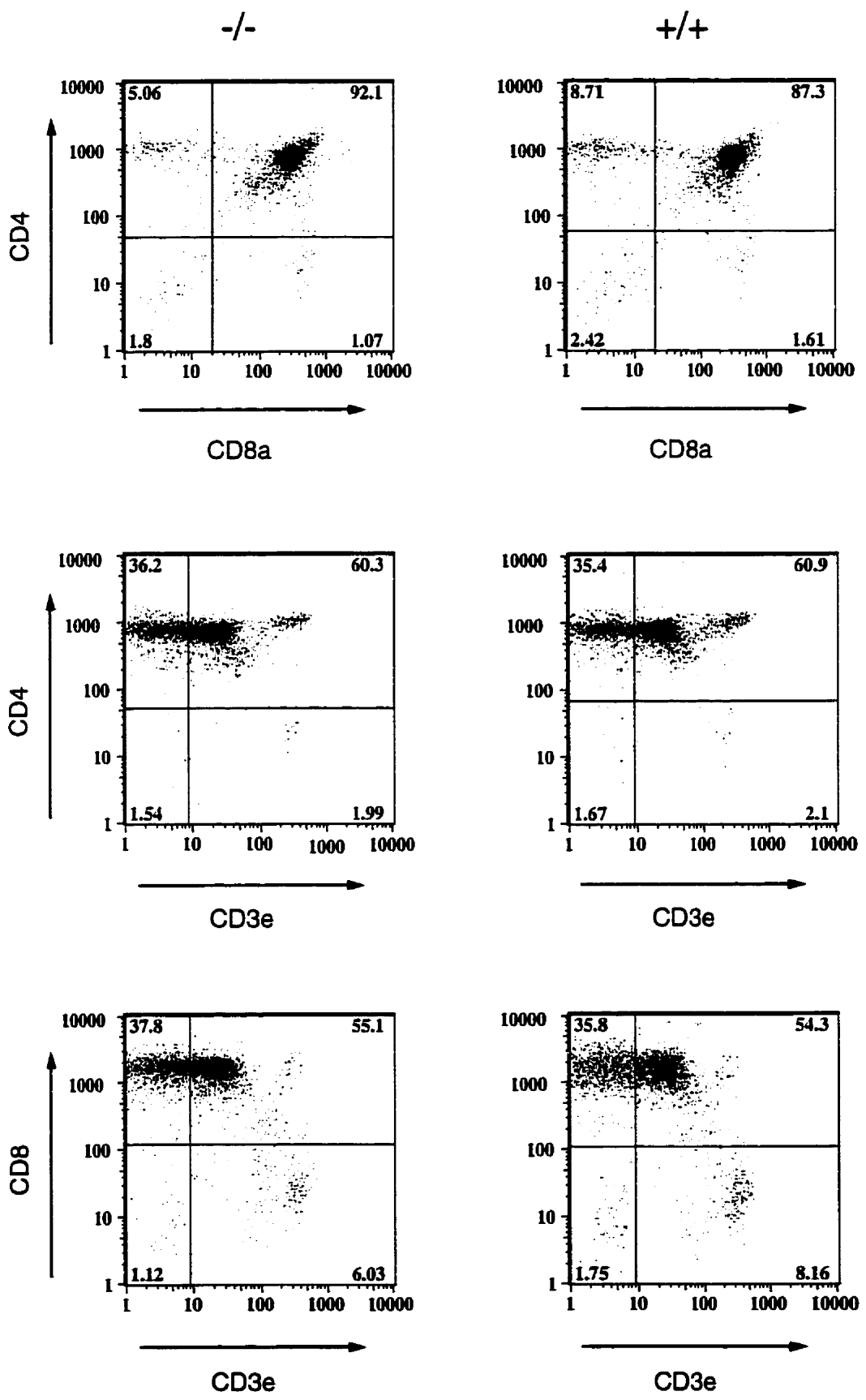
-/-
+/+
CD4
CD8a
5.06
92.1
1.8
1.07
8.71
87.3
2.42
1.61
CD4
CD3e
36.2
60.3
1.54
1.99
35.4
60.9
1.67
2.1
CD8
CD3e
37.8
55.1
1.12
6.03
35.8
54.3
1.75
8.16
1
10
100
1000
10000

Table 1.

Summary of the percent distribution of the indicated surface markers on thymocytes isolated from wild-type (WT) and SERCA3-deficient (KO) mice.

Surface protein	WT	KO
$CD4^+CD8^-$	7, 16	4, 23
$CD4^+CD8^+$	88, 79	93, 69
$CD4^-CD8$-	2, 1	2, 3
$CD4^-CD8^+$	2, 4	2, 5
$CD4^+CD3^-$	36, 42	38, 44
$CD4^+CD3^+$	60, 55	58, 52
$CD4^-CD3^-$	2, 0.4	2, 2
$CD4^-CD3^+$	2, 2	2, 2
$CD8^+CD3^-$	37, 27	39, 31
$CD8^+CD3^+$	54, 47	54, 45
$CD8^-CD3^-$	2, 2	1, 5
$CD8^-CD3^+$	8, 24	6, 18

Values were determined by performing two-colour flow cytometric analysis of cells stained with antibodies to the indicated surface proteins. The individual percentages for two independent experiments are shown.

Table 2.

Summary of the percent representation of surface markers on thymocytes and splenocytes isolated from wild-type (WT) and SERCA3-deficient (KO) mice.

Thymocytes

Surface marker	WT	KO
CD3ε	63, 56	61, 58
CD4	96, 95	97, 94
CD8α	91, 82	94, 75

Splenocytes

Surface marker	WT	KO	n
CD3ε	52 ± 3	49 ± 3	7
CD4	26 ± 2	25 ± 1	10
CD8α	16 ±2	15 ± 2	6
B220	43 ± 6	42 ± 5	4

Values were determined by flow cytometric analysis of cells stained with fluorphore-conjugated antibodies to the indicated surface proteins. Values shown for splenocyte samples are the mean percentages of cells ± SEM for the indicated number of independent experiments (n). For thymocytes, the individual percentages for two independent experiments are shown.

those of CD3ε, on the cell surface did not differ between the two genotypes (Figure 4). Finally, the percentage distribution of CD4 or CD8 positive thymocytes expressing CD3ε did not differ between SERCA3-deficient and wild-type animals (Figure 5 and Table 1). Therefore, based on the expression patterns of these cell surface markers, which identify thymocytes at different stages of development, it can be concluded that SERCA3 activity is not required for T cell maturation in the mouse thymus.

Lymphocytes migrate from their primary sites of maturation (thymus for T cells, and bone marrow for B cells) to the periphery, where they are exposed to antigen. Antigen receptor stimulates increases in intracellular Ca^{2+} levels, leading to cellular responses including proliferation, and in some instances, cell death (Crabtree and Clipstone, 1994). From the results obtained for splenocytes of both genotypes, it can be seen that B cells ($B220^+$) and T cells ($CD3\varepsilon^+$) were roughly equally represented, and together comprised 80-91% of the cells isolated from the spleen (Figure 6; Table 2). Similar results were observed when the percentage of T cells positive for both CD4 and CD8 were compared to $B220^+$ B cells (Figure 6 and Table 3). This is not surprising since virtually all $CD4^+$ and $CD8^+$ splenic T cells were also positive for CD3ε (Figure 7 and Table 3). Unlike in thymocytes, CD3ε expression on splenocytes was uniformly high (Figure 8), and $CD4^+$ and $CD8^+$ cells expressed similar levels of CD3ε (Figure 7). It was evident that expression of CD4 and CD8 proteins on splenocytes was mutually exclusive (Figure 7 and Table 3) and that $CD4^+$ cells were more abundant than $CD8^+$ cells (~25% $CD4^+$ vs. ~16% $CD8^+$) (Table 2).

Comparing the expression and representation of these surface markers on SERCA3-deficient and wild-type cells, it was found that the mutation of *serca3* does not alter the expression levels of CD3ε, CD4, CD8 or B220 on the cell surface. Similarly, the percentage of splenocytes expressing these surface proteins were not found to differ

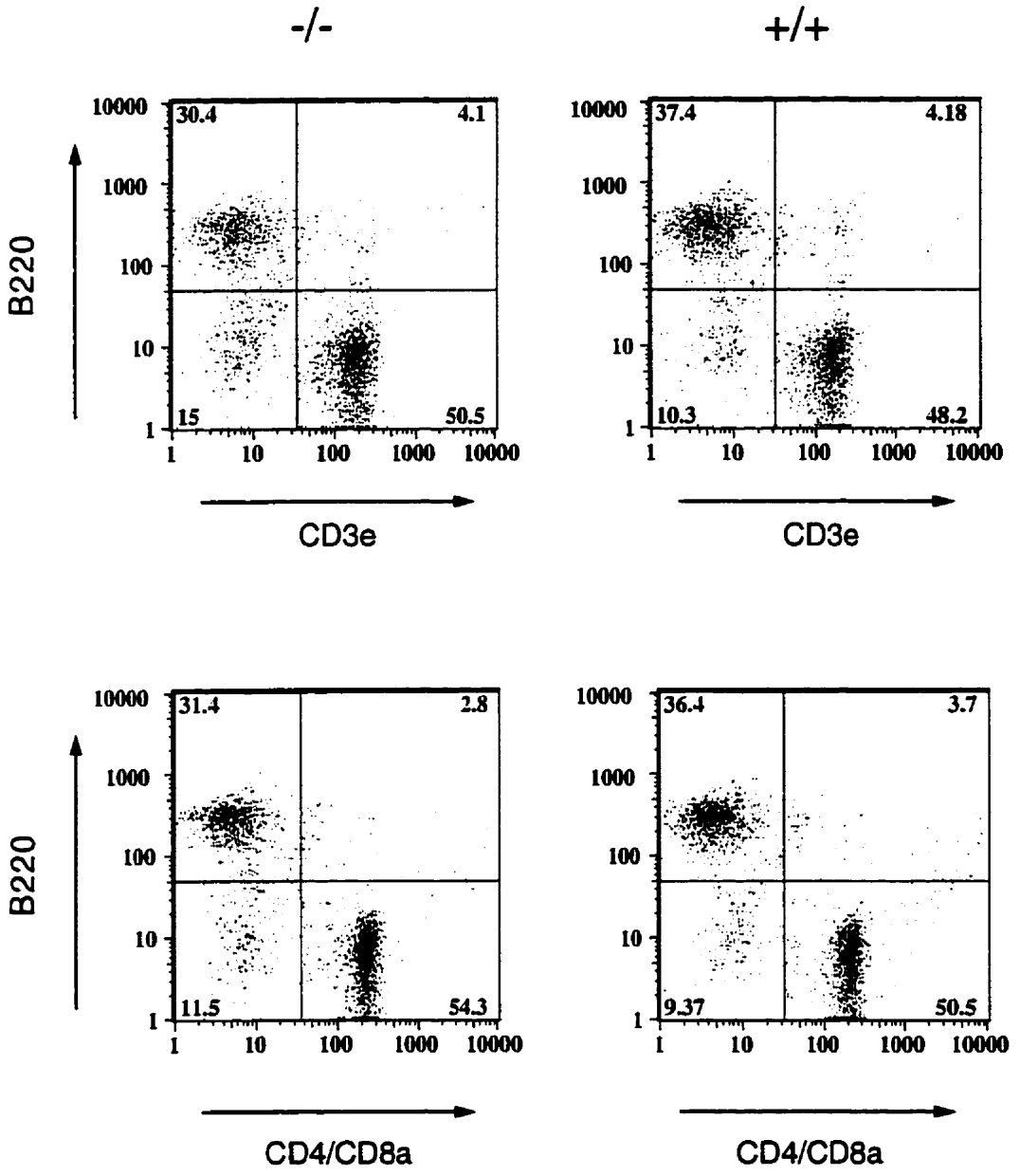

Fig. 6. **Fluorescence-activated cell sorting analysis of splenocytes isolated from wild-type and SERCA3-deficient mice for B and T cell surface markers.** Co-expression of the indicated proteins on splenocytes was performed using two-colour flow cytometric analysis, as described in Materials and Methods. See legend to Figure 5 for further details. Representative results from three similar experiments are presented.

Table 3.

Summary of percent representation of surface markers on splenocytes isolated from wild-type (WT) and SERCA3-deficient (KO) mice.

Surface protein	WT	KO	n
$B220^+CD3^-$	32 ± 5	38 ± 5	3
$B220^+CD3^+$	3 ± 1	4 ± 2	3
$B220^-CD3^-$	8 ± 2	8 ± 2	3
$B220^-CD3^+$	48 ± 8	47 ± 4	3
$B220^+CD4^-CD8^-$	33 ± 6	36 ± 5	3
$B220^+CD4^+CD8^+$	3 ± 1	2 ± 0.2	3
$B220^-CD4^-CD8^-$	8 ± 2	9 ± 2	3
$B220^-CD4^+CD8^+$	56 ± 5	48 ± 5	3

Surface protein	WT	KO	n
$CD4^+CD3^-$	0.4, 0.7	0.4, 2	2
$CD4^+CD3^+$	20, 28	25, 24	2
$CD4^-CD3^-$	53, 49	47, 56	2
$CD4^-CD3^+$	27, 22	22, 18	2
$CD8^+CD3^-$	1	4	1
$CD8^+CD3^+$	15	17	1
$CD8^-CD3^-$	53	55	1
$CD8^-CD3^+$	31	23	1
$CD4^+CD8^-$	22, 31	26, 26	2
$CD4^+CD8^+$	0.7, 0.6	1, 2	2
CD4-CD8-	56, 52	55, 55	2
$CD4^-CD8^+$	22, 16	18, 17	2

Values were determined by performing two-colour flow cytometric analysis of cells stained with antibodies to the indicated surface proteins. Either individual values or mean percentages ± SEM for the indicated number of experiments (n) are shown.

Fig. 7. **Fluorescence-activated cell sorting analysis of T cell markers on splenocytes isolated from wild-type and SERCA3-deficient mice.** Dots plots are shown of two-colour flow cytometric analysis of isolated splenocytes doubly-labelled with fluorophore-conjugated antibodies to the indicated surface markers. See legend to Figure 5 for further details. Representative result from one to two experiments are shown.

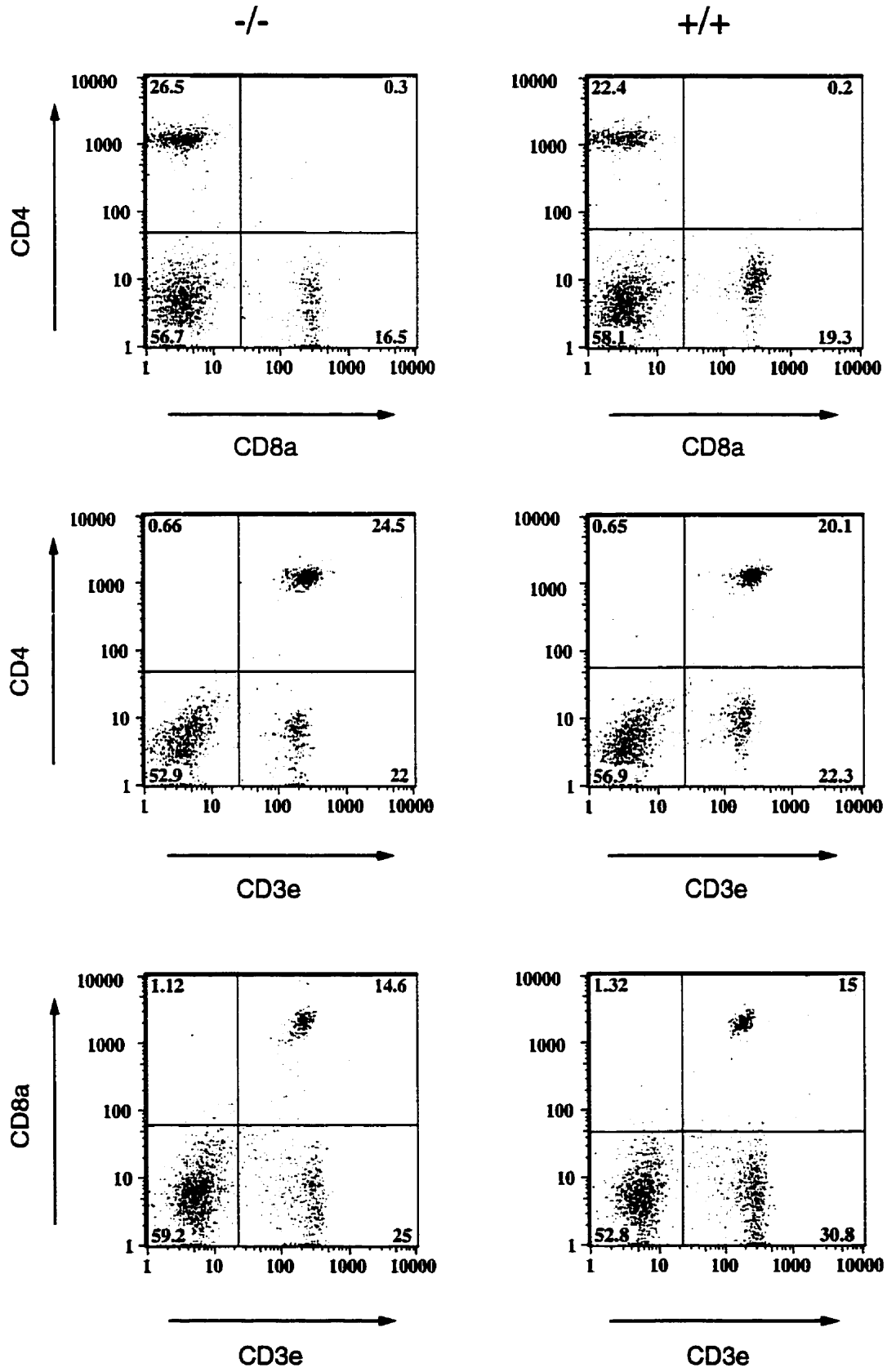
-/-
+/+
CD4
CD8a
26.5
0.3
56.7
16.5
22.4
0.2
58.1
19.3
CD4
CD3e
0.66
24.5
52.9
22
0.65
20.1
56.9
22.3
CD8a
CD3e
1.12
14.6
59.2
25
1.32
15
52.8
30.8
1
10
100
1000
10000

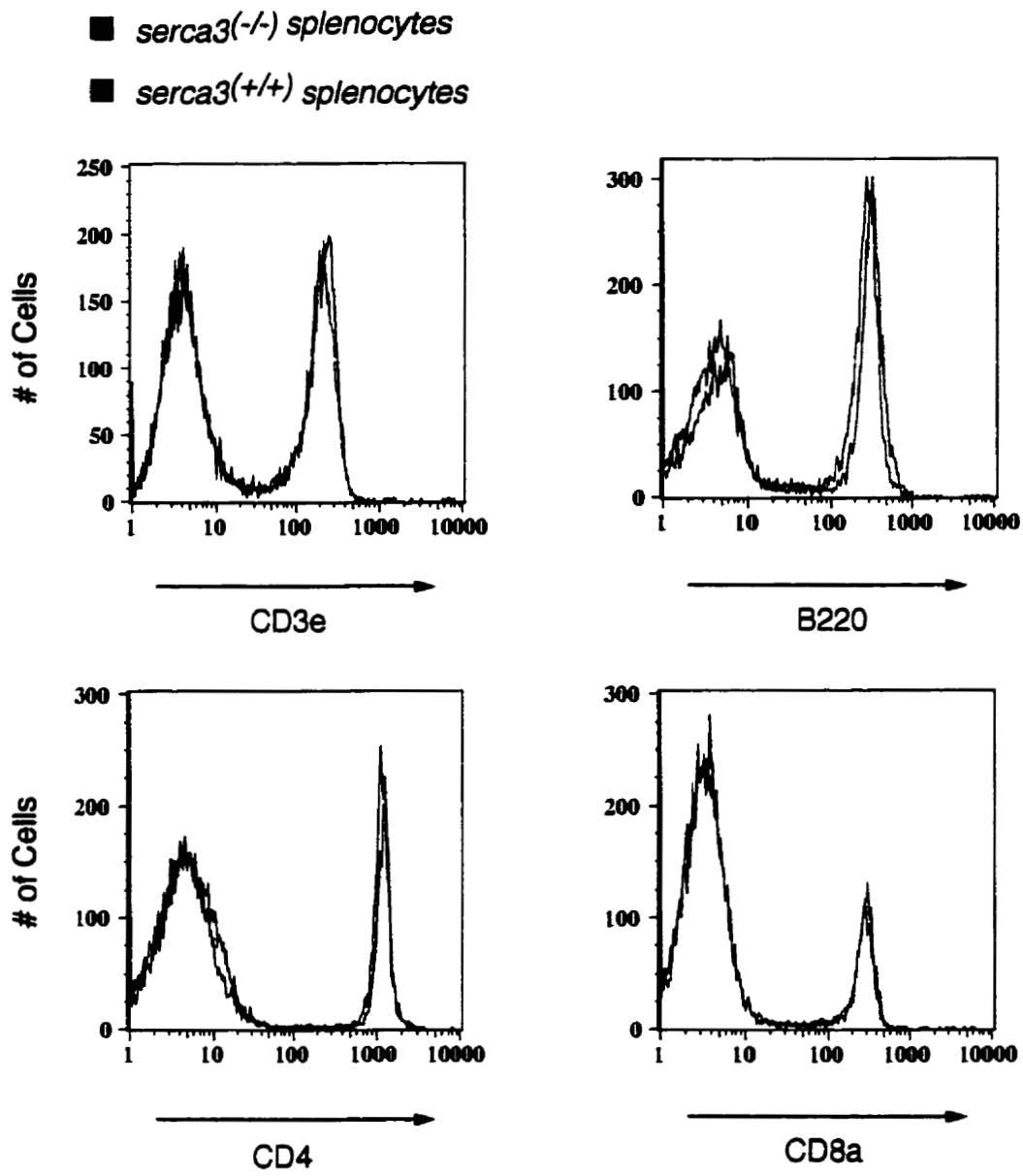

Fig. 8. **Expression levels of surface proteins on splenocytes isolated from *serca3* mutant and wild-type mice.** Superimposed histograms are shown, illustrating the fluorescence intensity of wild-type (■) and SERCA3-deficient (■) cells stained with fluorophore-conjugated antibodies to the indicated B and T cell markers, and detected using flow cytometry. In each graph, the cell population with a fluorescence level of less than ~10 corresponds to the background fluorescence observed for cells not stained with primary antibody, as determined by the analysis of similar cells with an isotype control antibody or without antibody.

between the two genotypes (Table 2), revealing that the lack of SERCA3 expression does not affect the representation of B cells and T cell subtypes in the mouse spleen.

Confirmation of lack of SERCA3 expression in *serca3*$^{(-/-)}$ lymphocytes

Previously published results of Northern blot analysis of total mRNA isolated from gene-targeted mice revealed a *serca3* message that was shown to possess a 28 codon deletion and an intact reading frame (Liu et al., 1997). Western blot analysis of microsomes prepared from human embryonic kidney cells (HEK293 cells) transiently expressing the SERCA3 cDNA used for gene targeting, showed that the message transcribed from this construct is not translated into protein, and functional assays detected only background levels of SERCA activity in these samples (Liu et al., 1997).

To confirm that SERCA3 was not endogenously expressed in the lymphocytes of these mice, immunoblot analysis was performed using an anti-SERCA3 antibody, PA1–910, directed against a peptide corresponding to an N-terminal sequence conserved in rat and mouse SERCA3 proteins. The specificity of PA1-910 for SERCA3 is demonstrated in Figure 9A, where it was reacted against microsome preparations from HEK293 cells (previously isolated by others in the lab), that were transiently transfected with either rat SERCA2a, SERCA2b,or SERCA3 cDNA expression constructs.

Given its specificity for SERCA3, PA1-910 was reacted against 20 or 40 µg of total protein isolated from *serca3*$^{(-/-)}$ splenocytes and thymocytes and wild-type control cells, as described in Materials and Methods. 5 µg of a microsomal preparation from HEK293 cells overexpressing rat SERCA3 was also loaded on gels as a positive control. As illustrated in Figure 9B, a band of predicted size was detected in the protein samples prepared from wild-type splenocytes and thymocytes, that was absent in the samples

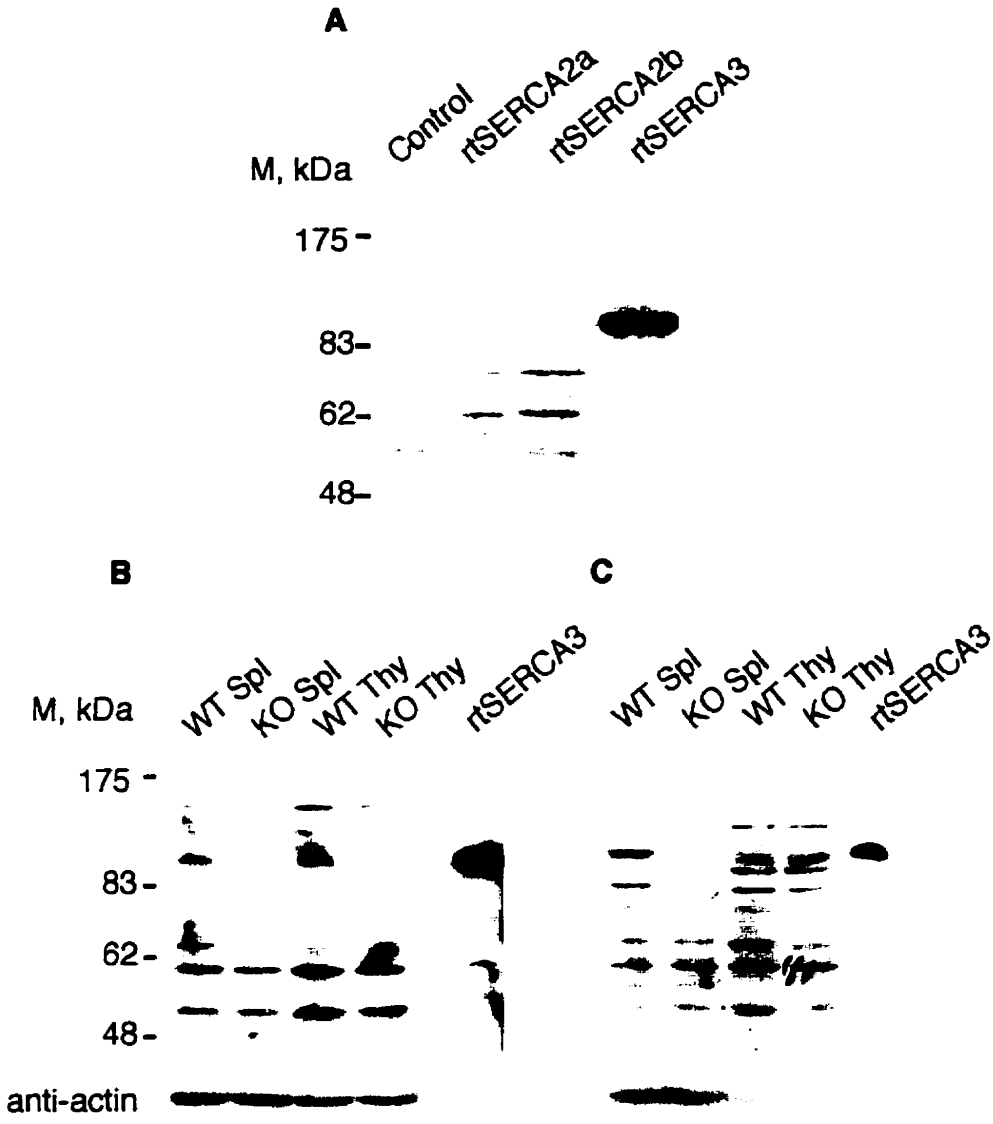

Fig. 9. **Lack of SERCA3 expression in lymphocytes of *serca3* gene-targeted mice. A.** Immunoblot of 5 μg of microsomes isolated from HEK293 cells transfected with the indicated rat SERCA constructs. Cells transfected with SERCA cDNA inserted into vector in the reverse orientation served as Control. **B.** and **C.** Immunoblot of 20 μg (B) or 40 μg (C) of cell lysate isolated from wild-type (WT) or *serca3*$^{(-/-)}$ (KO) splenocytes (Spl) or thymocytes (Thymo). 5 μg of microsomes from same preparation as in A, served as positive control. In all cases proteins were separated by SDS-PAGE, transferred onto nitrocellulose membranes and reacted with PA1-910 antibody (2 μg/mL (A and B) or 10 μg/mL of a different stock (C)). Actin expression was detected by subsequent incubation of blots with anti-actin antibody (0.1 μg/mL).

isolated from cells with mutant *serca3*. Subsequent incubation of the membrane with an anti-actin antibody revealed comparable protein levels between samples.

The results of additional attempts to confirm this finding, using subsequent protein preparations and a new lot of the PA1-910 antibody, are shown in Figure 9C. The lot of antibody currently available is not as sensitive as the previously available one, as demonstrated by a lower level of detection of rat SERCA3 in 2.5μg of the same microsome preparation (Figure 9C), even though 5-fold more antibody was used. However, as shown in Figure 9C, a band of predicted size was observed in the *serca3*$^{(+/+)}$ splenocytes that was absent from the *serca3*$^{(-/-)}$ splenocytes. This band was not, however, observed in either of the thymocyte samples. Although preliminary, these results indicate that as expected SERCA3 protein is not present in the lymphocytes of these gene-targeted mice.

Examination of SERCA2b expression in *serca3*$^{(-/-)}$ lymphocytes

It has previously been reported that myocytes from mice heterozygous for *serca2* deletion, have a ~45% reduction in SERCA2 mRNA, and a ~35% reduction in both SERCA2a protein and SERCA activity when compared to levels in *serca2*$^{(+/+)}$ myocytes. Therefore, mechanisms exist in these cells to partially compensate for the loss of a single copy of the SERCA2 gene (Periasamy et al., 1999). Given the importance of SERCA activity in regulating Ca^{2+} homeostasis, various compensatory mechanisms may operate in lymphocytes to minimize the effects of ablated SERCA3 expression.

As discussed in Chapter 1, the SERCA2b isoform is also expressed in lymphocytes. To test the possibility that SERCA2b expression may be altered in the lymphocytes of gene-targeted mice, SERCA2b protein levels were examined by immunoreactivity, using the commercially available anti-SERCA2 antibody, 2A7-A1. The ability of 2A7-A1 to detect SERCA2b is demonstrated in Figure 10A, which shows a

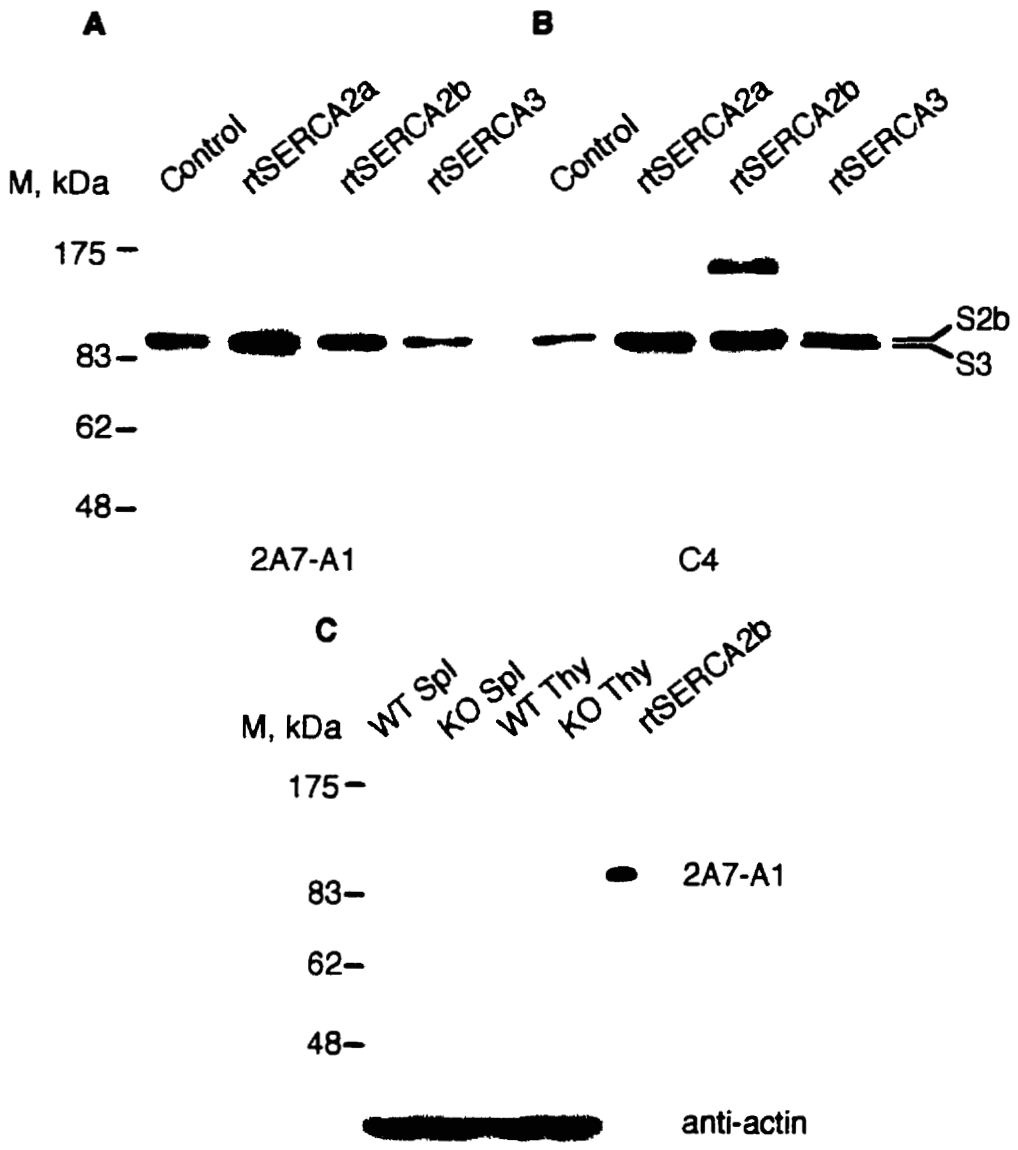

Fig. 10. **Failure of 2A7-A1 antibody to detect mouse SERCA2b in cell lysates. A.** and **B.** Immunoblots of 5 μg of microsomes isolated from HEK293 cells transfected with the indicated rat (rt) SERCA constructs. Rat SERCA cDNA inserted into vector in the reverse orientation served as Control. Blots were reacted with either monoclonal anti-SERCA2 antibody, 2A7-A1 (8 μg/mL), or polyclonal anti-SERCA antibody, C4 (2 μg/mL), as indicated. The band at ~175 kDa in **B** is a rtSERCA2b aggregate seen previously by others (Lytton et al., 1992). **C.** Immunoblot of 30 μg of cell lysate isolated from wild-type (WT) and *serca3*$^{(-/-)}$ (KO) splenocytes (Spl) and thymocytes (Thy) were reacted with 2A7-A1 (upper blot) and actin (0.1 μg/mL; lower blot) antibodies. Microsomes from HEK293 cells expressing rat SERCA2b served as a positive control. Migration position of SERCA2b (S2b) and SERCA3 (S3) are indicated.

Western blot of the same microsome preparations as described above that were isolated from HEK293 cells. Figure 10B is a Western blot of these same microsomal samples, where SERCA proteins were detected using the C4 antibody, which recognizes all SERCA isoforms. Comparing the two figures it is evident that although 2A7-A1 was specific for SERCA2 compared to SERCA3 (compare right-hand lanes of Panels A and B), it was not particularly sensitive at detecting overexpressed rat SERCA2a and 2b above the background levels of human SERCA2b (Control sample).

However, given its specificity for SERCA2 isoforms, 2A7-A1 was used to examine SERCA2b expression levels in splenocytes and thymocytes of *serca3*$^{(-/-)}$ and wild-type cells. As shown in Figure 10C, this antibody was unable to detect SERCA proteins in lymphocyte post-nuclear cell lysates. Protein was present in these samples as revealed by the detection of actin.

Due to the failure of 2A7-A1 to detect SERCA2b in these protein samples, the anti-SERCA antibody, N1, was used, which recognizes all SERCA isoforms. When N1 was reacted against protein samples containing both SERCA2b and SERCA3 proteins, a doublet was detected, with the lower band corresponding to SERCA3 (97 kDa) and the upper band corresponding to SERCA2b (110 kDa) (Figure 11B, lane 3). Therefore, it was thought that N1 may be useful for detecting SERCA2b expression in lymphocyte post-nuclear cell lysates. Figure 11A shows the result of an immunoblot analysis of total protein isolated from *serca3*$^{(+/+)}$ or *serca3*$^{(-/-)}$ splenocytes and thymocytes. Bands corresponding to SERCA proteins were detected in all samples. The band detected in the *serca3*$^{(-/-)}$ splenocyte sample is less intense than that in the wild-type sample, even though more protein appears to have been loaded in this lane as shown by the higher level of actin in this sample. No differences in band intensity were observed between the thymocyte samples, although more protein appears to have been loaded in the wild-type sample based on the greater intensity

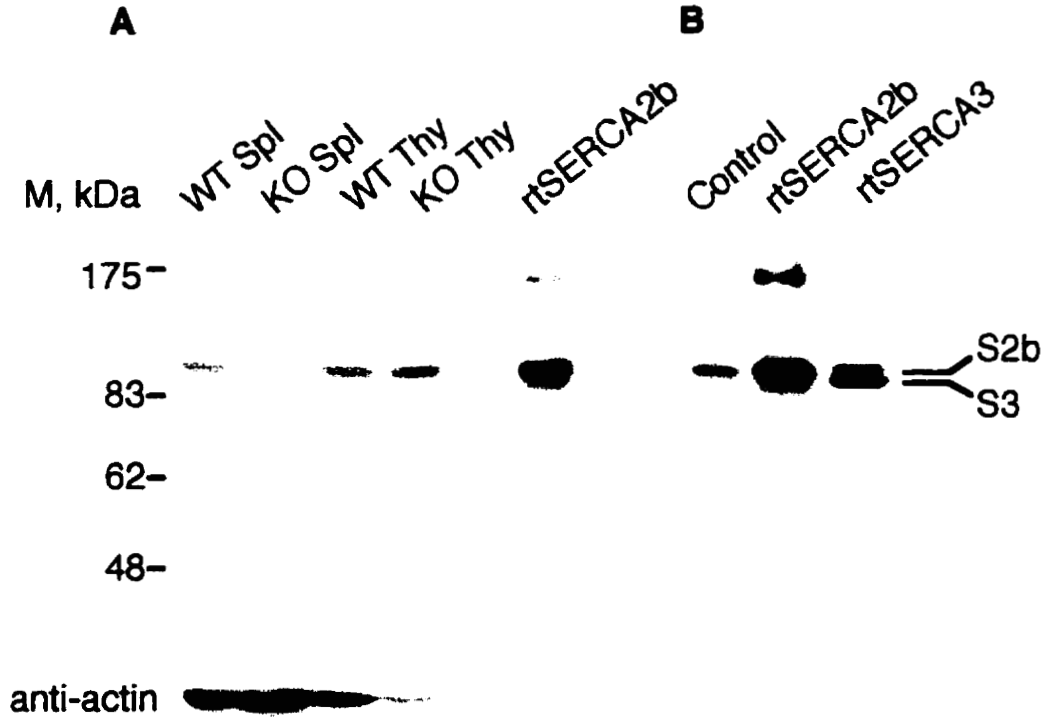

Fig. 11. **Detection of SERCA2b in cell lysates from SERCA3-deficient mice. A.** Immunoblot of 40 μg of cell lysate from wild-type (WT) and *serca3*$^{(-/-)}$ (KO) splenocytes (Spl) or thymocytes (Thy). 2.5 μg of microsomes isolated from HEK293 cells transiently expressing rat SERCA2b was included as a positive control.The blot in subsequently probed with anti-actin (0.1 μg/mL) antibody. **B.** Immunoblot of 2.5 μg of microsomes from HEK293 cells transfected with the indicated rat (rt) SERCA constructs. SERCA cDNA inserted into the expression vector in the reverse orientation served as Control. The band at ~175 kDa in is a rtSERCA2b aggregate seen previously by others (Lytton et al. (1992). Blots in A and B were reacted with polyclonal anti-SERCA antibody, N1 (1:4000). The migration positions of SERCA2b (S2b) and SERCA3 (S3) are shown.

of the actin band. Importantly, SERCA2b and SERCA3 proteins could not be distinguished in the post-nuclear cell lysates of *serca3*$^{(+/+)}$ lymphocytes, therefore the intensities of the bands observed in the *serca3*$^{(-/-)}$ lymphocyte samples that presumably represent only SERCA2b, could not be compared with SERCA2b levels in the wild-type cells. Given these results, possible alterations in SERCA2b expression in SERCA3-deficient lymphocytes remain unknown.

II. IL-2 secretion and cell viability following cellular stimulation *in vitro*

Decreased levels of IL-2 secreted by stimulated *serca3*$^{(-/-)}$ splenocytes

As discussed in Chapter 1, IL-2 is a cytokine secreted by mature T cells in response to antigen receptor stimulation, and is the principle growth factor responsible for inducing T cell proliferation during cellular activation (Abbas et al., 1997; Cantrell and Smith, 1984; Meuer et al., 1984). Its transcription has been shown to be dependent on a sustained elevation in intracellular Ca^{2+} levels for ~2 hours (Wacholtz and Lipsky, 1993; Weiss et al., 1987). The expression of IL-2 therefore serves as an important indicator of an altered biological response resulting from changes in Ca^{2+} signaling in T cells

To test the role of SERCA3 in mediating Ca^{2+}-dependent responses to TCR stimulation, SERCA3-deficient splenocytes were stimulated *in vitro* for 24 hours with compounds previously shown to induce IL-2 expression in T cells. The stimulators used were ones that either act at the level of the TCR, or act on signaling pathways downstream of the receptor. The former type included plate-bound anti-CD3ε antibodies and ConA (Weiss et al., 1987), while the latter type included PMA and A23187, which activate PKC

and increase $[Ca^{2+}]_i$. Together, these two signals are sufficient to induce IL-2 expression (Truneh et al., 1985).

Given the role of capacitative Ca^{2+} entry in mediating the influx of extracellular Ca^{2+}, and thus IL-2 expression by T cells in response to cellular stimulation (Fanger et al., 1995; Timmerman et al., 1996), it was predicted that the ablation of SERCA3 may stimulate a greater degree of IL-2 expression if SERCA3-regulated stores were associated with store-operated channels in the plasma membrane that are responsive to antigen receptor stimulation.

As shown in Figure 12, and summarized in Table 4, 10 nM PMA in combination with 100nM A23187 induced the greatest production of IL-2 by cells of both genotypes. Stimulation of the TCR alone by plate-bound anti-CD3ε antibodies resulted in small IL-2 responses by both serca3$^{(-/-)}$ and *serca3*$^{(+/+)}$ cells. A sizable response to plate-bound anti-CD3ε antibody required a co-stimulatory signal provided by the activation of the CD28 surface protein ((Stein et al., 1994), Figure 12 and Table 4). CD28 stimulation is believed to both enhance the magnitude of the signal from the TCR, and activate Ca^{2+}-independent signal transduction pathways that synergize with those induced downstream of the TCR (Sprent, 1999). ConA has been shown to specifically interact with the TCR (Weiss et al., 1987). For cells of both genotypes, treatment with this lectin stimulated IL-2 secretion at levels slightly higher than those induced in response to plate-bound anti-CD3ε plus anti-CD28 mAbs. Minimal IL-2 was found to be secreted by cells treated with PMA, A23187, or cell culture medium alone (Figure 12 and Table 4), as well as cell culture medium containing vehicle solutions (DMSO/ethanol or PBS) (data not shown).

Comparison of the IL-2 production by *serca3*$^{(-/-)}$ and *serca3*$^{(+/+)}$ cells reveals that, with the exception of PMA alone and plate-bound anti-CD3ε, cells deficient in SERCA3

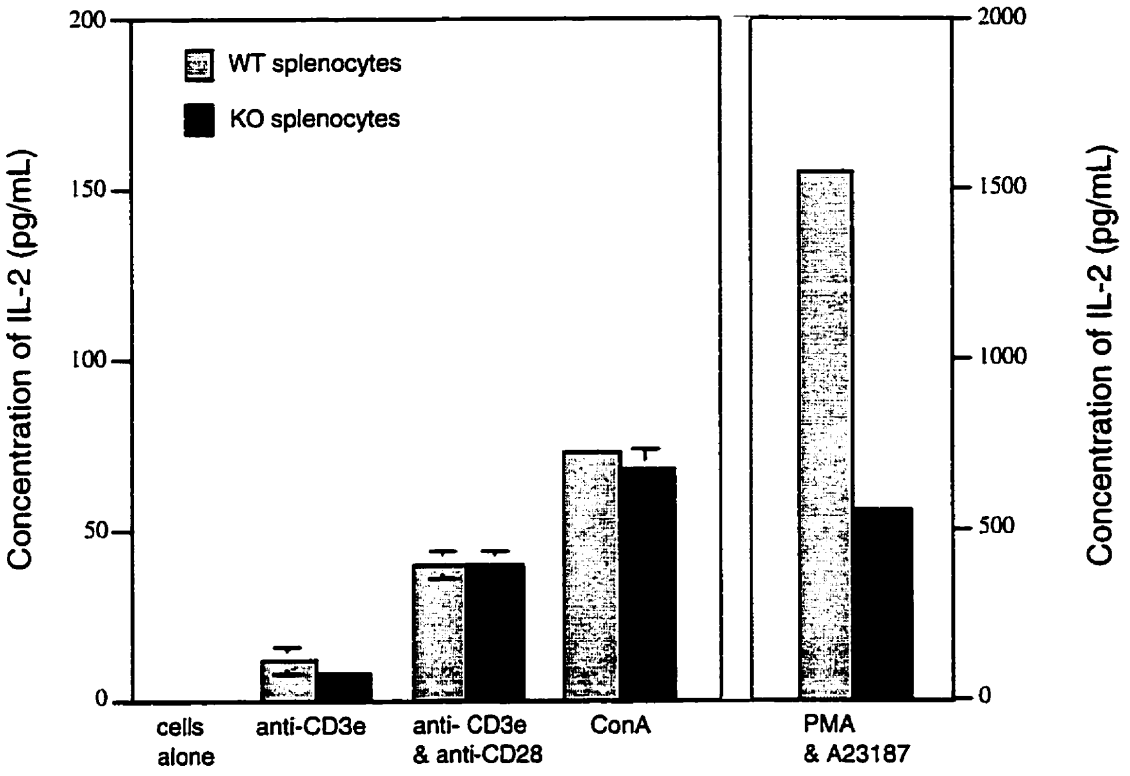

Fig. 12. **IL-2 secretion by cultured splenocytes.** The concentrations of secreted IL-2 in cell culture supernatants from wild-type (WT, □) and SERCA3-deficent (KO, ■) splenocytes following 24 hours of stimulation with cell culture medium alone (cells alone), plate-bound anti-CD3e (10 μg/mL), plate-bound anti-CD3e (10 μg/mL) plus anti-CD28 (10 μg/mL), ConA (5 μg/mL), or PMA (10 nM) plus A23187 (100 nM). IL-2 concentrations were determined by ELISA, as described in Materials and Methods. Shown are the means of triplicate wells ± SEM. A representative result from five similar experiments is shown.

Table 4.

Concentrations of secreted IL-2 (pg/mL) by wild-type (WT) and SERCA3-deficient (KO) splenocytes following stimulation *in vitro*.

Stimulus	WT	KO	n	p-value
Cell culture medium alone	0	0	5	--
A23187 alone	0, 0	0, 4	2	0.5
PMA alone	0, 4	3, 17	2	0.5
Plate-bound anti-CD3ε Ab	38 ± 10	45 ± 23	5	0.8
Plate-bound anti-CD3ε + anti-CD28 Abs	349 ± 179	164 ± 63	5	0.27
ConA	312 ± 104	186 ± 43	5	0.09
PMA + A23187	5320 ± 1300	2170 ± 718	5	**0.01**

IL-2 concentrations (pg/mL) in cell culture supernatants collected after 24 hours of culturing were determined by ELISA. Individual values from duplicate experiments, or the mean ± SEM for the indicated number of experiments (n) are shown.

secreted reduced amounts of IL-2 following cellular stimulation (Figure 12 and Table 4). However, only the mean concentration of IL-2 secreted by *serca3*$^{-/-}$ splenocytes in response to PMA and A23187 was significantly less than that secreted by *serca3*$^{+/+}$ cells (Table 4).

The concentration of secreted IL-2 was highly variable between experiments, even though similar trends were observed when comparing wild-type and SERCA3-deficient cells (Table 4). In an attempt to diminish the variability in the data, the concentrations of secreted IL-2 were normalized to the maximum secreted IL-2 concentration for each experiment. In all cases, this corresponded to the IL-2 concentration secreted by wild-type cells treated with PMA plus A23187. Similar to what was observed before data normalization, SERCA3-deficient splenocytes showed a reduced level of IL-2 secretion in response to both anti-CD3ε/anti-CD28 antibodies and ConA treatment, and a marked reduction in response to PMA plus A23187 (Figure 13). Secreted levels of IL-2 following stimulation with anti-CD3ε antibody alone, which were very low, did not differ significantly between SERCA3-deficient and wild-type cells. T-tests of statistical significance comparing the results obtained for anti-CD3ε/anti-CD28 antibodies and ConA, revealed that the secreted IL-2 concentration by SERCA3-deficient cells following ConA treatment was significantly different from that of wild-type control cells ($p = 0.03$, $n = 5$).

For both SERCA3-deficient and wild-type cells, the concentration of secreted IL-2 in response to PMA plus A23187 were more than 10-fold greater than the levels secreted in response to ConA or anti-CD3ε/anti-CD28 (Table 4). The concentrations of IL-2 secreted by both cell types following PMA/A23187 treatment were therefore considered to represent the maximum capacity of the cells to respond to stimulation, and that less potent stimuli induced a reduced IL-2 response. Based on these assumptions, the concentration of IL-2

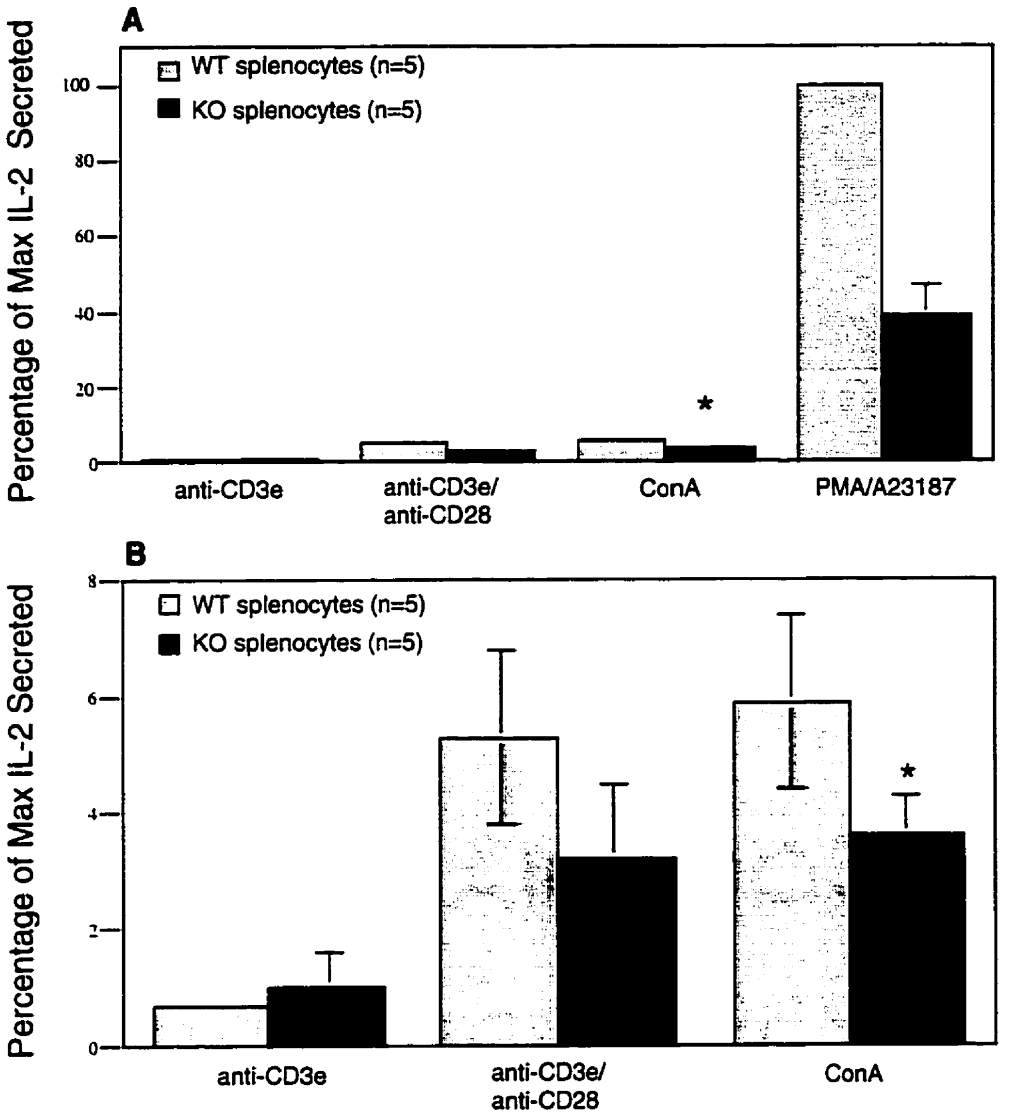

Fig. 13. **IL-2 secretion by cultured splenocytes normalized to the experimental maximum.** IL-2 secreted by wild-type (WT, □) and SERCA3-deficient (KO, ■) splenocytes following 24 hours of stimulation *in vitro* with the indicated compounds is shown. Graph B is an enlarged version of A, with the results for PMA/A23187 treatment omitted. IL-2 concentrations were determined by ELISA, as described in Materials and Methods. Percentages are relative to the concentration secreted by wild-type cells in response to PMA/A23187. The error bars indicate the standard error of the mean for five experiments. The asterisks (*) indicates a significant difference between the WT and KO cells in response to ConA treatment (p=0.03).

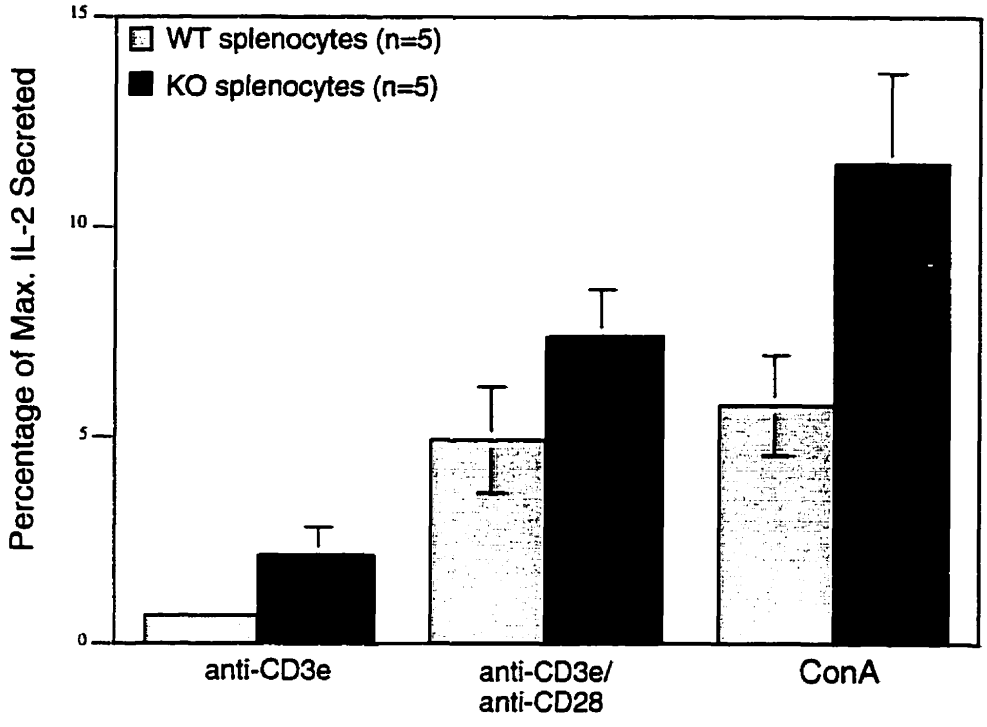

Fig. 14. **IL-2 secretion from cultured splenocytes normalized to the genotype maximum.** IL-2 secreted by wild-type (WT, □) and SERCA3-deficient (KO, ■) splenocytes following 24 hours of stimulation *in vitro* with the indicated compounds is shown. IL-2 concentrations in cell culture supernatants were determined by ELISA, as described in Materials and Methods. Percentages are relative to the amount secreted by cells of each genotype in response to PMA plus A23187. The error bars indicate the standard error of the mean for five similar experiments.

secreted in response to anti-CD3ε Ab, anti-CD3ε/anti-CD28 Abs and ConA treatment was compared to the maximum response induced by PMA/A23187 separately for cells of each genotype. The purpose of this comparison was to determine if SERCA3-deficient cells were capable of responding to anti-CD3ε Ab, anti-CD3ε/anti-CD28 Abs and ConA to the same degree as wild-type cells. The results show that the fractional IL-2 responses of SERCA3-deficient cells to all three stimuli were slightly greater than those of wild-type cells, although the differences were not statistically significant (Figure 14).

Viability of *serca3*$^{(-/-)}$ splenocytes following stimulation

A reduction in IL-2 concentration in cell culture supernatants could reflect the presence of fewer IL-2 producing cells, or be due to a reduced amount of IL-2 being secreted by individual cells. In an attempt to distinguish between these two possibilities, the viability of *serca3*$^{(-/-)}$ and *serca3*$^{(+/+)}$ splenocytes was determined both before and following cellular stimulation with plate-bound anti-CD3ε plus anti-CD28 mAbs and PMA/A23187. Since IL-2 is predominantly secreted by CD4$^+$ T cells, the viability of these cells within the splenocyte population was specifically examined using FITC-anti-CD4 antibodies. The viability of all T cells was also assessed using an FITC-anti-CD3ε antibody. At the time of isolation, the viability of CD4$^+$ T cells and CD3ε$^+$ T cells from SERCA3-deficient animals were found to be similar to those of wild-type cells (Figure 15). Following 24 hours of culturing in the presence of anti-CD3ε/anti-CD28 or PMA/A23187, the viability of CD4$^+$ and CD3ε$^+$ *serca3*$^{(-/-)}$ cells were slightly less than *serca3*$^{(+/+)}$ cells, but the differences were not significantly different for either of the treatment conditions. Similarly, the viability of *serca3*$^{(-/-)}$ and *serca3*$^{(+/+)}$ splenocytes (i.e. T cells and B cells), were not found to be significantly different either before or after 24 hours of treatment (Figure 15).

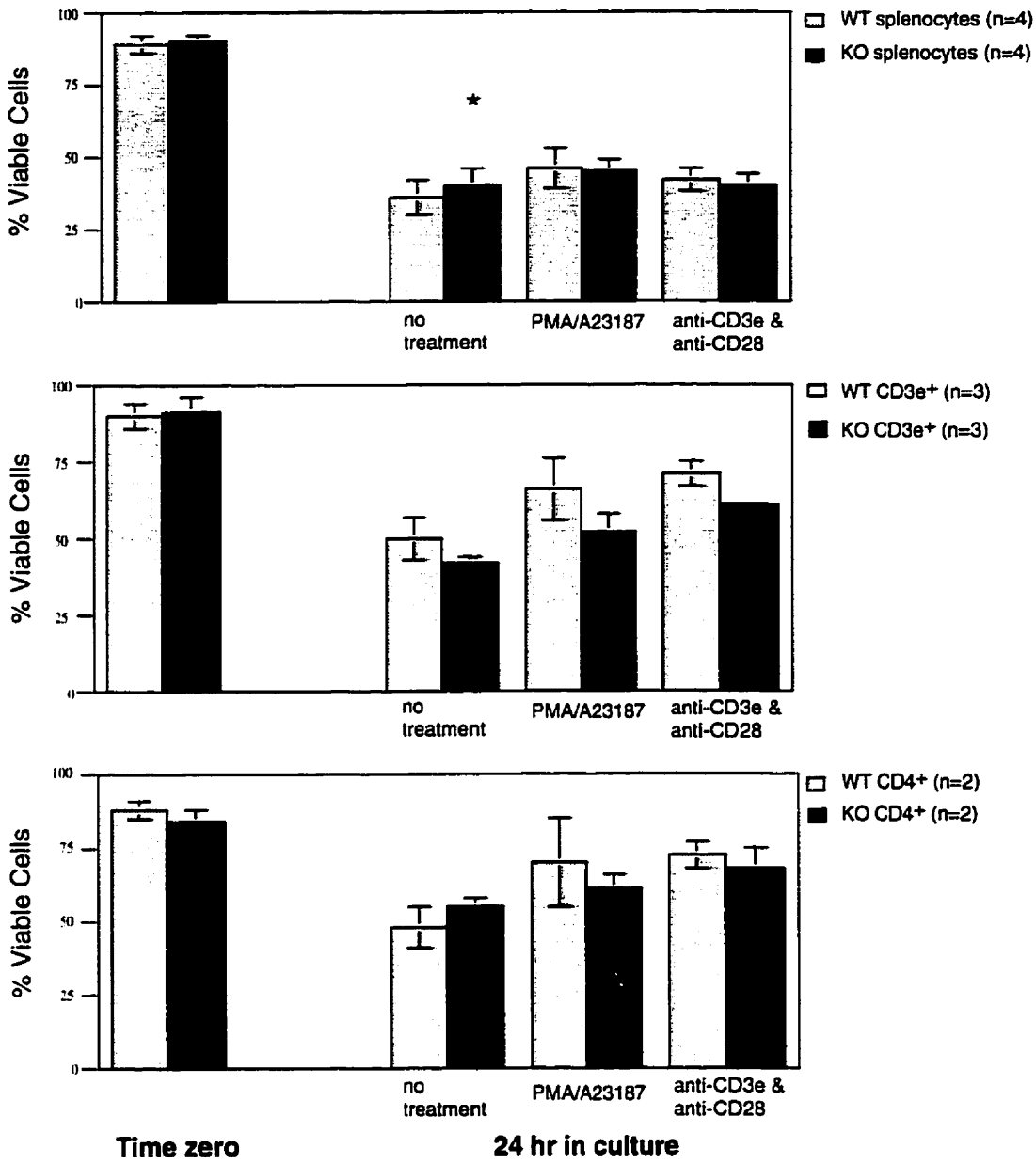

Fig. 15. **Viability of splenocytes following *in vitro* stimulation.** The percentages of viable wild-type (WT, □) and SERCA3-deficient (KO, ■)splenocytes are shown at the time of isolation (time zero) and following 24 hours of culture with the indicated compounds. Viability was determined by propidium iodide exclusion, which was measured using flow cytometry. CD3e+ and CD4+ cells were identified by staining with FITC-conjugated antibodies. The error bars indicate the standard error of the mean for two to four experiments, as labelled. The asterisks indicates a significant difference between WT and KO cells for that time point (p=0.01).

Given that the viability of SERCA3-deficient and wild-type splenocytes following cellular stimulation did not significantly differ, the general trend of reduced IL-2 secretion by *serca3*$^{(-/-)}$ cells in response to cellular stimulation suggests that SERCA3 activity is a component of the signaling pathway that regulates IL-2 expression in individual cells. A highly significant deficit in IL-2 secretion was observed in response to treatment with PMA plus A23187, suggesting that the disruption of *serca3* alters the ability of IL-2-producing cells to respond to potent stimuli.

III. Calcium transients of *serca3*$^{(-/-)}$ lymphocytes following antigen receptor stimulation

The observed alteration of Ca^{2+}-dependent IL-2 expression in stimulated *serca3*$^{(-/-)}$ T cells, suggested that SERCA3 may regulate Ca^{2+} transients in response to antigen receptor stimulation. To test this hypothesis, B cells of the spleen and T cells of the spleen and thymus isolated from *serca3*$^{(-/-)}$ mice were stimulated by antigen receptor cross-linking, and induced changes in $[Ca^{2+}]_i$ were determined using the Ca^{2+}-indicating dye, fluo-3, and flow cytometry. Cells isolated from sex- and age-matched *serca3*$^{(+/+)}$ mice that were either unrelated or siblings, served as controls.

Kinetic analysis of fluo-3 fluorescence by flow cytometry

To demonstrate how the results presented in this chapter were obtained, the different stages of data acquisition for a representative experiment are presented in Figure 16. Panel A shows a dot plot of splenocytes, where cells were plotted based on their degree

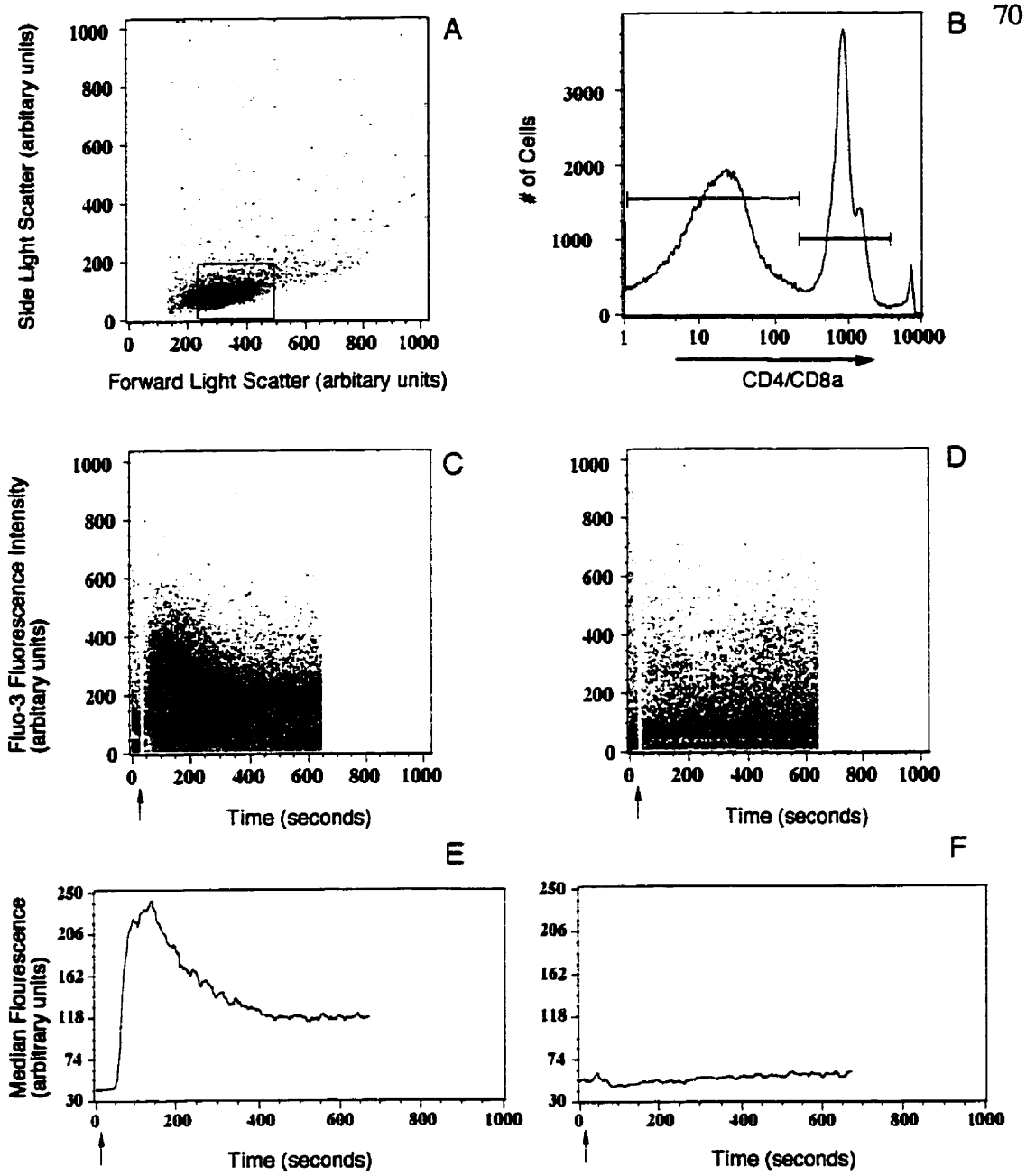

Fig. 16. **Illustration of the steps of data analysis for Ca^{2+} flux experiments. A.** Dot plot showing light scattering properties of the cells within the sample. The box denotes a gate that was placed around lymphocytes. **B.** Histogram showing fluorescence intensity of gated cells stained with both PE-anti-CD4 and PE-anti-CD8a antibodies. Two predominant populations are revealed. Marker placement was based on background fluorescence of cell sample labelled with PE-isotype control, and distinguishes positively stained cells at right and unstained cells at left. **C.** and **D.** Pseudo-density dot plots of kinetic changes in fluo-3 fluorescence intensity in B cells (ie. unstained cells in B) (C), and in CD4+CD8+ cells (D) following anti-IgG stimulation (indicated by arrow). Increasing densities of cells are shown with a rainbow scale from low (blue) to high (red). **E** and **F.** Kinetic curves showing the median fluo-3 fluorescence of data presented in C and D, respectively.

of forward- and side-scattering of light. The box denotes a gate that was placed around the lymphocytes, which are characterized by their small size and low degree of granularity. These cells were stained with both PE-anti-CD4 and CD8α antibodies. Panel B shows a histogram of the gated cells detected by the FL-2 detector, and reveals two predominant populations. The marker dividing the two populations represents the level of background PE fluorescence, which was determined by staining similar cells with a PE-conjugated isotype control antibody. The population of cells that falls to the right of the marker (above 200), therefore represents cells that are positive for both CD4 and CD8, and the population on the left represents cells that were not stained by either antibody. These negative staining cells were considered to represent B cells. As shown in Figure 7 and listed in Table 3, ~40% of splenocytes are negative for both CD4 and CD8, and ~33-36% of splenocytes are B cells, as determined by their expression of B220.

This particular experiment was aimed at examining B cell responses to surface IgG cross-linking. Therefore, the $CD4^-CD8^-$ splenocytes, which will be referred to as B cells, were gated and, as shown in Panel C, changes in fluo-3 fluorescence intensity over time were selectively examined in these cells. It can be seen in Panel C that there was a fair number of cells within the gated population that did not respond to the anti-mouse IgG stimulus. Although SERCA3-deficient and wild-type animals did not significantly differ with respect to the number of non-responding cells (see Table 5), a threshold of fluo-3 fluorescence was set such that subsequent analyses focused only on cells that responded to the stimulus applied. Panel D shows that no increase in fluo-3 fluorescence intensity in response to anti-IgG was observed in cells that stained positively with anti-CD4 and anti-CD8α antibodies. When the fluo-3 fluorescence intensity for a given time slice was examined, the responding cells depicted in Panel C fell into a slightly positive-skewed distribution. Because a calculated *mean* fluorescence could potentially be biased by the high

responders, the *median* fluo-3 fluorescence intensity of cells, above a set threshold, was therefore calculated for each time interval (see Panel E). These values were converted to median measures of $[Ca^{2+}]_i$, as described in Materials and Methods. Panel F shows the median fluo-3 fluorescence in $CD4^+$ and $CD8^+$ cells.

Ca^{2+} transients of serca3$^{(-/-)}$ lymphocytes in response to antigen-receptor cross-linking

Figures 17, 18,19, 20, and 21, show typical kinetic profiles of changes in median $[Ca^{2+}]_i$ observed in serca3-deficient and wild-type splenic B cells, $CD4^+$ or $CD8^+$ splenic T cells, and $CD4^+$ or $CD4^-$ thymocytes, respectively, following the addition of antibody. The measured Ca^{2+} transients possessed the characteristic biphasic increase in $[Ca^{2+}]_i$, where a peak increase in Ca^{2+} levels was followed by a decline to a sustained Ca^{2+} concentration that was above baseline levels. The baseline, peak and plateau $[Ca^{2+}]_i$ obtained for each experiment are presented in Tables 5 through 9. Pair-wise t-tests revealed no significant differences between the mean values obtained for serca3-deficient cells and wild-type control cells (see Tables 5 through 9).

Although the peak and plateau levels of $[Ca^{2+}]_i$ in *serca3*$^{(-/-)}$ and *serca3*$^{(+/+)}$ B cells and thymocytes did not differ significantly, the half-time ($t_{1/2}$) of the decline of $[Ca^{2+}]_i$ between these two levels was found to be significantly slower in SERCA3-deficient B cells, $CD4^+$ thymocytes, and $CD4^-$ thymocytes (Tables 5, 8 and 9, and Figures 17, 20 and 21). No significant difference in the rate of decline of Ca^{2+} levels was observed between *serca3*$^{(-/-)}$ and *serca3*$^{(+/+)}$ $CD4^+$ or $CD8^+$ splenic T cells in response to CD3ε cross-linking with 5 μg/mL goat anti-hamster secondary antibody (Tables 6 and 7, and Figures 18 and 19).

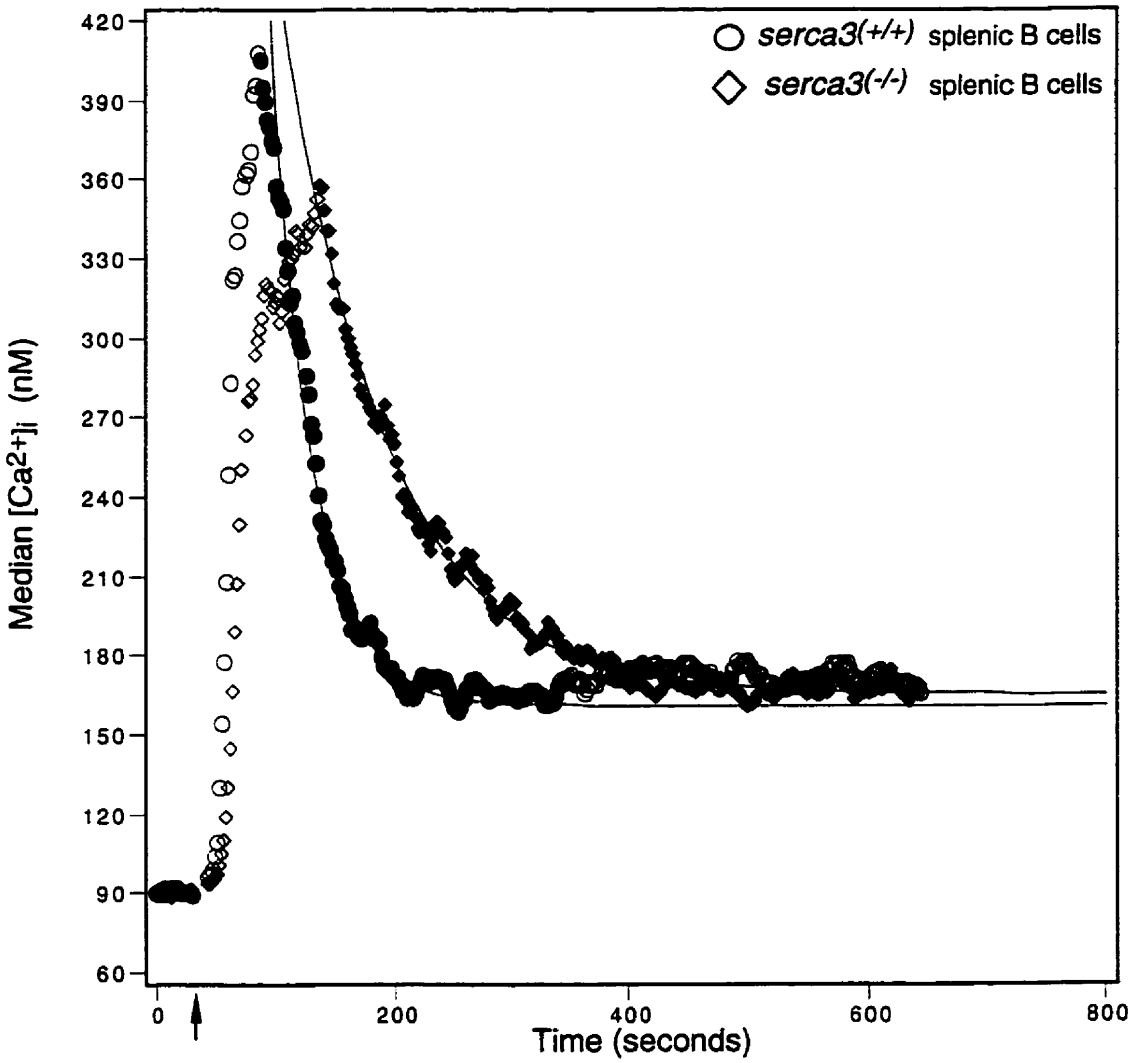

Fig. 17. **Calcium transients in splenic B cells (ie. CD4$^-$CD8$^-$ splenocytes).** Kinetic changes in median $[Ca^{2+}]_i$ are shown for wild-type (○) and SERCA3-deficient cells (◇) that were loaded with fluo-3. Ca^{2+} transients were initated by the addition of secondary antibody (indicated by arrow) to cross-link surface IgG. Fluo-3 fluorescence intensity was monitored with time using flow cytometric analysis. Specific responses of CD4-CD8- cells were determined by gating on the cell population that stained negatively with both PE-anti-CD4 and PE-anti-CD8a antibodies. Arbitrary fluorescence values were converted to measures of median $[Ca^{2+}]_i$, as described in Materials and Methods. The filled symbols indicate data points that were fit to exponential equations to obtain rate constants for the declining portion of the curves. The resultant lines of best fit are shown. This is a representative result of four independent experiments.

Table 5.

Summary of the Ca^{2+} signaling parameters in wild-type (WT) and SERCA3-deficient (KO) splenic B cells (ie. $CD4^-CD8^-$ cells) following the cross-linking of surface IgG.

Experiment		Baseline $[Ca^{2+}]_i$ (nM)	After sIgG cross-linking: Peak $[Ca^{2+}]_i$ (nM)	After sIgG cross-linking: Plateau $[Ca^{2+}]_i$ (nM)	$t_{1/2}$ of decline (seconds)	% non-responding $CD4^-CD8^-$ cells
1	WT1	110	195	145	34	33
	WT2	135	190	145	36	32
	KO1	105	280	154	75	54
	KO2	100	180	130	87	37
2	WT1	82	225	133	42	37
	WT2	81	290	147	29	37
	KO1	105	230	137	44	41
	KO2	110	275	151	47	38
3	WT	90	400	170	24	19
	KO	90	350	170	60	26
4	WT1	115	280	150	20	66
	WT2	87	350	175	23	52
	KO1	87	290	170	112	54
	KO2	88	360	175	64	55
	KO3	88	320	180	87	55
Mean±SEM	**WT**	99±9	202 ± 59	154 ± 7	**29 ± 4**	37 ± 8
	KO	97±5	289 ± 28	158 ± 9	**69 ± 10**	41 ± 6
		(p=0.87)	(p=0.33)	(p=0.39)	**(p =0.04)**	(p = 0.28)

The results of four independent experiments and the resultant mean ± SEM, are presented. Within an experiment, two or more values for one genotype refer to duplicate or triplicate cell samples from the same animal. The mean of these samples was used in the calculation of the resultant mean. The Ca^{2+} concentrations before (baseline) and after stimulation are shown, as well as the half-time ($t_{1/2}$) of the declining portion of the transient. Values in bold indicate statistically significant differences between mutant and wild-type cells. Non-responding cells were excluded from all analyses.

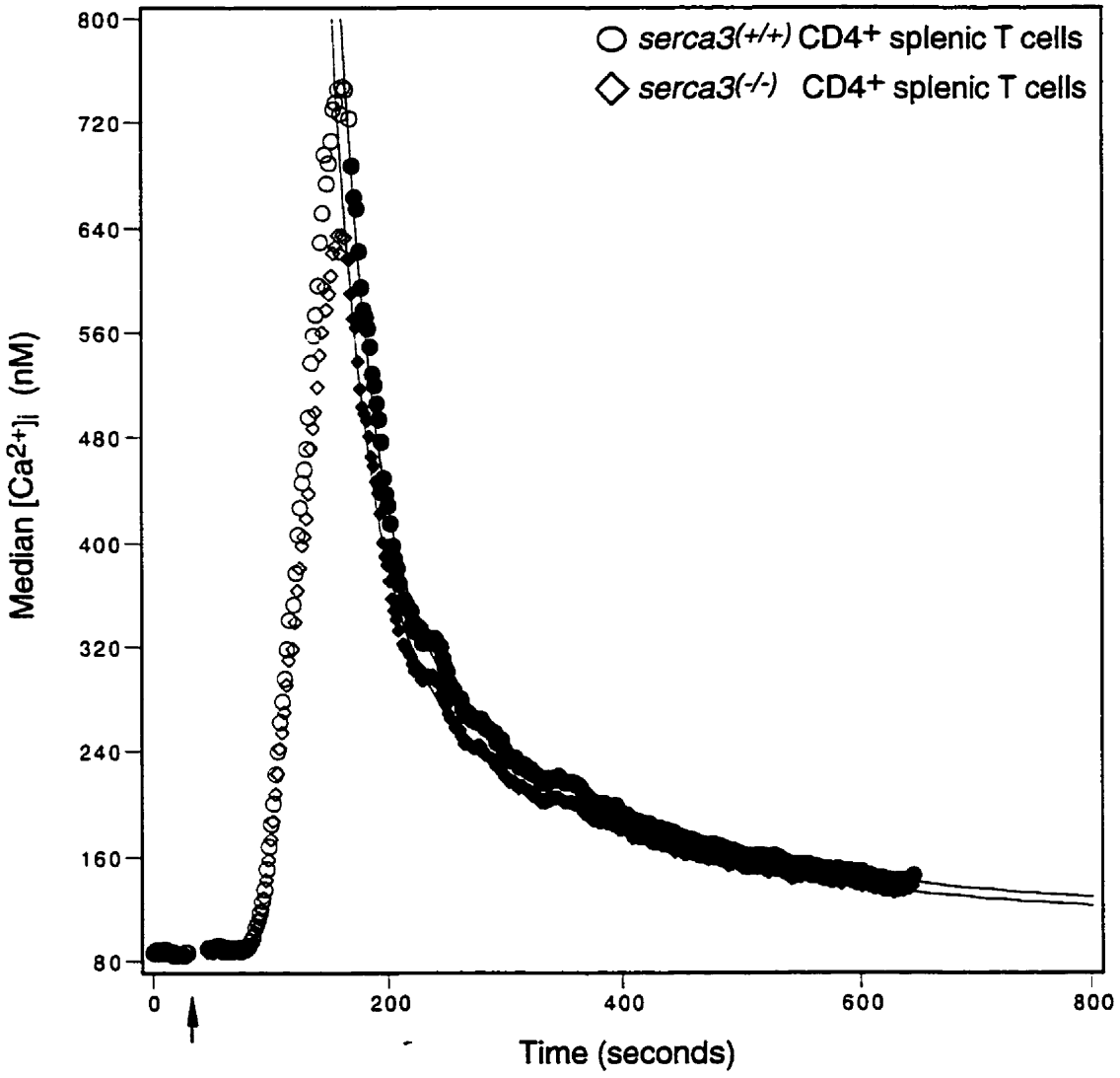

Fig. 18. **Calcium transients in CD4+ splenic T cells.** Kinetic changes in median $[Ca^{2+}]_i$ are shown for wild-type (○) and SERCA3-deficient cells (◇) that were loaded with fluo-3. Ca^{2+} transients were initated by the addition of secondary antibody (indicated by arrow) to cross-link anti-CD3e antibody already on the cell surface. Specific responses of CD4+ cells were determined by gating on the cell population that stained positively with PE-anti-CD4 antibodies. See legend for Figure 17 for more details. This is a representative result of four independent experiments.

Table 6.

Summary of the Ca^{2+} signaling parameters in wild-type (WT) and SERCA3-deficient (KO) $CD4^+$ splenic T cells following the cross-linking of anti-CD3ε antibody.

Experiment		Baseline $[Ca^{2+}]_i$ (nM)	After CD3ε cross-linking: Peak $[Ca^{2+}]_i$ (nM)	After CD3ε cross-linking: Plateau $[Ca^{2+}]_i$ (nM)	$t_{1/2}$ of decline (seconds)	% non-responding $CD4^+$ T cells
1	WT	85	400	121	97	14
	KO	90	650	160	32	12
2	WT	87	740	141	20, *140*	6
	KO	85	630	133	21, *140*	8
3	WT	82	558	172	28, *110*	6
	KO	100	830	500	32, *110*	9
4	WT	90	1000	150	21, *197*	9
	KO1	155	613	140	60, *197*	13
	KO2	216	800	235	68, *197*	15
Mean±SEM	WT	86 ± 2	675 ± 128	146 ±11	42 ± 19	9 ± 2
	KO	115 ±24	704 ± 45	245 ±86	37 ± 9	11 ± 1
		(p=0.29)	(p = 0.84)	(p =0.29)	(p = 0.86)	(p = 0.22)

The results of four independent experiments and the resultant mean ±SEM are presented. Within an experiment, two values for one genotype refer to duplicate cell samples from the same animal. The mean of these two samples was used in the calculation of the resultant mean. The Ca^{2+} concentrations before (baseline) and after stimulation are shown, as well as the half-time ($t_{1/2}$) of the declining portion of the transient. When curves were fit to two rate constants, the slower component was made equal for mutant and wild-type cells (in italics), and the fast component was compared. See Materials and Methods for further details. Non-responding cells were excluded from all analyses.

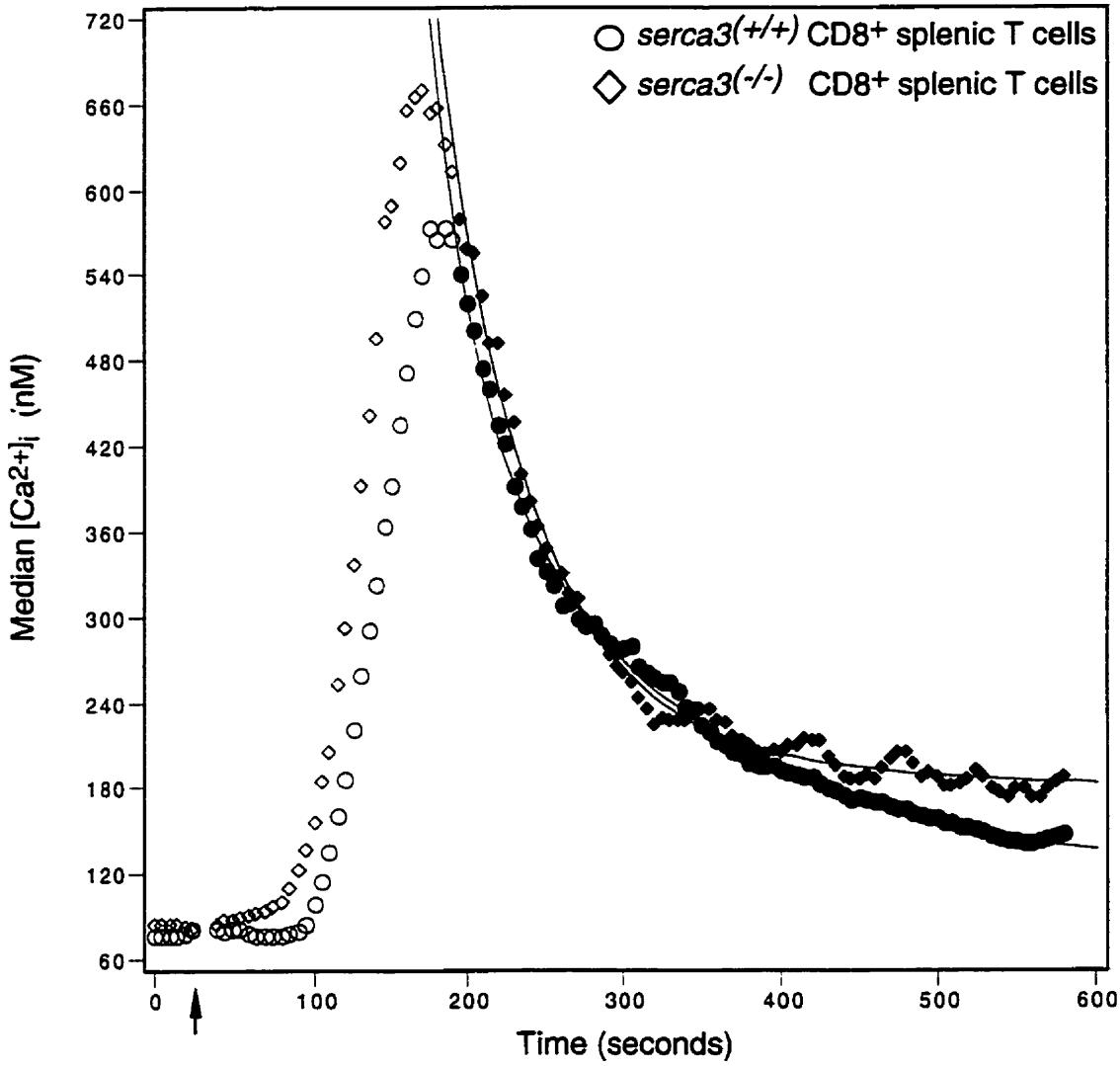

Fig. 19. **Calcium transients in CD8+ splenic T cells.** Kinetic changes in median $[Ca^{2+}]_i$ are shown for wild-type (○) and SERCA3-deficient cells (◇) that were loaded with fluo-3. Ca^{2+} transients were initated by the addition of secondary antibody (indicated by arrow) to cross-link anti-CD3e. Specific responses of CD8+ cells were determined by gating on the cell population that stained positively with PE-anti-CD8a antibodies. Refer to Figure 17 for further details. This is a representative result of four independent experiments.

Table 7.

Summary of the Ca^{2+} signaling parameters in wild-type (WT) and SERCA3-deficient (KO) $CD8^+$ splenic T cells following the cross-linking of anti-CD3ε antibody.

Experiment		Baseline $[Ca^{2+}]_i$ (nM)	After CD3ε cross-linking		$t_{1/2}$ of decline (seconds)	% non-responding $CD8^+$ cells
			Peak $[Ca^{2+}]_i$ (nM)	Plateau $[Ca^{2+}]_i$ (nM)		
1	WT	100	560	150	--	18
	KO	113	550	138	--	18
2	WT	133	740	190	--	9
	KO	92	930	180	--	11
3	WT	80	570	145	22, *116*	7
	KO	82	660	175	39, *116*	7
4	WT	90	480	128	24, *161*	9
	KO	112	445	125	23, *161*	9
Mean±SEM	WT	101 ±11	588 ±55	153 ±13	23 ± 1	11 ± 2
	KO	100 ± 8	646 ±104	155 ±14	31 ± 9	11 ± 2
		(p=0.95)	(p = 0.34)	(p = 0.91)	(p = 0.57)	(p = 0.39)

The results of four independent experiments and the resultant mean ±SEM are presented. The Ca^{2+} concentrations before (baseline) and after stimulation are shown, as well as the half-time ($t_{1/2}$) of the declining portion of the transient. Curves were fit to two rate constants. The slower component was made equal for mutant and wild-type cells (in italics), and the fast component was compared. See Materials and Methods for further details. Non-responding cells were excluded from all analyses. Dashes (--) indicate data that could not be fit accurately to exponential equations due to random variations in the values.

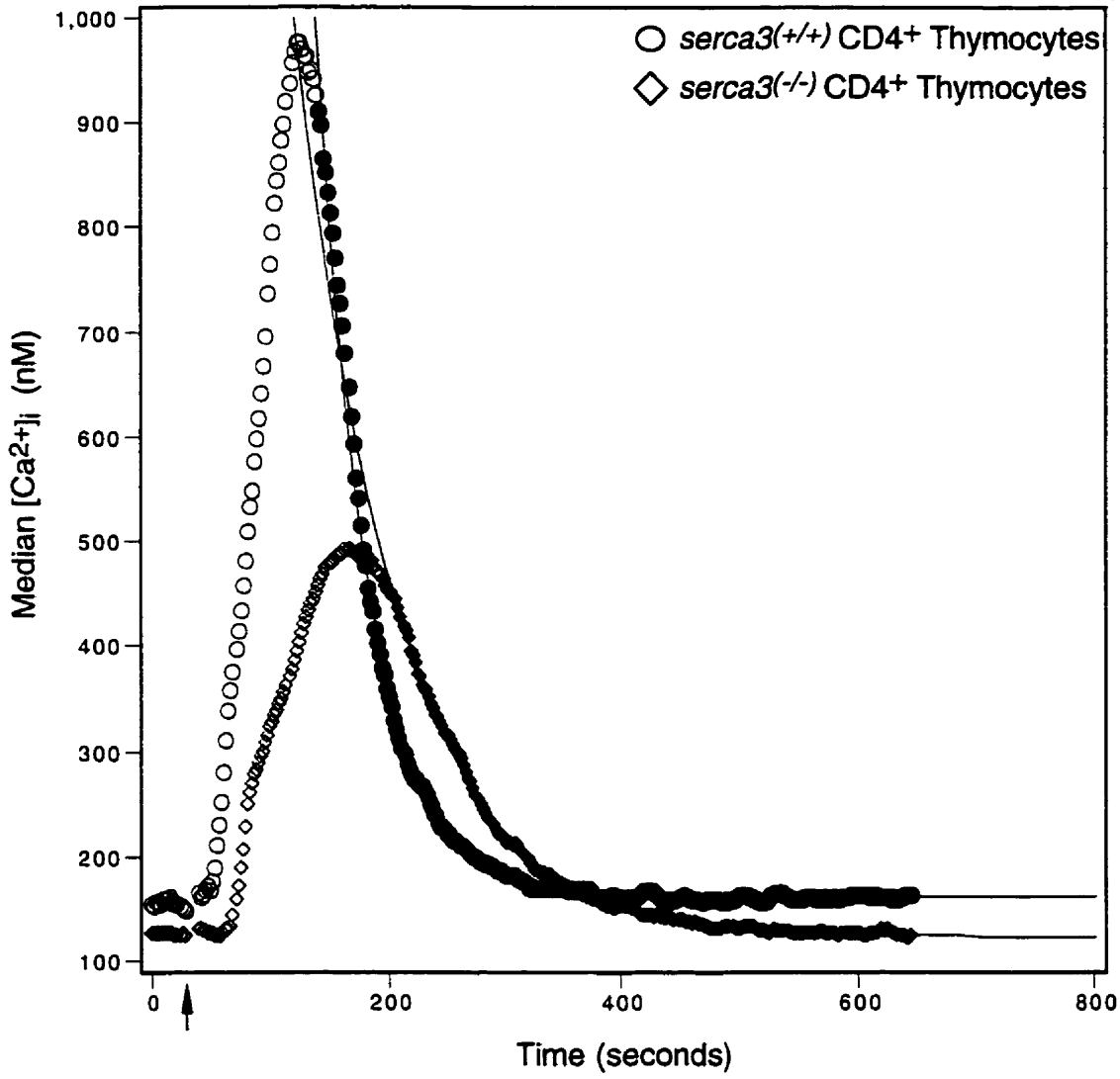

Fig. 20. **Calcium transients in CD4+ thymocytes.** Kinetic changes in median $[Ca^{2+}]_i$ are shown for wild-type (○) and SERCA3-deficient cells (◇) that were loaded with fluo-3. Ca^{2+} transients were initated by the addition of secondary antibody (indicated by arrow) to cross-link anti-CD3e. Specific responses of CD4+ cells were determined by gating on the cell population that stained postively with PE-anti-CD4 antibodies, using flow cytometric analysis. Refer to Figure 17 for further details. A representative result of five independent experiments is shown.

Table 8.

Summary of the Ca^{2+} signaling parameters in wild-type (WT) and SERCA3-deficient (KO) $CD4^+$ thymocytes (ie. $CD4^+CD8^+$/$CD4^+CD8^-$ cells) following the cross-linking of anti-CD3ε antibody on the cell surface.

Experiment		Baseline $[Ca^{2+}]_i$ (nM)	After CD3ε cross-linking: Peak $[Ca^{2+}]_i$ (nM)	After CD3ε cross-linking: Plateau $[Ca^{2+}]_i$ (nM)	$t_{1/2}$ of decline (seconds)	% non-responding $CD4^+CD8^+$ & $CD4^+CD8^-$ cells
1	WT	110	665	123	35	54
	KO	110	600	117	43	56
2	WT	126	3,550	132	27	34
	KO	126	744	185	51	57
3	WT	155	970	160	30	56
	KO	125	490	125	57	57
4	WT	145	1,400	170	22	50
	KO	118	1,220	125	30	47
5	WT	121	500	140	32	74
	KO	113	590	120	45	57
Mean±SEM	WT	134 ± 10	1647 ±652	146 ±11	**29 ± 2**	54 ± 6
	KO	120 ± 4	764 ± 161	138± 16	**45 ± 5**	55 ± 2
		(p=0.18)	(p = 0.26)	(p=0.73)	**(p =0.02)**	(p = 0.88)

The results of five independent experiments and the resultant mean ± SEM, are presented. The mean of these samples was used in the calculation of the resultant mean. The Ca^{2+} concentrations before (baseline) and after stimulation are shown, as well as the half-time ($t_{1/2}$) of the declining portion of the transient. Values in bold indicate statistically significant differences between mutant and wild-type cells. Non-responding cells were excluded from all analyses.

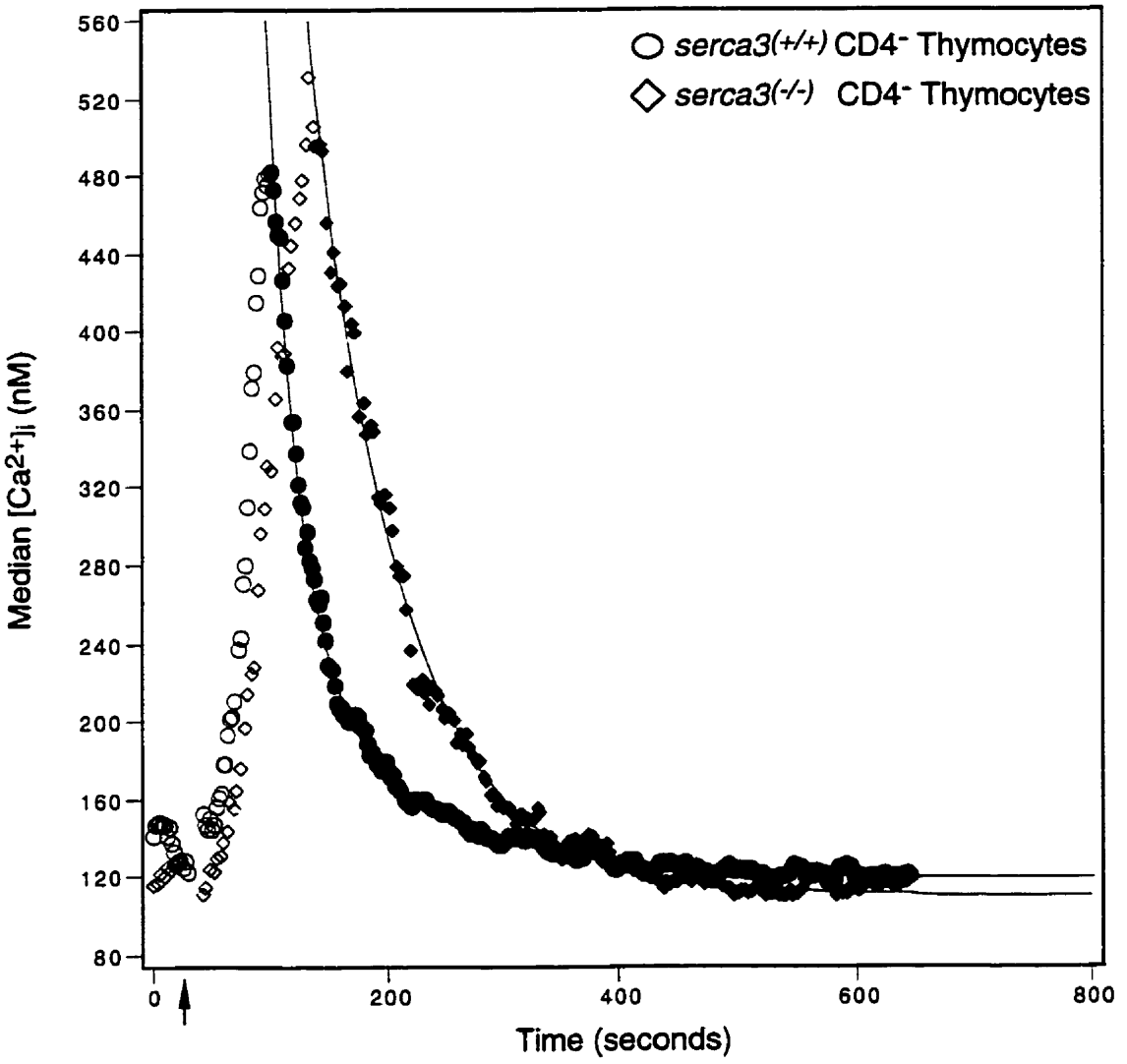

Fig. 21. **Calcium transients in CD4- thymocytes.** Kinetic changes in median $[Ca^{2+}]_i$ are shown for wild-type (O) and SERCA3-deficient cells (◇) that were loaded with fluo-3. Ca^{2+} transients were initated by the addition of secondary antibody (indicated by arrow) to cross-link anti-CD3e. Specific responses of $CD4^-$ cells were determined by gating on the cell population that stained negatively with PE-anti-CD4 antibodies. See Figure 17 for further details. This is a representative result of four independent experiments.

Table 9.

Summary of the Ca^{2+} signaling parameters in wild-type (WT) and SERCA3-deficient (KO) $CD4^-$ thymocytes (ie. $CD4^-CD8^-$/$CD4^-CD8^+$ cells) following the cross-linking of anti-CD3ε antibody on the cell surface.

Experiment		Baseline $[Ca^{2+}]_i$ (nM)	After CD3ε cross-linking: Peak $[Ca^{2+}]_i$ (nM)	After CD3ε cross-linking: Plateau $[Ca^{2+}]_i$ (nM)	$t_{1/2}$ of decline (seconds)	% non-responding $CD4^-CD8^-$ & $CD4^-CD8^+$ cells
1	WT	105	400	110	14, *88*	61
	KO	--	--	--	--	73
2	WT	115	345	120	11, *71*	56
	KO	115	270	110	40, *71*	84
3	WT	135	480	120	18, *85*	62
	KO	120	500	115	47, *85*	65
4	WT	--	--	--	--	68
	KO	--	--	--	--	71
Mean ±SEM	WT	118 ± 9	408 ± 39	146 ± 11	**15 ± 4**	62 ± 3
	KO	118 ± 3	385 ± 115	138 ± 16	**42 ± 2**	73 ± 4
		(p = 0.5)	(p = 0.67)	(p = 0.2)	**(p=0.047)**	(p = 0.15)

The results of four independent experiments and the resultant mean ± SEM, are presented. The Ca^{2+} concentrations before (baseline) and after stimulation are shown, as well as the half-time ($t_{1/2}$) of the declining portion of the transient. Curves were fit to two rate constants. The slower component was made equal for mutant and wild-type cells (in italics), and the fast component was compared. See Materials and Methods for further details. Values in bold indicate statistically significant differences between mutant and wild-type cells. Non-responding cells were excluded from all analyses. Dashes (--) indicate data that could not be fit accurately to exponential equations due to random variations in the values.

Based on the results of these experiments conducted on cells present in a suspension, SERCA3 activity contributes significantly to the decline of Ca^{2+} levels following the attainment of peak $[Ca^{2+}]_i$ in stimulated B cells and thymocytes, but not in splenic T cells, following anti-CD3ε cross-linking. The results also show that the baseline, peak and plateau $[Ca^{2+}]_i$ following antigen receptor stimulation are not altered in cells lacking SERCA3, suggesting that SERCA3 activity is either functionally redundant, or is compensated for with respect to these components of the Ca^{2+} transient.

Altered Ca^{2+} influx in SERCA3-deficient $CD4^+$ splenic T cells

Although the kinetic changes in the $[Ca^{2+}]_i$ levels of splenic T cells generated following TCR stimulation did not significantly differ from those of wild-type cells, secreted IL-2 concentrations were significantly reduced in SERCA3-deficient splenocytes in response to 10 nM PMA plus 100 nM A23187, and to a lesser extent with ConA. Since IL-2 expression is dependent on a sustained increase in $[Ca^{2+}]_i$ resulting from the influx of extracellular Ca^{2+}, I tested that role of SERCA3 in regulating Ca^{2+} influx in $CD4^+$ splenic T cells, which are the predominant expressors of IL-2.

This was done by cross-linking CD3ε of fluo-3-loaded *serca3*$^{-/-}$ T cells that were present in nominally Ca^{2+}-free extracellular medium that contained BAPTA. In addition, the cells were treated with thapsigargin to inhibit SERCA pump activity and, thus, the re-uptake of Ca^{2+} into intracellular stores (Lytton et al., 1991; Thastrup et al., 1990). Moreover, 100 nM A23187 was added to the extracellular medium following the return of $[Ca^{2+}]_i$ to baseline levels, in order to assess the amount of Ca^{2+} remaining in intracellular Ca^{2+} stores. Since the stimulation of the cells by anti-CD3ε cross-linking, thapsigargin and A23187 was done in the absence of extracellular Ca^{2+}, the observed increases in intracellular Ca^{2+} levels in response to these stimuli would be solely due to the release of

stored Ca^{2+}, and can therefore be used as a measure of the filling status of these intracellular Ca^{2+} stores (Gouy et al., 1990; Liu et al., 1998; Mason et al., 1991). In addition, the combination of CD3ε cross-linking, thapsigargin and A23187 treatments were expected to release all available Ca^{2+} from the intracellular stores responsive to these stimuli, and as a result, fully deplete them. This in turn was expected to cause a maximal activation of the capacitative calcium entry pathway (Gouy et al., 1990; Mason et al., 1991). The increase in $[Ca^{2+}]_i$ following the subsequent addition of Ca^{2+} to the extracellular medium, was then used as a measure of this influx pathway (Hofer et al., 1998; Liu et al., 1998).

As shown in Figure 22 and summarized in Table 10, the baseline Ca^{2+} concentrations in the presence of BAPTA were slightly higher in SERCA3-deficient cells as compared to wild-type cells, although the differences were not statistically significant. Following anti-CD3ε cross-linking and thapsigargin treatment, the increase in $[Ca^{2+}]_i$ was significantly reduced in *serca3*$^{(-/-)}$ $CD4^+$ T cells, as determined by the mean difference between the baseline and peak $[Ca^{2+}]_i$ (*serca3*$^{(+/+)}$, 67± 4 nM; *serca3*$^{(-/-)}$, 34 ± 5 nM; p = 0.03, n = 4), suggesting that less Ca^{2+} was released in SERCA3-deficient cells as compared to wild-type cells in response to stimulation. However, the mean peak $[Ca^{2+}]_i$ of both cell types in response to stimulation did not differ significantly (Table 10). As would be expected in the absence of extracellular Ca^{2+}, the $[Ca^{2+}]_i$ corresponding to the plateau phase of the Ca^{2+} transient was essentially identical to the initial baseline concentration (Table 10).

The subsequent addition of 100 nM A23187 did not cause a significant increase in intracellular Ca^{2+} levels in either SERCA3-deficient or control cells, suggesting that all A23187-responsive Ca^{2+} stores were depleted by the combined treatment of anti-CD3ε antibodies plus thapsigargin (Figure 22 and Table 10). Upon the addition of Ca^{2+} to the

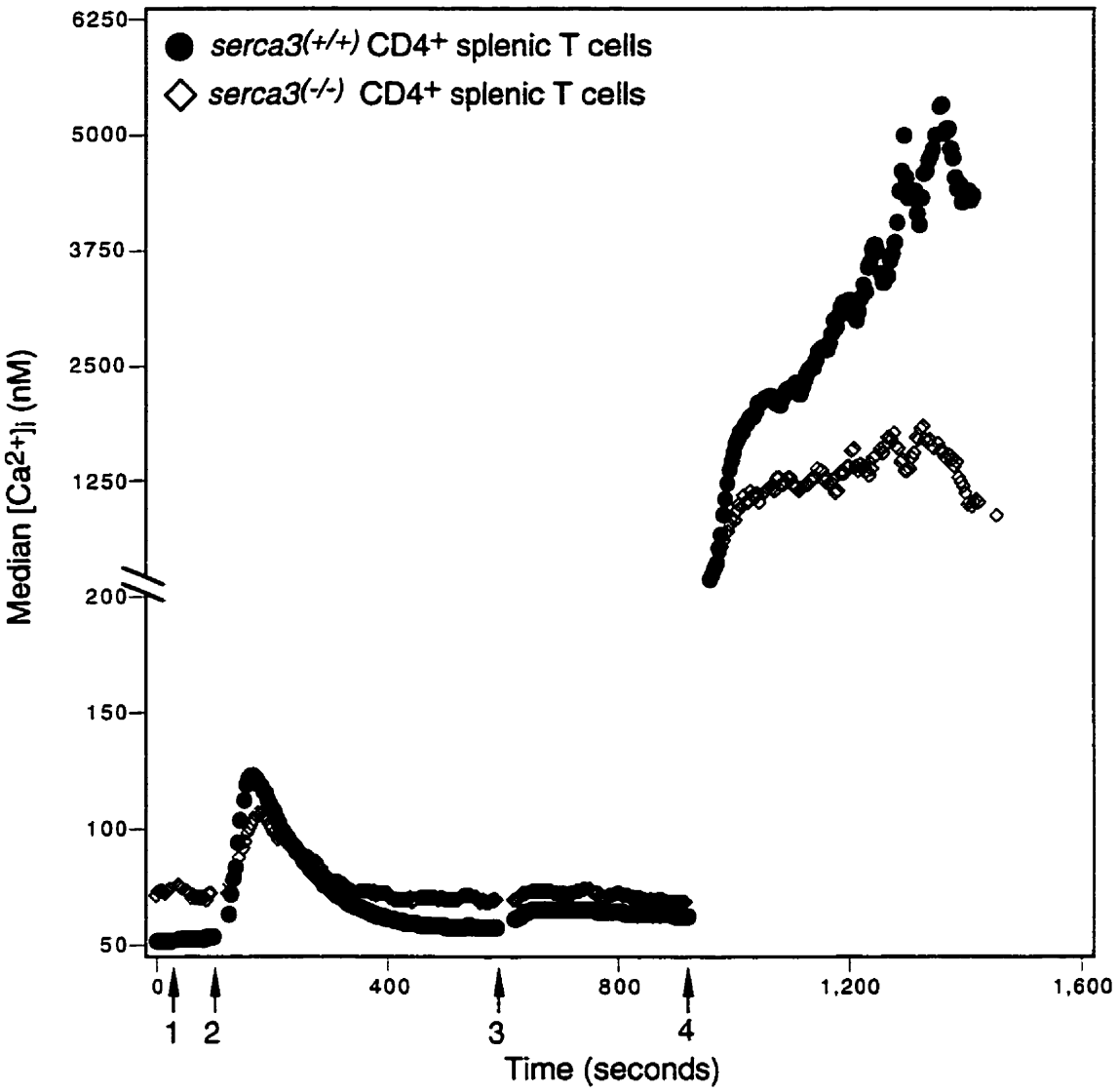

Fig. 22. **Examination of the size of intracellular Ca^{2+} stores and the Ca^{2+} influx pathway in CD4+ splenocytes.** Kinetic changes in $[Ca^{2+}]_i$ are shown for wild-type (●) and SERCA3-deficient (◇) cells that were loaded with fluo-3 and present in Ca^{2+}-free medium. The Ca^{2+} transient was initiated by the addition of anti-CD3e Ab plus thapsigargin (1). Anti-CD3e Ab was subsequently cross-linked with an anti-hamster IgG secondary Ab (2). Upon return to baseline Ca^{2+} levels, A23187 was added (3), followed by $CaCl_2$ (4). Resultant changes in fluorescence intensity were monitored with time using flow cytometric analysis. Specific responses of CD4+ splenocytes were determined by gating on the cell population that stained positively with a PE-anti-CD4 antibody. See Materials and Methods for more details. This is a representative result of four independent experiments.

Table 10.

Summary of the measurement of Ca^{2+} release and influx pathways in wild-type (WT) and SERCA3-deficient (KO) $CD4^+$ splenic T cells following the cross-linking of anti-CD3ε antibody and thapsigargin treatment.

Experiment		Baseline $[Ca^{2+}]_i$ (nM)	$[Ca^{2+}]_i$ After anti-CD3ε (nM)	After CD3ε cross-linking & thapsigargin treatment			
				Peak $[Ca^{2+}]_i$ (nM)	Plateau $[Ca^{2+}]_i$ (nM)	Mean $[Ca^{2+}]_i$ after A23187 (nM)	Peak $[Ca^{2+}]_i$ after $CaCl_2$ (nM)
1	WT	59	N/D	133	56	60	3,600
	KO	63	N/D	82	63	69	1,100
2	WT	52	53	123	58	64	5,000
	KO*	75	72	111	71	74	2,000
3	WT	56	57	114	61	66	10,500
	KO	56	70	95	58	64	8,880
4	WT	52	55	115	56	62	8,800
	KO	61	63	103	64	70	4,500
Mean±SEM	WT	55 ± 2	55 ± 1	121 ± 4	58 ± 1	63 ± 1	**6975±1608**
	KO	64 ± 4	68 ± 3	98 ± 6	64 ± 3	69 ± 2	**4120±1742**
		(p=0.17)	(p=0.05)	(p=0.09)	(p=0.16)	(p=0.11)	**(p = 0.01)**

The results of four independent experiments and the resultant mean ± SEM, are presented. The Ca^{2+} concentrations before (baseline) and after stimulation are shown, as well as the half-time ($t_{1/2}$) of the declining portion of the transient. Values in bold indicate statistically significant differences between mutant and wild-type cells. Sample marked with (*) had 25% non-responding cells, which were omitted from all analyses. N/D indicates "not done", because cells in this experiment were preincubated with anti-CD3ε antibody, which was cross-linked at the time of the experiment.

extracellular medium, the peak $[Ca^{2+}]_i$ observed in SERCA3-deficient cells was significantly reduced as compared to the levels observed in wild-type cells (Figure 22 and Table 10), revealing a marked decrease in the influx of Ca^{2+} in mutant cells in response to intracellular Ca^{2+} store depletion.

Together, these experiments showed that the intracellular Ca^{2+} stores of *serca3*$^{(-/-)}$ $CD4^+$ splenic T cells are more depleted than those of wild-type cells. This result suggest that SERCA3 has a functional role in maintaining the filling status of antigen- and thapsigargin-sensitive Ca^{2+} stores. Moreover, the results revealed a marked reduction in the Ca^{2+} influx pathway in the *serca3* mutant cells. The observed differences in calcium entry between mutant and wild-type $CD4^+$ splenic T cells shown in these experiments are in contrast with the results summarized in the previous section, where kinetic changes in the cytosolic Ca^{2+} concentration of SERCA3-deficient and wild-type $CD4^+$ splenic T cells bathed in HBS containing 1 mM Ca^{2+}, were not found to differ significantly following the cross-linking of anti-CD3ε antibodies.

Finally, the results reported here show that for both genotypes, the peak increase in intracellular Ca^{2+} levels in response to CD3ε ligation was markedly lower in the absence of extracellular Ca^{2+}, as compared to when Ca^{2+} was present in the extracellular medium (e.g. compare Table 6 to Table 10). A similar result has been shown by others examining Ca^{2+} fluxes in primary mouse $CD4^+$ splenic T cells (Liu et al., 1998). This result therefore demonstrates that the influx of extracellular Ca^{2+} is the major component that determines the magnitude of both the peak and sustained levels of intracellular Ca^{2+} following the stimulation of the antigen receptor on $CD4^+$ splenic T cells.

CHAPTER FOUR: DISCUSSION

I. Overview

The aim of my research was to determine the physiological role of SERCA3 in lymphocytes. Previously published studies have revealed the importance of Ca^{2+} signals in mediating lymphocyte maturation and activation (Clipstone and Crabtree, 1992; Nakayama et al., 1992; Weiss and Littman, 1994), as well as both T cell mobility and contact with antigen-presenting cells (Negulescu et al., 1996). Increases in $[Ca^{2+}]_i$ following antigen receptor ligation result from the release of stored Ca^{2+}, and capacitative Ca^{2+} influx. As demonstrated by the results reported here, the influx of extracellular Ca^{2+} is the predominant determinant of the magnitude of the Ca^{2+} signal. Therefore, the maintenance of the Ca^{2+} stores, and the resequestration of Ca^{2+} after its release, likely play a critical role in mediating cellular responses to antigen.

The abundance of SERCA3 in lymphocytes, together with its distinct biochemical properties suggest that it may have a unique role in regulating lymphocyte Ca^{2+} signaling and cellular activation. This hypothesis was tested by examining kinetic changes in $[Ca^{2+}]_i$ following antigen receptor stimulation in cells isolated from SERCA3 homozygous mutant mice. In addition, the secretion of IL-2 in response to cellular stimulation *in vitro* was examined to determine if SERCA3 has a functional role in early T cell activation.

II. Role for SERCA3 in regulating Ca^{2+} fluxes in splenic B cells and thymocytes

In splenic B cells, and both $CD4^+$ and $CD4^-$ thymocytes lacking SERCA3, a slower rate of decline of intracellular Ca^{2+} levels was observed in response to antigen receptor

stimulation. Interestingly, when the decline phase of Ca^{2+} transients showed two distinct components, the mutant and wild-type cells consistently differed with respect to the fast component that occurs immediately after the peak $[Ca^{2+}]_i$ is reached. Peak intracellular levels are obtained when antigen-responsive stores have been depleted and a balance exists between the mechanisms of Ca^{2+} influx, reuptake and extrusion. The fast decline that follows is due to the rate of reuptake exceeding the rate of Ca^{2+} influx. SERCA2b has been shown to have a higher apparent Ca^{2+} affinity and a slower rate of Ca^{2+} transport and ATP hydrolysis, suggesting that the reaction cycle of this isozyme is slower compared to other SERCA proteins (Lytton et al., 1992). The slower decline of Ca^{2+} levels in the SERCA3-deficient cells may therefore reflect the inability of SERCA2b to fully compensate for SERCA3 activity when intracellular Ca^{2+} levels are at their highest (Lytton et al., 1992).

III. SERCA3 expression is not necessary for B cell or T cell maturation

The altered kinetics of the Ca^{2+} transients generated in B cells lacking SERCA3 were not found to be associated with changes in the representation of B cells in the spleen. These findings are supported by the results of more detailed experiments that showed the percent distribution of mature and maturing splenic B cells (determined by examining the surface expression of IgD and IgM) are unaffected in mice lacking SERCA3 (Liu unpublished results). In mature B cells, the activation of antigen receptors induces cell proliferation and the secretion of antibodies. It would be important therefore, to determine if the observed alteration in Ca^{2+} signaling effects these cellular responses following BCR stimulation.

A significant reduction in the rate of declining Ca^{2+} levels was also observed following antigen receptor stimulation of thymocytes. $CD4^+$ cells represent about 95% thymocytes (see Figure 5 and Table 2) and included 10-15% mature $CD4^+$ thymocytes (ie.

$CD4^+CD8^-$) and 80-85% $CD4^+CD8^+$ thymocytes, which are the cells that undergo intense selection in the thymus. The majority of $CD4^+$ cells expressed low levels of CDε on their cell surface, whereas a minority of $CD4^+$ cells, which may represent single positive mature cells, expressed high levels of CD3ε. Therefore, it is unclear if the Ca^{2+} responses observed in $CD4^+$ cells following anti-CD3ε antibody cross-linking are the same for both low and high CD3ε-expressing cells. It will be important to examine the calcium response in $CD8^-$ cells, most of which correspond to the CD4 single positives. Similarly, $CD4^-$ thymocytes are a mixture of both mature $CD8^+$ thymocytes (ie. $CD4^-CD8^+$; 3% of thymocytes), and the immature $CD4^-CD8^-$ thymocytes (2% of cells). Thus it is unclear if both cell populations have equally altered Ca^{2+} signaling kinetics.

SERCA3 is most abundantly expressed in the cortical region of the thymus (Wu et al., 1995), which contains maturing thymocytes undergoing selection (ie. $CD4^+CD8^+$ cells) (Abbas et al., 1997). This is consistent with my data demonstrating an important role for SERCA3 in buffering Ca^{2+} changes in $CD4^+CD8^+$ cells. Despite lower levels of SERCA3 in other thymic regions, my data support a significant role for SERCA3 in all thymocytes, no matter what state of maturation.

A significant reduction in *serca3*$^{-/-}$ thymocyte proliferation has been observed in response to *in vitro* stimulation with PMA/A23187, and to a lesser extent with ConA (L. Liu, unpublished results). Although thymocytes were stimulated by the activation of CD3ε in my experiments, the slower rate of decline in intracellular Ca^{2+} levels may be sufficient to alter the proliferative response of these cells to stimulation, or may induce the death of cells and thus decrease the proportion of cells capable of responding to stimulation. Flow cytometric analysis, however, revealed no difference in the distribution of immature versus maturing thymocytes, and no differences in the expression of CD3ε in cells lacking SERCA3. Similarly, the distribution of mature T cells in the periphery was not different

from that of wild-type control cells. Therefore, the expression of SERCA3 does not appear to be necessary for T cell maturation. The results, however, clearly show that SERCA3 has a role in the regulation of Ca^{2+} fluxes in thymocytes in response to antigen receptor stimulation.

IV. A role for SERCA3 in the regulation of IL-2 expression and Ca^{2+} influx in splenic T cells

SERCA3-deficient splenic T cells stimulated *in vitro* showed a significant reduction in IL-2 secretion in response to 10 nM PMA plus 100 nM A23187, that did not appear to be due to a decrease in cell viability, thus revealing a role for SERCA3 in early T cell activation. However, examination of the Ca^{2+} transients induced following cross-linking of anti-CD3ε antibodies on the surface of splenic T cells revealed no differences in the kinetic changes in $[Ca^{2+}]_i$, nor in the magnitude of the baseline, peak, or plateau phases of the Ca^{2+} signal.

IL-2 expression requires a sustained elevation of $[Ca^{2+}]_i$ that is dependent on capacitative Ca^{2+} influx (Wacholtz and Lipsky, 1993; Weiss et al., 1987). Examination of the filling status of the intracellular Ca^{2+} stores of both *serca3*$^{(-/-)}$ and *serca3*$^{(+/+)}$ $CD4^+$ splenic T cells, showed that the CD3ε- and thapsigargin-sensitive stores of the mutant cells are more depleted than those of wild-type cells (see Figure 22), revealing that SERCA3 regulates the filling status of these stores. Surprisingly, when the intracellular stores of both genotypes were maximally depleted by the subsequent addition of 100 nM A23187, and Ca^{2+} was then added to the cells, a significant reduction in the magnitude of Ca^{2+} influx was observed in the mutant cells as compared to the wild-type cells. These results therefore suggest an uncoupling of the depletion of intracellular stores, to the influx of extracellular Ca^{2+} in *serca3*$^{(-/-)}$ $CD4^+$ splenic T cells. In addition, the reduced magnitude of Ca^{2+} influx in

the *serca3* mutant cells may explain why lower levels of IL-2 were secreted by these cells in response to PMA plus A23187.

To determine if the deficit in IL-2 production in the SERCA3-deficient cells is a direct result of a reduction in the influx pathway, it will be necessary to determine if the cells are capable of producing similar levels of IL-2 as wild-type cells. This could be accomplished by transiently overexpressing a constitutively active form of calcineurin and examining secreted levels of IL-2 by *serca3*$^{(-/-)}$ and *serca3*$^{(+/+)}$ cells (O'Keefe et al., 1992). This mutant form of calcineurin in combination with PMA treatment has been shown to transcriptionally activate an IL-2 reporter gene construct independent of changes in $[Ca^{2+}]_i$ (O'Keefe et al., 1992). The results of such experiments would therefore confirm that the reduced levels of secreted IL-2 by SERCA3 mutant cells are a result of altered Ca^{2+} signaling, and are not due to alterations in the signaling pathway downstream of calcineurin activation. In addition, although the results suggest that the decrease in secreted levels of IL-2 following *in vitro* stimulation is due to a reduction in IL-2 expression by individual cells, this should be confirmed by examining intracellular IL-2 levels in permeabilized cells using flow cytometric analysis.

V. Coupling of intracellular stores to Ca^{2+} entry in *serca3*$^{(-/-)}$ cells

In lymphocytes, the influx of extracellular Ca^{2+} is believed to occur predominately through CRAC channels at the plasma membrane (Fanger et al., 1995; Lewis and Cahalan, 1995), and the magnitude of Ca^{2+} influx has been shown to be regulated by the degree of intracellular Ca^{2+} store depletion (Hofer et al., 1998). The mechanism by which store depletion is coupled to the influx of Ca^{2+} is not well understood. Moreover, CRAC channels have not as yet been identified molecularly. However, one way to determine if less Ca^{2+} is entering the SERCA3-deficient $CD4^+$ T cells, would be to measure the current

induced following cellular stimulation in both mutant and wild-type cells. In addition, based on macroscopic and single channel currents, and the average open probability of the channels, it may be possible to estimate the number of CRAC channels expressed on the cell surface of SERCA3-deficient lymphocytes, and determine if the number differs significantly from that estimated for wild-type cells (Kerschbaum and Cahalan, 1999).

A down-regulation of the influx pathway may explain why no differences were observed in the basal Ca^{2+} levels and the kinetic changes in intracellular Ca^{2+} in SERCA3-deficient and wild-type splenic T cells in response to anti-CD3ε antibody cross-linking. Although the stores may be more depleted in the absence of SERCA3, which would tend to activate influx, by decreasing influx capacity, cells are able to maintain intracellular Ca^{2+} homeostasis. Only when the influx of Ca^{2+} is maximally stimulated in the cells of both genotypes does the deficit in the influx pathway become apparent, with respect to intracellular Ca^{2+} levels and the expression of IL-2. Interestingly, the fraction of IL-2 secreted in response to less potent stimuli (ie. plate-bound anti-CD3ε plus anti-CD28 antibodies, and ConA) relative to the maximal response of each genotype tended to be similar, or slightly greater for the SERCA3-deficient cells, although the differences were not statistically significant. These results may indicate that lymphocytes lacking SERCA3 are capable of responding equally as well as wild-type cells to less potent stimuli, perhaps because down-regulation of the influx pathway compensates for increased activation due to greater store depletion.

A reduction in the magnitude of the influx of extracellular Ca^{2+} could be due to either a reduction in Ca^{2+} influx or an increase in the rate of Ca^{2+} extrusion. Thus, an alternative explanation for the reduced peak in $[Ca^{2+}]_i$ observed in *serca3*$^{(-/-)}$ cells following re-addition of Ca^{2+} to the medium, is that pathways such as the plasma membrane calcium pump (Lewis and Cahalan, 1995) or mitochondrial sequestration (Hoth and Fanger, 1997),

were increased. If the mechanisms responsible for the removal of cytosolic Ca^{2+} were up-regulated, one might have expected to see a decrease in the peak $[Ca^{2+}]_i$ in mutant cells in response to anti-CD3ε antibody cross-linking. The results, however, show that the peak Ca^{2+} concentration following CD3ε cross-linking and thapsigargin treatment was the same for both mutant and wild-type cells.

Thus, the amount of Ca^{2+} released from intracellular stores and the amount removed from the cytosol resulted in a net change in $[Ca^{2+}]_i$ in the mutant cells that was not different from that observed in wild-type cells. Moreover, a reduced amount of Ca^{2+} was released from the mutant cells in response to anti-CD3ε Ab cross-linking and thapsigargin treatment. Given that SERCA activity was inhibited by 1 μM thapsigargin in these experiments, theses results support the conclusion that mechanisms involved in decreasing cytosolic Ca^{2+} levels during signal transduction are not up-regulated in SERCA3-deficient cells, and instead either remained unchanged or may be down-regulated.

VI. SERCA expression and its contribution to Ca^{2+} handling in lymphocytes

The size of intracellular Ca^{2+} stores and the Ca^{2+} influx pathway should be similarly examined in B cells and thymocytes to determine if common mechanisms of compensation are observed here. In addition, it would be interesting to test the filling status of TCR-responsive Ca^{2+} stores using ConA. This lectin appears to specifically interact with the CD3ε/TCR complex of T cells and can be dissociated from the TCR by the addition of α-methyl mannoside, which binds ConA but not the TCR (Weiss et al., 1987). The reapplication of ConA, or subsequent CD3ε activation could then be used to examine the extent of refilling of intracellular Ca^{2+} stores in cells lacking SERCA3. Liu et al. showed that acetylcholine (Ach)-responsive Ca^{2+} stores in endothelial cells lacking SERCA3 are

more depleted and are not refilled following the removal of Ach, suggesting that SERCA3 regulates a Ca^{2+} pool that is distinct from that regulated by SERCA2b (Liu et al., 1997). It would be interesting therefore to determine the extent to which SERCA3 and SERCA2b regulate Ca^{2+} stores responsive to antigen receptor activation.

Although SERCA3-deficient splenic B cells and thymic T cells showed a slower rate of decline of Ca^{2+} in response to cellular stimulation, no such differences were observed in splenic T cells. Therefore, the ablation of SERCA3 has differential effects in these cell types. This could reflect differences in the contribution of SERCA3 to the handling of Ca^{2+} during signal transduction in these cells. For example, SERCA3 could play a more prominent role resequestering released Ca^{2+} in B cells and thymocytes. This notion is supported by the observation that SERCA3 is more abundantly expressed than SERCA2b in these cells (Wu et al., 1995). Therefore, the loss of SERCA3 function could be less well compensated for in splenic B cells and thymocytes. Conversely, compensation by increased SERCA2b expression or by other mechanisms may explain why the rate of decline $[Ca^{2+}]_i$ was not slower in splenic T cells lacking SERCA3.

In addition, given that IL-2 expression was altered in these cells, SERCA3 expression may be important for regulating the frequency of Ca^{2+} oscillations, which would not be evident with the experimental protocols employed here. This could be determined using Ca^{2+} imaging to examine the responses of single lymphocytes, loaded with Ca^{2+} indicating dye, to stimulation. These experiments would allow one to determine if the frequency of oscillating Ca^{2+} levels are altered in these cells in the absence of SERCA3.

Unfortunately, the experiments outlined in this thesis aimed at examining possible alterations in the expression of SERCA2b in *serca3*$^{-/-}$ lymphocytes were inconclusive. The fact that changes in the Ca^{2+} transients generated following cellular stimulation were observed in splenic B cells but not in splenic T cells, could reflect differences in the

compensatory changes adopted by these cells in response to the loss of SERCA3 activity. It may be important therefore to separate the two cell types when examining the expression levels of SERCA2b and other Ca^{2+}-regulating proteins. In addition, given the low sensitivity of the available SERCA2-specific antibody for detecting mouse SERCA2b in whole-cell lysates, it may be worthwhile to obtain microsomal fractions from cells in order to enrich for SERCA2b in protein samples.

VII. Conclusion

SERCA3 is abundantly expressed in lymphoid tissues, suggesting its expression is important for the regulation of Ca^{2+} homeostasis in these cells. Surprisingly, mice with an inactivated SERCA3 gene appear phenotypically normal. In addition, the results of my experiments on lymphocytes isolated from these animals indicate that there are no alterations in the distribution or maturation of B cells and T cell subtypes in the absence of SERCA3.

However, some changes in the dynamics of Ca^{2+} regulation were observed. Most notably was the reduction in the Ca^{2+} influx pathway in SERCA3-deficient $CD4^+$ splenic T cells, which correlated with a marked decrease in IL-2 expression by these cells in response to potent stimuli *in vitro* . Therefore, defects in cell function resulting from the ablation of *serca3* appear to be revealed only when the Ca^{2+} handling requirements of the cell are at there highest.

My results contrast those of Liu et al. who examined effects of serca3 mutation on endothelial cell function. They showed a marked reduction in the release of Ca^{2+} from these cells in response to acetylcholine stimulation, even at relatively low concentrations, suggesting that SERCA3 regulates a functionally distinct intracellular Ca^{2+} store in endothelial cells. The experiments presented in this thesis showed that SERCA3 activity

was only critically important when the demand on Ca^{2+} handling was high, suggesting that either SERCA2b expression, or other mechanisms of calcium regulation, compensate for the lack of SERCA3 expression in lymphocytes. Thus under a normal range of physiological conditions these cells are able to maintain Ca^{2+} homeostasis in the absence of SERCA3 expression. The identification of the compensatory changes may provide additional insight regarding the functional significance of high SERCA3 expression in lymphocytes.

BIBLIOGRAPHY

Abbas, A. K., Lichtman, A. H., and Pober, J. S. (1997). Cellular and Molecular Immunology, 3 Edition (Philadelphia: W. B. Saunders Company).

Akha, A. A. S., Wilmott, N. J., Brickley, K., Dolphin, A. C., Galione, A., and Hunt, S. V. (1996). Anti-Ig-induced calcium influx in rat B lymphocytes mediated by cGMP through a dihydropyridine-senstive channel. *J Biol Chem* **271**, 7297-7300.

Anger, M., Samuel, J. L., Marotte, F., Wuytack, F., Rappaport, L., and Lompre, A. M. (1993). The sarco(endo)plasmic reticulum Ca(2+)-ATPase mRNA isoform, SERCA 3, is expressed in endothelial and epithelial cells in various organs. *FEBS Lett* **334**, 45-8.

Ashton-Rickardt, P. G., Bandeira, A., Delaney, J. R., Van Kaer, L., Pircher, H. P., Zinkernagel, R. M., and Tonegawa, S. (1994). Evidence for a differential avidity model of T cell selection in the thymus [see comments]. *Cell* **76**, 651-63.

Ausubel, F. M., Brent, R., Kingston, R. E., Moore, D. D., Seidman, J. G., Smith, J. A., and Struhl, K. (1997). Current Protocols in Molecular Biology (New York, N. Y.: John Wiley & Sons).

Bayle, D., Weeks, D., and Sachs, G. (1995). The membrane topology of the rat sarcoplasmic and endoplasmic reticulum calcium ATPases by in vitro translation scanning. *J Biol Chem* **270**, 25678-84.

Berridge, M. J. (1997). The AM and FM of calcium signalling. *Nature* **386**, 759-760.

Berridge, M. J. (1997). Lymphocyte activation in health and disease. *Crit Rev Immunol* **17**, 155-78.

Berridge, M. J., and Irvine, R. F. (1989). Inositol phosphate and cell signaling. *Nature* **341**, 197-205.

Birnbaumer, L., Zhu, X., Jiang, M., Boulay, G., Peyton, M., Vannier, B., Brown, D., Platano, D., Sadeghi, H., Stefani, E., and Birnbaumer, M. (1996). On the molecular basis and regulation of cellular capacitative calcium entry: roles for Trp proteins. *Proc Natl Acad Sci U S A* **93**, 15195-202.

Blaustein, M. P., and Lederer, W. J. (1999). Sodium/calcium exchange: its physiological implications. *Physiol Rev* **79**, 763-854.

Bobe, R., Lacabaratz-Porret, C., Bredoux, R., Martin, V., Ozog, A., Launay, S., Corvazier, E., Kovacs, T., Papp, B., and Enouf, J. (1998). Expression of two isoforms of the third sarco/endoplasmic reticulum Ca2+ ATPase (SERCA3) in platelets. Possible recognition of the SERCA3b isoform by the PL/IM430 monoclonal antibody. *FEBS Lett* **423**, 259-64.

Brandl, C. J., deLeon, S., Martin, D. R., and MacLennan, D. H. (1987). Adult forms of the Ca2+ ATPase of sarcoplasmic reticulum: Expression in developing skeletal muscle. *J. Biol. Chem.* **262**, 3768-3774.

Bubien, J. K., Zhou, L. J., Bell, P. D., Frizzell, R. A., and Tedder, T. F. (1993). Transfection of the CD20 cell surface molecule into ectopic cell types generates a Ca2+ conductance found constitutively in B lymphocytes. *J Cell Biol* **121**, 1121-32.

Burk, S. E., Lytton, J., MacLennan, D. H., and Shull, G. E. (1989). cDNA cloning, functional expression, and mRNA tissue distribution of a third organellar Ca2+ pump. *J. Biol. Chem.* **264**, 18561-18568.

Camacho, P., and Lechleiter, J. D. (1995). Calreticulin inhibits repetitive intracellular Ca2+ waves. *Cell* **82**, 765-71.

Camacho, R., and Lechleiter, J. D. (1993). Increased frequency of calcium waves in *Xenopus laevis* oocytes that express a calcium-ATPase. *Science* **260**, 226-229.

Campbell, A. M., Kessler, P. D., and Fambrough, D. M. (1992). The alternative carboxyl termini of avian cardiac and brain sarcoplasmic reticulum/endoplasmic reticulum Ca(2+)-ATPases are on opposite sides of the membrane. *J Biol Chem* **267**, 9321-5.

Cantrell, D. A., and Smith, K. A. (1984). The interleukin-2 T-cell system: a new cell growth model. *Science* **224**, 1312-6.

Chen, L., Glover, J. N. M., Hogan, P. G., Rao, A., and Harrison, S. C. (1998). Structure of the DNA-binding domains from NFAT, Fos and Jun bound specifically to DNA. *Nature* **392**, 42-48.

Chow, C. W., Rincon, M., and Davis, R. J. (1999). Requirement for transcription factor NFAT in interleukin-2 expression. *Mol Cell Biol* **19**, 2300-7.

Clapham, D. E. (1995). Calcium Signaling. *Cell* **80**, 259-268.

Clipstone, N. A., and Crabtree, G. R. (1992). Identification of calcineurin as a key signalling enzyme in T-lymphocyte activation. *Nature* **357**, 695-697.

Coligan, J. E., Kruisbeek, A. M., Margulies, D. H., Shevach, E. M., and Strober, W. (1997). Current Protocols in Immunology (New York, N. Y.: John Wiley & Sons).

Crabtree, G. R., and Clipstone, N. A. (1994). Signal transmission between the plasma membrane and nucleus of T lymphocytes. *Annu. Rev. Biochem.* **63**, 1045-1083.

Csutora, P., Su, Z., Kim, H. Y., Bugrim, A., Cunningham, K. W., Nuccitelli, R., Keizer, J. E., Hanley, M. R., Blalock, J. E., and Marchase, R. B. (1999).

Calcium influx factor is synthesized by yeast and mammalian cells depleted of organellar calcium stores. *Proc Natl Acad Sci U S A* **96**, 121-6.

Dasgupta, J. D., Granja, c., Druker, B., Lin, L.-L., Yunis, E. J., and Relias, V. (1992). Phospholipase C-γ1 association with CD3 structure in T cells. *J. Exp. Med.* **175**.

DeFranco, A. L. (1997). The complexity of signaling pathways activated by the BCR. *Curr. Opin. Immunol.* **9**, 296-308.

Dode, L., De Greef, C., Mountian, I., Attard, M., Town, M. M., Casteels, R., and Wuytack, F. (1998). Structure of the human sarco/endoplasmic reticulum Ca2+-ATPase 3 gene. Promoter analysis and alternative splicing of the SERCA3 pre-mRNA. *J Biol Chem* **273**, 13982-94.

Dolmetsch, R. E., Lewis, R. S., Goodnow, C. C., and Healy, J. I. (1997). Differential activation of transcription factors induced by Ca2+ response amplitude and duration. *Nature* **386**, 855-858.

Dolmetsch, R. E., Xu, K., and Lewis, R. S. (1998). Calcium oscillations increase the efficiency and specificity of gene expression [see comments]. *Nature* **392**, 933-6.

Donnadieu, E., Bismuth, G., and Trautmann, A. (1992). Calcium fluxes in T lymphocytes. *J Biol Chem* **267**, 25864-72.

Donnadieu, E., Cefai, D., Tan, Y. P., Paresys, G., Bismuth, G., and Trautmann, A. (1992). Imaging early steps of human T cell activation by antigen-presenting cells. *J Immunol* **148**, 2643-53.

Fanger, C. M., Hoth, M., Crabtree, G. R., and Lewis. R. S. (1995). Characterization of T cell mutants with defects in capacitative calcium entry: Genetic evidence for the physiological roles of CRAC channels. *J. Cell Biol.* **131**, 655-667.

Gelfand, E. W., Cheung, R. K., Mills, G. B., and Grinstein, S. (1988). Uptake of extracellular Ca2+ and not recruitment from internal stores is essential for T lymphocyte proliferation. *Eur J Immunol* **18**, 917-22.

Girard, S., and Clapham, D. (1993). Acceleration of intracellular calcium waves in Xenopus oocytes by calcium influx. *Science* **260**, 229-32.

Givan, A. L. (1992). Flow Cytometry: First principles (New York, New York: John Wiley & Sons, Inc.).

Gold, M. R., and Aebersold, R. (1994). Both phosphatidylinositol 3-kinase and phosphatidylinositol 4-kinase products are increased by antigen receptor signaling in B cells. *J Immunol* **152**, 42-50.

Gold, M. R., Chan, V. W., Turck, C. W., and DeFranco, A. L. (1992). Membrane Ig cross-linking regulates phosphatidylinositol 3-kinase in B lymphocytes. *J Immunol* **148**, 2012-22.

Goldsmith, M. A., and Weiss, A. (1988). Early signal transduction by the antigen receptor without commitment to T cell activation. *Science* **240**, 1029-1031.

Gouy, H., Cefai, D., Christensen, S. B., Debre, P., and Bismuth, G. (1990). Ca2+ influx in human T lymphocytes is induced independently of inositol phosphate production by mobilization of intracellular Ca2+ stores. A study with the Ca2+ endoplasmic reticulum-ATPase inhibitor thapsigargin. *Eur J Immunol* **20**, 2269-75.

Grynkiewicz, G., Poenie, M., and Tsien, R. Y. (1985). A new generation of Ca^{2+} indicators with greatly improved fluorescence properties. *J. Biol. Chem.* **260**, 3440-3450.

Hakamata, Y., Nishimura, S., Nakai, J., Nakashima, Y., Kita, T., and Imoto, K. (1994). Involvement of the brain type of ryanodine receptor in T-cell proliferation. *FEBS Lett* **352**, 206-10.

Harnick, D. J., Jayaraman, T., Ma, Y., Mulieri, P., Go, L. O., and Marks, A. R. (1995). The human type I inositol 1,4,5-triphosphate receptor from T lymphocytes: Structure, localization, and tyrosine phosphorylation. *J. Biol. Chem.* **270**, 2833-2840.

He, H., Giordano, F. J., Hilal-Dandan, R., Choi, D.-J., Rockman, H. A., McDonough, P. M., Bluhm, W. F., Meyer, M., Sayen, M. R., Swanson, E., and Dillmann, W.

H. (1997). Overexpression of the rat sarcoplasmic reticulum Ca^{2+} ATPase gene in the heart of transgenic mice accelerates calcium transients and cardiac relaxation. *J. Clin. Invest.* **100**, 380-389.

Hesketh, T. R., Smith, G. A., Moore, J. P., Taylor, M. V., and Metcalfe, J. C. (1983). Free cytoplasmic calcium concentration and the mitogenic stimulation of lymphocytes. *J Biol Chem* **258**, 4876-82.

Hofer, A. M., Fasolato, C., and Pozzan, T. (1998). Capacitative Ca^{2+} entry is closely linked to the filling state of internal Ca^{2+} stores: A study using simultaneous measurements of I_{crac} and intraluminal $[Ca^{2+}]$. *J. Cell Biol.* **140**, 325-334.

Hoth, M., and Fanger, C. M. (1997). Mitochondrial regulation of store-operated calcium signaling in T lymphocytes. *J. Cell Biol.* **137**, 633-648.

Imboden, J. B., and Stobo, J. D. (1985). Transmembrane signaling by the T cell antigen receptor: Perturbation of the T3-antigen receptor complex generates inositol phosphates and releases calcium ions from intracellular stores. *J. Exp. Med.* **161**, 446-456.

Imboden, J. B., Weiss, A., and Stobo, J. D. (1985). The antigen receptor on a human T cell line initiates activation by increasing cytoplasmic free calcium. *J Immunol* **134**, 663-5.

Iwashima, M., Irving, B. A., van Oers, N. S., Chan, A. C., and Weiss, A. (1994). Sequential interactions of the TCR with two distinct cytoplasmic tyrosine kinases. *Science* **263**, 1136-1139.

Izquierdo, M., and Cantrell, D. A. (1992). T-cell activation. *Trends Cell Biol.* **2**, 268-271.

Jacinto, E., Werlen, G., and Karin, M. (1998). Cooperation between Syk and Rac1 leads to synergistic JNK activation in T lymphocytes. *Immunity* **8**, 31-41.

Janeway, C. A., Jr., and Bottomly, K. (1994). Signals and signs for lymphocyte responses. *Cell* **76**, 275-285.

Ji, Y., Loukianov, E., Loukianova, T., Jones, L. R., and Periasamy, M. (1999). SERCA1a can functionally substitute for SERCA2a in the heart. *Am J Physiol* **276**, H89-97.

Jiang, S., Chow, S. C., Nicotera, P., and Orrenius, S. (1994). Intracellular Ca2+ signals activate apoptosis in thymocytes: studies using the Ca(2+)-ATPase inhibitor thapsigargin. *Exp Cell Res* **212**, 84-92.

Kanzaki, M., Lindorfer, M. A., Garrison, J. C., and Kojima, I. (1997). Activation of the calcium-permeable cation channel CD20 by alpha subunits of the Gi protein. *J Biol Chem* **272**, 14733-9.

Kanzaki, M., Shibata, H., Mogami, H., and Kojima, I. (1995). Expression of calcium-permeable cation channel CD20 accelerates progression through the G1 phase in Balb/c 3T3 cells. *J Biol Chem* **270**, 13099-104.

Kao, J., Fortner, C. N., Liu, L. H., Shull, G. E., and Paul, R. J. (1999). Ablation of the SERCA3 gene alters epithelium-dependent relaxation in mouse tracheal smooth muscle. *Am J Physiol* **277**, L264-70.

Kao, J. P. Y. (1994). Practical aspects of measuring [Ca^{2+}] with fluorescent indicators. In A practical guide to the study of calcium in living cells, R. Nuccitelli, ed. (San Diego, CA: Academic Press, Inc.), pp. 155-181.

Kerschbaum, H. H., and Cahalan, M. D. (1999). Single-channel recording of a store-operated Ca2+ channel in Jurkat T lymphocytes. *Science* **283**, 836-9.

Kishimoto, H., and Sprent, J. (1999). Several different cell surface molecules control negative selection of medullary thymocytes. *J Exp Med* **190**, 65-73.

Kurosaki, T. (1999). Genetic analysis of B cell antigen receptor signaling. *Annu Rev Immunol* **17**, 555-92.

Kurosaki, T. (1997). Molecular mechanisms in B cell antigen receptor signaling. *Curr Opin Immunol* **9**, 309-18.

Launay, S., Bobe, R., Lacabaratz-Porret, C., Bredoux, R., Kovacs, T., Enouf, J., and Papp, B. (1997). Modulation of endoplasmic reticulum calcium pump expression during T lymphocyte activation. *Journal of Biological Chemistry* **272**, 10746-10750.

Launay, S., Gianni, M., Kovacs, T., Bredoux, R., Bruel, A., Gelebart, P., Zassadowski, F., Chomienne, C., Enouf, J., and Papp, B. (1999). Lineage-specific modulation of calcium pump expression during myeloid differentiation. *Blood* **93**, 4395-405.

Lee, M. G., Xu, X., Zeng, W., Diaz, J., Kuo, T. H., Wuytack, F., Racymaekers, L., and Muallem, S. (1997). Polarized expression of Ca2+ pumps in pancreatic and salivary gland cells. Role in initiation and propagation of [Ca2+]i waves. *J Biol Chem* **272**, 15771-6.

Lewis, R. S., and Cahalan, M. D. (1995). Potassium and calcium channels in lymphocytes. *Annu. Rev. Immunol.* **13**, 623-653.

Li, W., Llopis, J., Whitney, M., Zlokarnik, G., and Tsien, R. Y. (1998). Cell-permeant caged InsP3 ester shows that Ca2+ spike frequency can optimize gene expression [see comments]. *Nature* **392**, 936-41.

Liu, K.-Q., Bunnell, S. C., Gurniak, C. B., and Berg, L. J. (1998). T cell receptor-initiated calcium release is uncoupled from capacitative calcium entry in Itk-deficient T cells. *J. Exp. Med.* **187**, 1721-1727.

Liu, L. H., Paul, R. J., Sutliff, R. L., Miller, M. L., Lorenz, J. N., Pun, R. Y. K., Duffy, J. J., Doetschman, T., Kimura, Y., MacLennan, D. H., Hoying, J. B., and Shull, G. E. (1997). Defective endothelium-dependent relaxation of vascular smooth muscle and endothelial cell Ca^{2+} signaling in mice lacking sarco(endo)plasmic reticulum Ca^{2+}-ATPase isoform 3. *J. Biol. Chem.* **272**, 30538-30545.

Loh, C., Shaw, K. T.-Y., Carew, J., Viola, J. P. B., Luo, C., Perrino, B. A., and Rao, A. (1996). Calcineurin binds the transcription factor NFAT1 and reversibly regulates its activity. *J. Biol. Chem.* **271**, 10884-10891.

Loukianov, E., Ji, Y., Grupp, I. L., Kirkpatrick, D. L., Baker, D. L., Loukianova, T., Grupp, G., Lytton, J., Walsh, R. A., and Periasamy, M. (1998). Enhanced myocardial contractility and increased Ca2+ transport function in transgenic hearts expressing the fast-twitch skeletal muscle sarcoplasmic reticulum Ca2+-ATPase [see comments]. *Circ Res* **83**, 889-97.

Lytton, J., Westlin, M., Burk, S. E., Shull, G. E., and MacLennan, D. H. (1992). Functional comparisons between isoforms of the sarcoplasmic or endoplasmic reticulum family of calcium pumps. *J. Biol. Chem.* **267**, 14483-14489.

Lytton, J., Westlin, M., and Hanley, M. R. (1991). Thapsigargin inhibits the sarcoplasmic or endoplasmic reticulum Ca^{2+}-ATPase family of calcium pumps. *J. Biol. Chem.* **266**, 17067-17071.

Lytton, J., Zarain-Herzberg, A., Periasamy, M., and MacLennan, D. H. (1989). Molecular cloning of the mammalian smooth muscle sarco(endo)plasmic reticulum Ca2+-ATPase. *J. Biol. Chem.* **264**, 7059-7065.

MacLennan, D. H. (1970). Purification and properties of an adenosine triphosphatase from sarcoplasmic reticulum. *J Biol Chem* **245**, 4508-18.

MacLennan, D. H., Rice, W. J., and Green, N. M. (1997). The mechanism of Ca^{2+} transport by sarco(endo)plasmic reticulum Ca^{2+}-ATPase. *J. Biol. Chem.* **272**, 28815-28818.

Mariathasan, S., Bachmann, M. F., Bouchard, D., Ohteki, T., and Ohashi, P. S. (1998). Degree of TCR internalization and Ca2+ flux correlates with thymocyte selection. *J Immunol* **161**, 6030-7.

Mason, M. J., Mahaut-Smith, M. P., and Grinstein, S. (1991). The role of intracellular Ca2+ in the regulation of the plasma membrane Ca2+ permeability of unstimulated rat lymphocytes. *J Biol Chem* **266**, 10872-9.

McCaffrey, P. G., Luo, C., Kerppola, T. K., Jain, J., Badalian, T. M., Ho, A. M., Burgeon, E., Lane, W. S., Lambert, J. N., Curran, T., Verdine, G. L., Rao, A., and Hogan, P. G. (1993). Isolation of the cyclosporin-sensitive T cell transcription factor NFATp. *Science* **262**, 750-754.

Meszaros, L. G., Zahradnikova, A., and Volpe, P. (1998). Kinetic basis of quantal calcium release from intracellular calcium stores. *Cell Calcium* **23**, 43-52.

Meuer, S. C., Hussey, R. E., Cantrell, D. A., Hodgdon, J. C., Schlossman, S. F., Smith, K. A., and Reinherz, E. L. (1984). Triggering of the T3-Ti antigen-receptor complex results in clonal T- cell proliferation through an interleukin 2-dependent autocrine pathway. *Proc Natl Acad Sci U S A* **81**, 1509-13.

Minta, A., Kao, J. P., and Tsien, R. Y. (1989). Fluorescent indicators for cytosolic calcium based on rhodamine and fluorescein chromophores. *J Biol Chem* **264**, 8171-8.

Nakayama, T., Ueda, Y., Yamada, H., Shores, E. W., Singer, A., and June, C. H. (1992). In vivo calcium elevations in thymocytes with T cell receptors that are specific for self ligands. *Science* **257**, 96-9.

Negulescu, P. A., Krasieva, T. B., Khan, A., Kerschbaum, H. H., and Cahalan, M. D. (1996). Polarity of T cell shape, motility, and sensitivity to antigen. *Immunity* **4**, 421-30.

Negulescu, P. A., Shastri, N., and Cahalan, M. D. (1994). Intracellular calcium dependence of gene expression in single T lymphocytes. *Proc. Natl. Acad. Sci. USA* **91**, 2873-2877.

O'Keefe, S. J., Tamura, J., Kincaid, R. L., Tocci, M. J., and O'Neill, E. A. (1992). FK-506- and CsA-sensitive activation of the interleukin-2 promoter by calcineurin. *Nature* **357**, 692-694.

Odermatt, A., Taschner, P. E., Khanna, V. K., Busch, H. F., Karpati, G., Jablecki, C. K., Breuning, M. H., and MacLennan, D. H. (1996). Mutations in the gene-encoding SERCA1, the fast-twitch skeletal muscle sarcoplasmic reticulum Ca2+ ATPase, are associated with Brody disease. *Nat Genet* **14**, 191-4.

Ozog, A., Pouzet, B., Bobe, R., and Lompre, A. M. (1998). Characterization of the 3' end of the mouse SERCA 3 gene and tissue distribution of mRNA spliced variants. *FEBS Lett* **427**, 349-52.

Patterson, R. L., van Rossum, D. B., and Gill, D. L. (1999). Store-operated Ca2+ entry: evidence for a secretion-like coupling model. *Cell* **98**, 487-99.

Periasamy, M., Reed, T. D., Liu, L. H., Ji, Y., Loukianov, E., Paul, R. J., Nieman, M. L., Riddle, T., Duffy, J. J., Doetschman, T., Lorenz, J. N., and Shull, G. E. (1999). Impaired cardiac performance in heterozygous mice with a null mutation in the sarco(endo)plasmic reticulum Ca2+-ATPase isoform 2 (SERCA2) gene. *J Biol Chem* **274**, 2556-62.

Poch, E., Leach, S., Snape, S., Cacic, T., MacLennan, D. H., and Lytton, J. (1998). Functional characterization of alternatively spliced human SERCA3 transcripts. *Am J Physiol* **275**, C1449-58.

Pozzan, T., Rizzuto, R., Volpe, P., and Meldolesi, J. (1994). Molecular and cellular physiology of intracellular calcium stores. *Physiol Rev* **74**, 595-636.

Putney, J. W., Jr. (1990). Capacitative calcium entry revisited: Review article. *Cell Calcium* **11**, 611-624.

Putney, J. W., Jr. (1993). Excitement about calcium signaling in inexcitable cells. *Science* **262**, 676-678.

Qian, D., and Weiss, A. (1997). T cell antigen receptor signal transduction. *Curr. Opin. Cell Biol.* **9**, 205-212.

Randriamampita, C., and Tsien, R. Y. (1993). Emptying of intracellular Ca2+ stores releases a novel small messenger that stimulates Ca2+ influx [see comments]. *Nature* **364**, 809-14.

Rao, A., Luo, C., and Hogan, P. G. (1997). Transcription factors of the NFAT family: Regulation and function. *Annu. Rev. Immunol.* **15**, 707-747.

Reth, M. (1989). Antigen receptor tail clue [letter]. *Nature* **338**, 383-4.

Rijkers, G. T., Justement, L. B., Griffioen, A. W., and Cambier, J. C. (1990). Improved method for measuring intracellular Ca++ with fluo-3. *Cytometry* **11**, 923-7.

Sakuntabhai, A., Ruiz-Perez, V., Carter, S., Jacobsen, N., Burge, S., Monk, S., Smith, M., Munro, C. S., O'Donovan, M., Craddock, N., Kucherlapati, R., Rees, J. L., Owen, M., Lathrop, G. M., Monaco, A. P., Strachan, T., and Hovnanian, A. (1999). Mutations in ATP2A2, encoding a Ca2+ pump, cause Darier disease [see comments]. *Nat Genet* **21**, 271-7.

Sasaki, D. T., Dumas, S. E., and Engleman, E. G. (1987). Discrimination of viable and non-viable cells using propidium iodide in two color immunofluorescence. *Cytometry* **8**, 413-20.

Schnetkamp, P. P. M., Li, X.-B., Basu, D. K., and Szerencsei, R. T. (1991). Regulation of free cytosolic Ca2+ concentration in the outer segments of bovine retinal rods by Na-Ca-K exchange measured with fluo-3. I. Efficiency of transport and interactions between cations. *J. Biol. Chem.* **266**, 22975-22982.

Schwartz, R. H. (1997). T cell clonal anergy. *Curr. Opin. Immunol.* **9**, 351-357.

Sei, Y., Gallagher, K. L., and Basile, A. S. (1999). Skeletal muscle type ryanodine receptor is involved in calcium signaling in human B lymphocytes. *J Biol Chem* **274**, 5995-6002.

Sei, Y., and Reich, H. (1995). Thapsigargin induces IL-2 receptor alpha-chain in human peripheral and Jurkat T cells via a protein kinase C-independent mechanism. *Immunol Lett* **45**, 75-80.

Shibasaki, F., Price, E. R., Milan, D., and McKeon, F. (1996). Role of kinases and the phosphatase calcineurin in the nuclear shuttling of transcription factor NF-AT4. *Nature* **382**, 370-373.

Sprent, J. (1999). Presidential address to the American Association of Immunologists. Stimulating naive T cells. *J Immunol* **163**, 4629-36.

Stein, P. H., Fraser, J. D., and Weiss, A. (1994). The cytoplasmic domain of CD28 is both necessary and sufficient for costimulation of interleukin-2 secretion and association with phosphatidylinositol 3'-kinase. *Mol. Cell. Biol.* **14**, 3392-3402.

Su, B., Jacinto, E., Hibi, M., Kallunki, T., Karin, M., and Ben-Neriah, Y. (1994). JNK is involved in signal integration during costimulation of T lymphocytes. *Cell* **77**, 727-736.

Sugawara, H., Kurosaki, M., Takata, M., and Kurosaki, T. (1997). Genetic evidence for involvement of type 1, type 2 and type 3 inositol 1,4,5-trisphosphate receptors in signal transduction through the B-cell antigen receptor. *Embo J* **16**, 3078-88.

Takahashi, A., Camacho, P., Lechleiter, J. D., and Herman, B. (1999). Measurement of intracellular calcium. *Physiol Rev* **79**, 1089-125.

Takata, M., Homma, Y., and Kurosaki, T. (1995). Requirement of phospholipase C-gamma 2 activation in surface immunoglobulin M-induced B cell apoptosis [see comments]. *J Exp Med* **182**, 907-14.

Thastrup, O., Cullen, P. J., Drobak, B. K., Hanley, M. R., and Dawson, A. P. (1990). Thapsigargin, a tumor promoter, discharges intracellular Ca2+ stores by specific inhibition of the endoplasmic reticulum Ca2(+)-ATPase. *Proc Natl Acad Sci U S A* **87**. 2466-70.

Thomis, D. C., Lee, W., and Berg, L. J. (1997). T cells from Jak3-deficient mice have intact TCR signaling, but increased apoptosis. *J Immunol* **159**, 4708-19.

Timmerman, L. A., Clipstone, N. A., Ho, S. N., Northrop, J. P., and Crabtree, G. R. (1996). Rapid shuttling of NF-AT in discrimination of Ca^{2+} signals and immunosuppression. *Nature* **383**, 837-840.

Toyofuku, T., Kurzydlowski, K., Lytton, J., and MacLennan, D. H. (1992). The nucleotide binding/hinge domain plays a crucial role in determining isoform-specific Ca2+ dependence of organellar Ca^{2+}-ATPase. *J. Biol. Chem.* **267**, 14490-14496.

Truneh, A., Albert, F., Golstein, P., and Schmitt-Verhulst, A. M. (1985). Early steps of lymphocyte activation bypassed by synergy between calcium ionophores and phorbol ester. *Nature* **313**, 318-20.

Tsien, R. Y., Pozzan, T., and Rink, T. J. (1982). T-cell mitogens cause early changes in cytoplasmic free Ca2+ and membrane potential in lymphocytes. *Nature* **295**, 68-71.

van Oers, N. S. C., Killeen, N., and Weiss, A. (1996). Lck regulates the tyrosine phosphorylation of the T cell receptor subunits and ZAP-70 in murine thymocytes. *J. Exp. Med.* **183**, 1053-1062.

Vandenberghe, P. A., and Ceuppens, J. L. (1990). Flow cytometric measurement of cytoplasmic free calcium in human peripheral blood T lymphocytes with fluo-3, a new fluorescent calcium indicator. *J Immunol Methods* **127**, 197-205.

Varadi, A., Lebel, L., Hashim, Y., Mehta, Z., Ashcroft, S. J., and Turner, R. (1999). Sequence variants of the sarco(endo)plasmic reticulum Ca(2+)-transport ATPase 3 gene (SERCA3) in caucasian type II diabetic patients (UK prospective diabetes study 48) [In Process Citation]. *Diabetologia* **42**, 1240-3.

Venkataraman, L., Francis, D. A., Wang, Z., Liu, J., Rothstein, T. L., and Sen, R. (1994). Cyclosporin-A sensitive induction of NF-AT in murine B cells. *Immunity* **1**, 189-96.

Wacholtz, M. C., and Lipsky, P. E. (1993). Anti-CD3-stimulated Ca2+ signal in individual human peripheral T cells. Activation correlates with a sustained increase in intracellular Ca2+1. *J Immunol* **150**, 5338-49.

Wange, R. L., and Samelson, L. E. (1996). Complex complexes: Signaling at the TCR. *Immunity* **5**, 197-205.

Ward, S. G. (1996). CD28: A signalling perspective. *Biochem. J.* **318**, 361-377.

Weiss, A., and Littman, D. R. (1994). Signal transduction by lymphocyte antigen receptors. *Cell* **76**, 263-274.

Weiss, A., Shields, R., Newton, M., Manger, B., and Imboden, J. (1987). Ligand-receptor interactions required for commitment to the activation of the interleukin 2 gene. *J Immunol* **138**, 2169-76.

Wesselborg, S., Fruman, D. A., Sagoo, J. K., Bierer, B. E., and Burakoff, S. J. (1996). Identification of a physical interaction between calcineurin and nuclear factor of activated T cells (NFATp). *J. Biol. Chem.* **271**, 1274-1277.

Woodrow, M., Clipstone, N. A., and Cantrell, D. (1993). $p21^{ras}$ and calcineurin synergize to regulate the nuclear factor of activated T cells. *J. Exp. Med.* **178**, 1517-1522.

Wu, K.-D., Lee, W.-S., Wey, J., Bungard, D., and Lytton, J. (1995). Localization and quantification of endoplasmic reticulum Ca^{2+}-ATPase isoform transcripts. *Am. J. Physiol.* **269**, C775-C784.

Wuytack, R., Papp, B., Verboomen, H., Raeymaekers, L., Dode, L., Bobe, R., Enouf, J., Bokkala, S., Authi, K., and Casteels, R. (1994). A sarco/enodplasmic reticulum Ca^{2+}-ATPase 3-type Ca^{2+} pump is expressed in platelets, in lymphoid cells, and in mast cells. *J. Biol. Chem.* **269**, 1410-1416.

Yao, Y., Ferrer-Montiel, A. V., Montal, M., and Tsien, R. Y. (1999). Activation of store-operated Ca2+ current in Xenopus oocytes requires SNAP-25 but not a diffusible messenger. *Cell* **98**, 475-85.

Zhang, P., Toyoshima, C., Yonekura, K., Green, N. M., and Stokes, D. L. (1998). Structure of the calcium pump from sarcoplasmic reticulum at 8-A resolution. *Nature* **392**, 835-9.

Zweifach, A., and Lewis, R. S. (1993). Mitogen-regulated Ca2+ current of T lymphocytes is activated by depletion of intracellular Ca2+ stores. *Proc Natl Acad Sci U S A* **90**, 6295-9.